

REPORT ON
1997 GEOLOGICAL AND GEOPHYSICAL SURVEYS
(work carried out from June 14 to August 4, 1997)
on the
KLU PROPERTY

<u>Grant Number</u>	<u>Claim Name</u>
YB 54998	KLU 3122
YB 54999	KLU 3123
YB 55007	KLU 3221
YB 55008	KLU 3222
YB 55009	KLU 3223
YB 55017	KLU 3321
YB 55018	KLU 3322
YB 55019	KLU 3323
YB 55027	KLU 3421
YB 55028	KLU 3422
YB 55126	KLU 4412
YB 55156	KLU 4610
YB 58166	KLU 1810
YB 58168	KLU 1910

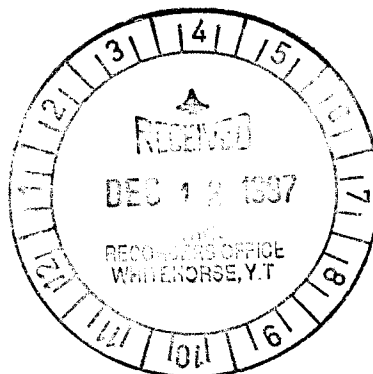
093726

NTS 115G/2

Latitude 61° 10'N; 139° 48'W

Whitehorse Mining District

Yukon Territory



Katherine Hattie
Inco Limited
Anchorage, AK
December 4, 1997

This report has been examined by
the Geological Evaluation Unit
under Section 53 (4) Yukon Quartz
Mining Act and is allowed as
representation work in the amount
of \$ 60,000.

M. B. ...
for Regional Manager, Exploration and
Geological Services for Commissioner
of Yukon Territory.

A112-11-11

TABLE OF CONTENTS

1.0 INTRODUCTION.....	1
2.0 LOCATION, ACCESS AND TOPOGRAPHY	1
3.0 PROPERTY	1
4.0 PREVIOUS WORK.....	4
5.0 REGIONAL GEOLOGY	5
6.0 PROPERTY GEOLOGY AND MINERALIZATION	5
6.1 Property Geology.....	5
6.2 Mineralization.....	9
7.0 1997 WORK PROGRAM.....	10
7.1 Line Cutting.....	10
7.2 Geology.....	11
7.3 Geophysics.....	11
7.3.1 Ground Magnetic Survey.....	11
7.3.2 UTEM Geophysical Survey.....	11
7.4 Geochemistry	12
7.4.1 Rock Geochemical Survey.....	12
7.4.2 Silt Geochemical Survey.....	12
8.0 CONCLUSIONS AND RECOMMENDATIONS	12
9.0 PERSONNEL.....	14
10.0 COST STATEMENT	15
10.1 AEM Conductor A (Sheet 8).....	15
10.2 AEM Conductor B (Sheet 10).....	16
10.3 AEM Conductor C (Sheet 3).....	17
11.0 STATEMENT OF QUALIFICATIONS.....	18
12.0 REFERENCES.....	19

LIST OF FIGURES

Figure		Page
1	Property Location Map	2
2	Klu Property Claim Location Map	3
3	Klu Property Generalized Geology Map	6

LIST OF TABLES

Table		Page
1	Klu Claims to be Considered for Renewal	4
2	Summary of Rock Formations, Klu Project	7

LIST OF MAPS

Map		Scale	Page
1	Detailed Claim Location Map	1:25,000	in pocket
2	Claim Map: Sheets 3, 8, 10	1:5,000	in pocket
3	Geology and Sample Location Map: Sheets 3, 8, 10	1:5,000	in pocket
4	Ground Magnetic & UTEM Survey Results: Sheet 8	1:5,000	in pocket

LIST OF APPENDICES

Appendix 1	UTEM & Magnetometer Surveys Logistics Report on the Klu Project
Appendix 2	Rock Sample Descriptions
Appendix 3	Rock Sample Analytical Results
Appendix 4	Silt Sample Descriptions
Appendix 5	Silt Sample Analytical Results

1.0 INTRODUCTION

The Klu property was staked in October of 1994 to cover Ni-Cu-PGE showings discovered during a reconnaissance exploration program carried out in 1993 and 1994. The showings occur at the base of a Triassic peridotite sill hosted in Permian Hasen Creek Formation sediments. These occurrences are in the vicinity of a Ni-Cu showing documented in a 1973 assessment report. Massive, disseminated and net textured sulphides occur in the marginal gabbro phase of the sill. Massive sulphide lenses (up to 2.0 x 0.25 m) and fracture controlled sulphides occur in siltstone in the footwall of the sill. Samples of these lenses contain up to 3.1% Ni, 27.6 % Cu, 0.09% Co, 75.8 g/t Pt, 7.9 g/t Pd and 7.0 g/t Au.

This report documents exploration work carried out on the property in 1997. The program consisted primarily of line cutting, ground magnetic and UTEM geophysical surveys. Limited geological mapping, rock geochemical sampling and silt sampling were also conducted.

2.0 LOCATION, ACCESS AND TOPOGRAPHY

The Klu property is centered eight kilometres south of the village of Destruction Bay and 20 kilometres southeast of the village of Burwash Landing. Whitehorse is approximately 200 kilometres southeast of the property (Figure 1). The property parallels the Alaska Highway with its northeast boundary being five kilometres southwest from the highway. Kluane National Park borders the property to the southeast and southwest. The property is completely within the Kluane Game Sanctuary.

Primary access to the property is by helicopter. A permanent helicopter base is in Haines Junction, 70 kilometres to the southeast. Secondary gravel roads run off the Alaska Highway along the southeast banks of Nines Creek and Bock's Brook. These roads both end approximately two kilometres from the northeast boundary of the property.

Topography on the property is extremely rugged. Elevations range from 3,500 to 8,200 feet. Treeline is generally at about 4,200 feet with treed areas only occurring in the Congdon, Nines, Bock's and Lewis Creek valleys. Several glaciers occur on the property above the 7,000 foot level.

3.0 PROPERTY

The property consists of 526 contiguous quartz claims located in the Whitehorse Mining District. A total of 508 were staked in October of 1994. An additional 18 claims, staked in August of 1995, connect the original claims which were previously in two separate blocks. The claims are 100% owned by Inco Limited. Figure 2 shows the claim boundary and the boundaries of the claim blocks staked in 1994 and 1995. A detailed property claim map showing individual claims, claim names, and grant numbers is included as Map 1 (in pocket). Claims upon which exploration was conducted in 1997 are indicated in red.

Table 1 lists the claim names and grant numbers for 160 claims considered for renewal in this assessment report. Work on the claims was done for Inco Limited by Inco personnel, line cutting contractors, and geophysical contractors.



YUKON TERRITORY PROPERTY LOCATION

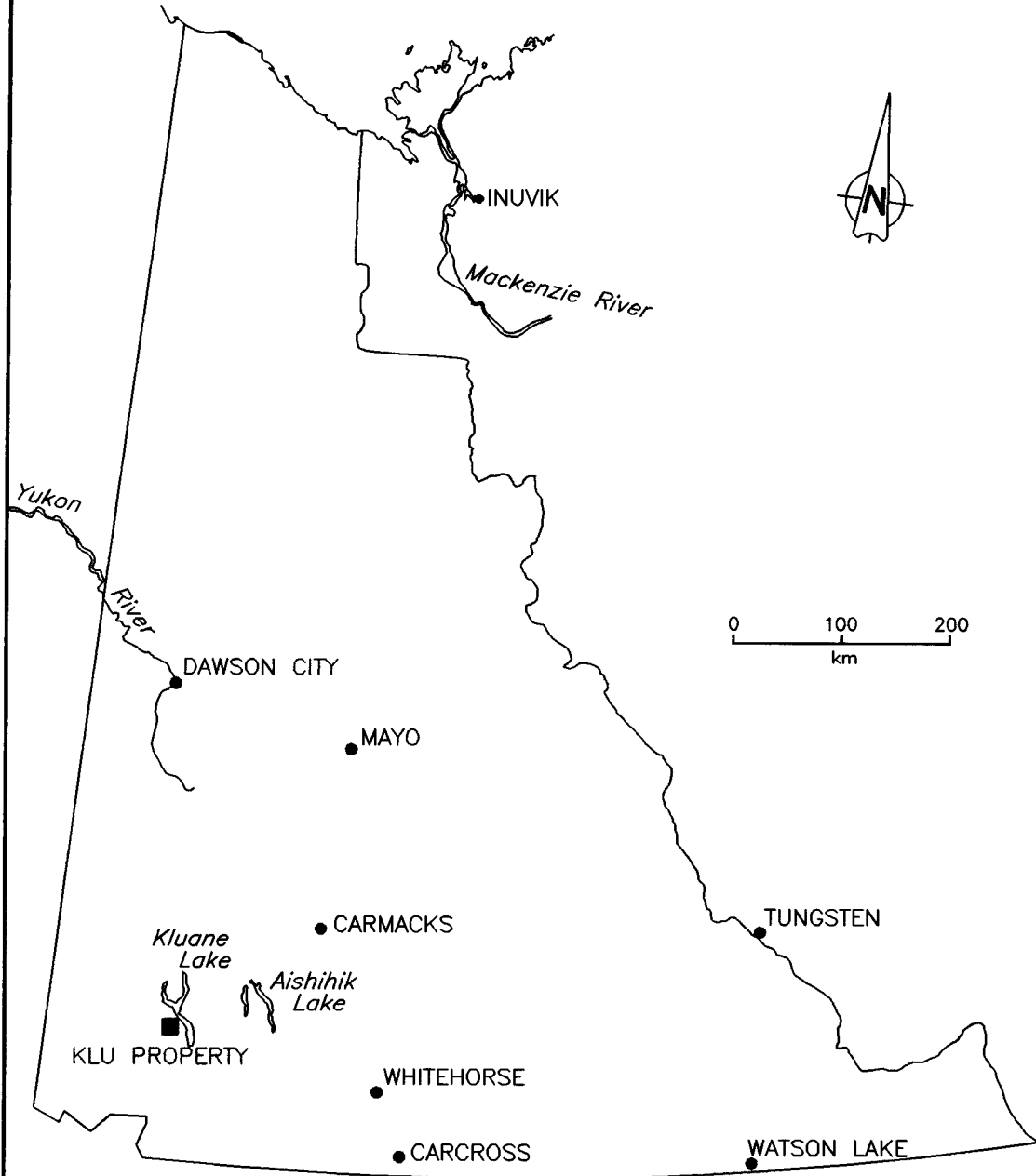
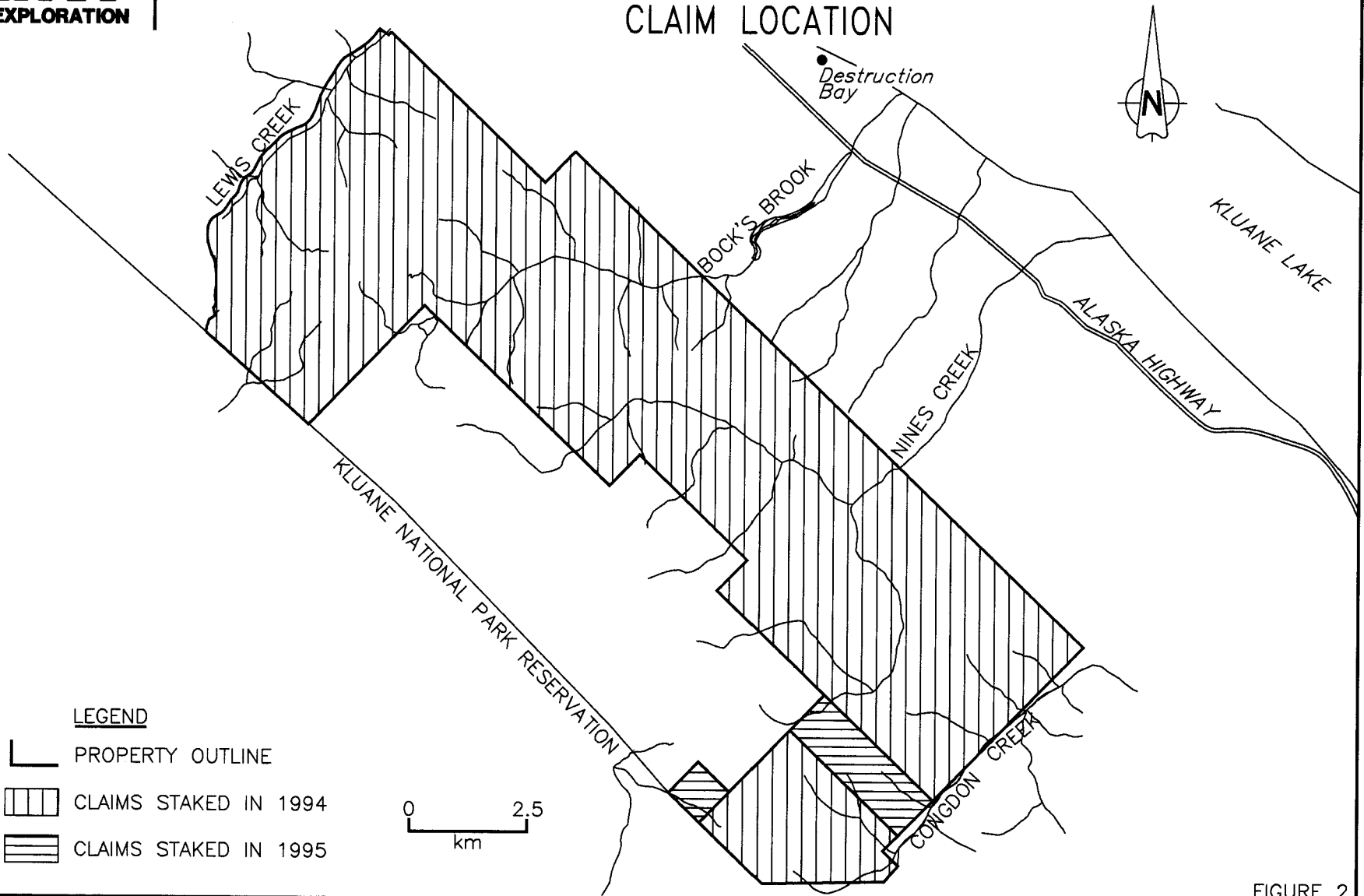

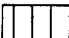
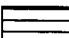


FIGURE 1

YUKON, KLU PROPERTY CLAIM LOCATION



LEGEND

-  PROPERTY OUTLINE
-  CLAIMS STAKED IN 1994
-  CLAIMS STAKED IN 1995

0 2.5
km

FIGURE 2

Table 1: Klu Claims held by Inco Limited to be considered for renewal.

Grant Number	Claim Name	Grant Number	Claim Name
YB 54846	KLU 1610	YB 54847	KLU 1611
YB 54856 to YB 54857	KLU 1622 to KLU 1623	YB 54862 to YB 54863	KLU 1710 to KLU 1711
YB 54872 to YB 54873	KLU 1722 to KLU 1723	YB 54881 to YB 54884	KLU 1821 to KLU 1824
YB 54890 to YB 54894	KLU 1920 to KLU 1924	YB 54900 to YB 54904	KLU 2020 to KLU 2024
YB 54910 to YB 54914	KLU 2120 to KLU 2124	YB 54920 to YB 54924	KLU 2220 to KLU 2224
YB 54930 to YB 54934	KLU 2320 to KLU 2324	YB 54940 to YB 54944	KLU 2420 to KLU 2424
YB 54948 to YB 54952	KLU 2520 to KLU 2524	YB 54956 to YB 54960	KLU 2620 to KLU 2624
YB 54964 to YB 54968	KLU 2720 to KLU 2724	YB 54972 to YB 54976	KLU 2820 to KLU 2824
YB 54980 to YB 54984	KLU 2920 to KLU 2924	YB 54988 to YB 54992	KLU 3020 to KLU 3024
YB 54996 to YB 55000	KLU 3120 to KLU 3124	YB 55005 to YB 55009	KLU 3219 to KLU 3223
YB 55015 to YB 55019	KLU 3319 to KLU 3323	YB 55025 to YB 55028	KLU 3419 to KLU 3422
YB 55035 to YB 55038	KLU 3519 to KLU 3522	YB 55045 to YB 55048	KLU 3619 to KLU 3622
YB 55055 to YB 55058	KLU 3719 to KLU 3722	YB 55065 to YB 55068	KLU 3819 to KLU 3822
YB 55075 to YB 55078	KLU 3919 to KLU 3922	YB 55085 to YB 55088	KLU 4019 to KLU 4022
YB 55095 to YB 55098	KLU 4119 to KLU 4122	YB 55105 to YB 55108	KLU 4219 to KLU 4222
YB 55115 to YB 55118	KLU 4319 to KLU 4322	YB 55124 to YB 55127	KLU 4410 to KLU 4413
YB 55132 to YB 55136	KLU 4418 to KLU 4422	YB 55140 to YB 55143	KLU 4510 to KLU 4513
YB 55148 to YB 55152	KLU 4518 to KLU 4522	YB 55156 to YB 55159	KLU 4610 to KLU 4613
YB 55164 to YB 55168	KLU 4618 to KLU 4622	YB 55180 to YB 55181	KLU 4718 to KLU 4719
YB 58166 to YB 58167	KLU 1810 to KLU 1811	YB 58168 to YB 58169	KLU 1910 to KLU 1911

4.0 PREVIOUS WORK

The earliest recorded exploration on the present Klu property was carried out by John S. Vincent Ltd., for the Nickel Syndicate during 1972-73 (MacEy et al, 1973). This work consisted of geological mapping and rock sampling on the Spy 1-12 claims. The claims were located on the northeast facing slope above the southern branch of Nines Creek. John S. Vincent Ltd. mapped a series of gabbro to peridotite sills intruding the Hasen Creek Formation. Sulphide mineralization was reported to occur at the base of a "gabbro-peridotite" sill. Values up to 1.47% Ni and 0.49% Cu were reported for sulphides occurring in "quartz xenoliths" at the base of the sill. Additional sulphide mineralization consisting of disseminated chalcopyrite, pyrrhotite and pyrite with values of 0.5% Ni and 0.5% Cu was reported to occur in gabbro along strike from the original showing. The occurrences are in the same area as the Ni-Cu-PGE rich sulphide showings discovered by Inco personnel in 1994. Elsewhere on the Spy claims, sphalerite-galena mineralization was reported on the margins of a quartz vein. Samples from this showing contain values of 1.25% Zn and 0.25% Pb.

Aurum Geological Consultants Inc. conducted an exploration program for Walhala Explorations Ltd. in 1987. Assessment was filed on the Tony 1-28 and Tony 29-60 claim blocks. This work consisted of geologic mapping and lithochemical sampling (Keyser, 1987).

During 1995, Inco personnel completed an exploration program consisting of geological mapping, lithochemical sampling, stream sediment sampling and limited soil geochemistry. In 1996, a helicopter-borne frequency domain EM and magnetometer survey was flown over the entire property.

5.0 REGIONAL GEOLOGY

The Klu property is situated within Wrangellia, an accreted terrane extending 2,340 kilometres from Alaska to southern British Columbia. Certain geological elements are common throughout the terrane, including an Upper Paleozoic island arc basement overlain by a thick Triassic flood basalt sequence.

The eastern part of Wrangellia, in southwest Yukon, is bounded to the northeast by the Denali Fault System and to the southwest by the Duke River Fault. The oldest Wrangellian rocks in the belt are the Pennsylvanian to Lower Permian Skolai Group. The Station Creek Formation occurs at the base of the Skolai Group and consists of tuffs, pyritic black tuff, mafic volcanics and argillite. This is overlain by the Hasen Creek Formation which consists of tuffs, mafic volcanics, argillite and limestone. The Skolai Group is stratigraphically overlain by Pennsylvanian to Triassic mafic meta-volcanics, Upper Triassic Nikolai basalt, and Upper Triassic McCarthy Formation limestone and phyllite. Tertiary volcanics and sediments unconformably overlie the sequence. Quaternary surficial deposits locally cover the Paleozoic, Mesozoic and Cenozoic strata.

There are two major suites of intrusive rocks in the belt. The oldest suite includes Triassic ultramafic sills, marginal gabbro, and the Maple Creek Gabbro. These intrusions are thought to be cogenetic with the Nikolai flood basalt. Cretaceous Kluane Range Intrusions are dioritic to granodioritic in composition and occur throughout northern Wrangellia. Minor Tertiary sills, dikes and stocks of felsic to intermediate composition are also present.

The major Triassic ultramafic intrusions (Kluane-type) are sill-like bodies which intrude the Hasen Creek and Station Creek Formations. The dips of the sills range from vertical to steeply overturned to as shallow as 30 degrees. Maximum dimensions of the sills are estimated to be up to 18 kilometres in length and 600 metres in thickness.

Peridotite is the dominant ultramafic phase with lesser dunite and pyroxenite. The peridotite ranges in composition from wehrlitic to lherzolitic and contains varying amounts of olivine, clinopyroxene, orthopyroxene, plagioclase, phlogopite and oxides. Serpentinization of ultramafic rocks varies locally from weak to strong. Many of the ultramafic sills have a marginal gabbro at their base which makes up approximately 4% of the thickness of each sill. Clinopyroxenite layers locally are present above the marginal gabbro layer. Some of the sills also have marginal gabbro at their upper contacts. Field relationships suggest that these marginal gabbros represent an initial pulse of magma which was followed by progressively more ultramafic magma. The apparent "reverse layering" of these intrusions is probably a result of the sequential tapping of a compositionally layered magma chamber at depth.

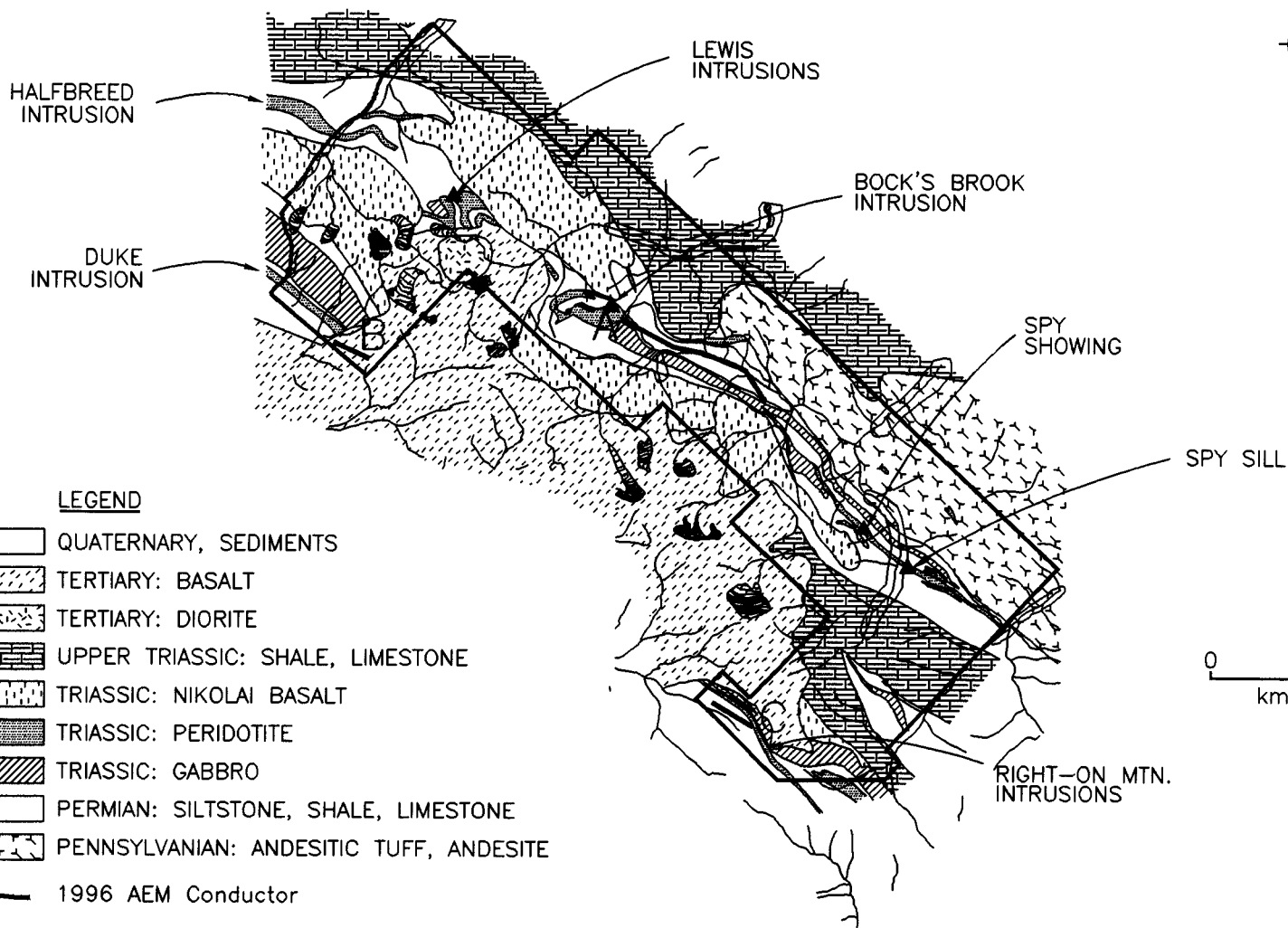
Permo-Triassic rocks of the belt are faulted and tightly folded about steeply dipping axial planes and shallow northwest trending axes. Faulting includes bedding-plane slip faults and strike-slip faults which trend normal to the Denali Fault (a terrane-bounding transcurrent fault).

6.0 PROPERTY GEOLOGY AND MINERALIZATION

6.1 Property Geology

The geology of the property is dominated by several fault bounded slices of folded Paleozoic and Mesozoic strata. These rocks are overlain by gently dipping Tertiary sediments and volcanics. Figure 3 shows a generalized geological map of the property. The bounding faults trend southeast to northwest and are believed to dip steeply. The axial planes of the folds also trend from southeast to northwest and appear to dip steeply; fold axes are assumed to be near horizontal. Much of the folding is inferred; no large scale

YUKON TERRITORY, KLU PROPERTY GENERALIZED GEOLOGY



- LEGEND**
- QUATERNARY, SEDIMENTS
 - ▨ TERTIARY: BASALT
 - ▩ TERTIARY: DIORITE
 - ▧ UPPER TRIASSIC: SHALE, LIMESTONE
 - ▦ TRIASSIC: NIKOLAI BASALT
 - ▥ TRIASSIC: PERIDOTITE
 - ▤ TRIASSIC: GABBRO
 - ▣ PERMIAN: SILTSTONE, SHALE, LIMESTONE
 - ▢ PENNSYLVANIAN: ANDESITIC TUFF, ANDESITE
 - 1996 AEM Conductor

FIGURE 3

KLU067

folds were observed on the property. Scarcity of outcrop in the valley bottoms of Congdon Creek, Nines Creek, Bock's Brook and Lewis Creek make some structural interpretations tenuous. Certain faults and folds shown on GSC Open File Map 381 are not shown on maps accompanying this report.

A table summarizing rock formations present on the Klu property is shown in Table 2. Geological age, map symbol, unit name and a brief description of each unit are listed in the table.

Table 2: Summary of Rock Formations, Klu Property

STRATIFIED ROCK FORMATIONS

AGE	SYMBOL	UNIT	DESCRIPTION
Tertiary (Miocene- Pliocene)	NW	Wrangell Lava (Undivided)	Basalt to andesite flows, minor white to yellow felsic pyroclastics and flows
Tertiary (Oligocene)	Os	Amphitheatre Formation	Yellow-buff to gray-buff sandstone, pebbly sandstone, polymictic conglomerate
U. Triassic- Cretaceous	uTrKp		Dark gray phyllite, minor greywacke and conglomerate
U. Triassic	uTrM	McCarthy Formation	Argillaceous limestone and dark gray argillite
U. Triassic	uTrC	Chitistone and Nizina Formations	Massive light gray limestone, limestone breccia, and dark gray well bedded limestone
U. Triassic	uTre		White to creamy-white gypsum and anhydrite
U. Triassic	uTrN	Nikolai Greenstone	Dark green and maroon amygdaloidal to massive basaltic and andesitic flows, locally interbedded with tuff, breccia, shale, limestone; pillow lava and conglomerate occur at base
L. Permian	Ps	Hasen Creek Formation	Thin bedded siliceous argillite, siltstone, shale, greywacke, conglomerate, local thin basalt flows
L. Permian	Pc	Hasen Creek Formation	Buff to gray bioclastic limestone
Pennsylvanian	Pv	Station Creek Formation	Andesitic to basaltic tuffs and flows

INTRUSIVE ROCKS

AGE	SYMBOL	UNIT	DESCRIPTION
Tertiary (Miocene)	lMf	Wrangell Plutonic Suite	Buff to creamy-white granodiorite, diorite, gabbro dykes and sills, fine grained
Tertiary (Miocene)	lMdi	Bock's Brook Stock	Light buff-gray biotite diorite, medium grained
Triassic	Trb	Maple Creek Gabbro (Kluane- type)	Gabbro and anorthositic gabbro sills, medium grained
Triassic	Trub	Kluane-type Ultramafics	Peridotite, feldspathic peridotite sills with minor pyroxenite and dunite, medium grained
Triassic	Trmg	Kluane-type Marginal Gabbro	Gray medium grained to fine grained locally chilled gabbro, forms along margins of peridotite

The Triassic Kluane-type intrusions form sills in Hasen Creek Formation strata and to a lesser extent in the Station Creek Formation. The location of the major ultramafic intrusions on the property is shown on Figure 3. The geology of the property is summarized below with reference to the major Kluane-type intrusions on the property.

The Spy Sill in the southeastern part of the property is a 75 to 100 metre thick, 6-kilometre long (minimum) intrusion of dominantly unserpentinized feldspathic peridotite. The Spy Sill is emplaced within Hasen Creek Formation siltstone. Marginal gabbro up to 10 metres thick is locally present at the top and base of the sill. Maple Creek gabbro sills occur stratigraphically above and below the Spy Sill as well as directly at its base. The most continuous Maple Creek gabbro sill occurs 230 metres down-section from the base of the peridotite and is up to 160 metres thick. This sill is intermittently exposed over a 10-kilometre strike. The northwestern end of the Spy Sill is cut by a 200-metre thick section of Maple Creek gabbro. Elsewhere, smaller bodies of Maple Creek gabbro also cut and form lens-shaped bodies within the peridotite. Three stacked lenses of peridotite occur below the main sill on the ridge between Congdon Creek and the southern branch of Nines Creek. These lenses are up to 600 metres long and 30 metres thick. Smaller lenses of peridotite occur below the main sill elsewhere. The lower contact of the main peridotite sill occurs 100 metres above a distinctive chert + siltstone pebble conglomerate bed, while the upper contact is approximately 20 metres below a buff weathering limestone bed with positive weathering relief. Down-section from the Spy Sill on the opposite side of the southern branch of Nines Creek, two apparently unconnected feldspathic peridotite intrusions up to 65 metres thick occur within the Station Creek Formation. Two kilometres northwest of the northwest extremity of the Spy Sill is an additional peridotite intrusion up to 200 metres thick with poor strike continuity. This sill is emplaced near the Station Creek-Hasen Creek Formation contact. The Hasen Creek and Station Creek Formations have a constant southeast-northwest strike and dip averaging 40 degrees to the southwest. The strata in the Spy Sill area do not appear to be overturned. Nikolai basalt caps the ridge above the Spy Sill. The lower contact of the basalt is approximately 450 metres up-section from the top of the peridotite. The contact between the Hasen Creek Formation and the Nikolai basalt appears to be disconformable.

The Right-On Mountain Intrusions occur at the southern extremity of the property in a package of Hasen Creek Formation shale, chert and limestone which trend southeast-northwest and dip steeply to the southwest (60-90 degrees). These beds may be overturned. Two major peridotite sills occur here, the largest of which is 200 metres thick. Some of this thickness may be due to fault repetition. These sills trend into Kluane National Park to the southeast. The large peridotite sill is truncated a short distance (approximately 150 metres) into the property while the narrower peridotite sill (60 metres thick) trends into Kluane Park to the northwest where it is locally obscured by Tertiary cover. The southwestern contact of the narrower peridotite sill is locally part of the Duke River Fault which forms the boundary between Wrangellia and Alexander Terrane. A Maple Creek gabbro sill up to 250 metres thick occurs to the northeast of the peridotite sills.

Portions of the Duke and Halfbreed Intrusions occur in the northwestern part of the property. Both intrusions trend northwest into the Native Land Claim Staking Withdrawal. These sills are emplaced within Hasen Creek Formation siltstone and conglomerate which are part of a synclinal structure cored by overlying Nikolai basalt. The Duke Intrusion is a mafic/ultramafic sill emplaced within Hasen Creek Formation strata which trend southeast-northwest and dip at approximately 50 degrees to the southwest. The base of the intrusion consists of a lower peridotite section which is approximately 200 metres thick. The peridotite varies from partially to totally serpentinized. This is overlain by 30 to 50 metre thick screen of Hasen Creek Formation siltstone and chert. The cherty sediment may be silicified siltstone. Above these sediments is a 350 metre thick section of gabbro. This gabbro is believed to be of the Maple Creek-type and contains multiple intrusions. Marginal gabbro is not exposed at the base of the peridotite in the Duke Intrusion. The Duke Intrusion trends below Tertiary cover to the southeast.

Only the southeastern extremity of the Halfbreed Intrusion is present on the property. The majority of the Intrusion occurs on the Native Land Claim Staking Withdrawal. On the Klu property, the Halfbreed Intrusion consists of two peridotite sills which are individually up to 125 metres thick. These sills occur

in siltstone, conglomerate and limestone beds of the Hasen Creek Formation which strike southeast-northwest and dip to the southwest at 50 to 60 degrees. Thin discontinuous marginal gabbro lenses occur at the base of these sills. Maple Creek gabbro sills occur both up-section and down-section from the peridotite sills. The peridotite and gabbro sills here are poorly exposed due to extensive glacial moraine, beneath which the sills terminate. A detailed description of the Duke and Halfbreed intrusions is given in GSC Bulletin 506 (Hulbert, 1997).

The Lewis Intrusions occur in the north-central part of the property two kilometres southeast of the terminus of the Halfbreed Intrusion. The Lewis Intrusions appear to consist of three relatively un-serpentinized peridotite to pyroxenite sills of complex morphology. The sills intrude a package of siltstone, chert and argillite of the Hasen Creek Formation. These rocks have variable orientations, but generally trend southwest-northeast and dip between 20 and 85 degrees to the southeast. An irregular body of Maple Creek gabbro with local cumulate layering appears to intrude the western-most sill. A thin gabbro, possibly Marginal-type, occurs at the base of the southeastern-most sill. The sills are overlain by Tertiary volcanics to the southeast. South of the Lewis Intrusions is a circular stock of Tertiary diorite approximately 1.2 kilometres in diameter. The Lewis Intrusions were difficult to map due to the extreme ruggedness of the area.

The Bock's Brook Intrusion is located in the central part of the property between the Spy Sill and the Lewis Intrusions. This peridotite intrusion is the largest on the property with the main intrusion being approximately 500 metres thick at its maximum. At least one smaller sill occurs below the main sill. The peridotite is strongly serpentinized and appears to be fault bounded along part of its northern contact. The thickness of the sill may be exaggerated due to fault repetition. The top of the sill and part of the base are in contact with Hasen Creek Formation limestone, siltstone and conglomerate. These beds have inconsistent orientations, but generally trend east-west and dip at approximately 50 degrees to the south. Much of the intrusion occupies a boulder choked cirque at the head of a tributary of Bock's Brook. Downstream of the main sill along the tributary are complicated fault slices of Hasen Creek Formation sediment, Nikolai basalt, Upper Triassic shale, a narrow fault bounded peridotite sill and Upper Triassic gypsum and limestone. The Nikolai basalt to the north of the Bock's Brook Intrusion contains numerous small (2x3x1 metre) rafts of gypsum. At the eastern end of the Bock's Brook Intrusion, the peridotite is in contact with a gabbro sill. This sill may be a continuation of the Maple Creek gabbro sill emplaced below the Spy Sill.

Upper Triassic gypsum and limestone beds occur directly above the Nikolai basalt. Several exposures of these beds occur between the Bock's Brook Intrusion - Lewis Intrusions trend and the northeast boundary of the property. Locations with gypsum interlayered with basalt may be in-part due to interbedding, but are probably repeated tectonically to some degree.

6.2 Mineralization

Ni-Cu-PGE mineralization on the property is associated with the basal marginal gabbro phase of the Spy Sill. Sulphide mineralization at the Spy Showing occurs in siltstone in the footwall of the sill, marginal gabbro and feldspathic peridotite. Massive chalcopyrite-pyrrhotite lenses in footwall siltstone are up to 2.0 x 0.25 metres; these lenses grade up to 2.6% Ni, 10.45% Cu, 0.09% Co, 75.8 g/t Pt, 7.9 g/t Pd and 7.0 g/t Au (1994 sample from 2.0 x 0.25 metre lens). The host siltstone is weakly altered, but highly fractured with chalcopyrite-pyrrhotite mineralization occurring along the fractures.

The basal marginal gabbro unit hosts massive sulphide lenses, net-textured sulphide and disseminated sulphide. Gabbro hosted massive pyrrhotite-chalcopyrite lenses grade up to 3.1% Ni, 2.8% Cu, 0.2% Co, 3.1 g/t Pt, 1.4 g/t Pd and 1.0 g/t Au. These lenses are up to 20 centimetres thick and occur at the gabbro-siltstone contact and within zones of gabbro-hosted semi-massive sulphide. Disseminated and net-textured pyrrhotite and chalcopyrite within marginal gabbro grade up to 1.2% Ni, 1.0% Cu, 0.009% Co, 290 ppb Pt, 180 ppb Pd and 88 ppb Au in grab samples. A 1.2-metre chip sample of net-textured

pyrrhotite-chalcocopyrite mineralization in marginal gabbro assayed 0.2% Ni, 1.4% Cu, 1.9 g/t Pt, 1.0 g/t Pd and 0.7 g/t Au. Ni-Cu-PGE mineralization at the base of the Spy Sill has been traced over a strike of 3.6 kilometres. Gabbro/sulphide talus from the base of the sill, 900 metres northwest of the Spy Showing, contained 1.5% Ni, 0.4% Cu, 0.7 g/t Pt and 1.4 g/t Pd. A gabbro boulder with coarse blebs of pyrrhotite was found at the base of the Spy Sill, 2.7 kilometres southeast of the Spy Showing. This boulder contained 0.3% Ni, 0.4% Cu, 0.4 g/t Pt and 0.7 g/t Pd.

Several pyrrhotite-magnetite horizons occur between the Spy Sill and the base of the Nikolai basalt. One magnetite horizon is up to 10 metres thick, while pyrrhotite horizons are up to four metres thick. A four metre thick pyrrhotite horizon discovered in 1995 was named the Claimpost Showing. This pyrrhotite body, hosted within silicified siltstone, is capped by gabbro and magnetite. Minor magnetite and chalcocopyrite occur with the pyrrhotite. Chip samples across the horizon contain 0.1 to 0.3% Cu and anomalous Co (330-640 ppm). The maximum Ni value from these samples is 520 ppm. Pt and Pd are not anomalous. It is not clear whether these horizons represent skarn-type mineralization or are a type of syngenetic iron formation. However, common skarn minerals such as garnet, epidote and clinopyroxene are not present in sediments adjacent to the pyrrhotite-magnetite bodies. The sediments are locally highly silicified, probably due to the presence of numerous Maple Creek Gabbro sills. Most of the pyrrhotite-magnetite horizons are not in contact with gabbro sills. The 10-metre thick magnetite horizon abruptly changes to a thinner pyrrhotite-rich zone. No bedding is visible in either pyrrhotite or magnetite rich horizons.

Exposure on the property is good at elevations above glacial sediments and valley filling talus fans, but the bases of the various peridotite intrusions are generally poorly exposed. The best exposed peridotite intrusion on the property is the Spy Sill. Even here, the base of the sill is relatively poorly exposed as mineralized marginal gabbro and massive sulphide lens weather recessively relative to the peridotite. A thin layer of fine talus was observed covering gossanous material at several places along the base of the sill; this makes locating sulphide mineralization difficult. Other intrusions such as the Duke Intrusion have almost no exposure at their basal contacts.

7.0 1997 WORK PROGRAM

Property work took place between June 14 and August 4, 1997, inclusive. The exploration crew was based at Burwash Landing Resort. Crew and equipment were flown to and from the property by helicopter from Burwash Landing Resort. A Bell 206 helicopter based in Haines Junction, operated by Trans North, was used during the project.

Exploration work carried out on the property in 1997 consisted of geologic mapping, geochemical sampling, silt sampling, line cutting, ground magnetic and UTEM geophysical surveys. Details of the various surveys are given below.

7.1 Line Cutting

Twin Mountain Exploration Inc. was awarded the line cutting contract. A total of 12.3 line-kilometres of grid was established as control for geophysical surveys. Topography was used to locate a starting point for the grid. The baseline was established with a survey transit and slope corrected to maintain grid control and provide accurate spacing of cross lines. Cross lines were turned 90° from the baseline azimuth with the transit and sight pickets were established along the cross lines for control. Cross lines were not slope corrected.

7.2 Geology

Geological traverses were carried out in conjunction with ground follow up of airborne EM conductors. Location of conductors A, B, and C are shown on Figure 3. Geology depicted on the three 1:5,000 scale geology maps submitted with this report has been compiled from traverses carried out in 1995, 1996, and 1997 and GSC Open File Map 381. Mapping completed in 1997 is indicated in green.

Mapping was conducted north of Nines Creek valley (Map 3, Sheet 8) during ground evaluation of airborne conductor A. The trace of the airborne conductor was walked but no outcrop was visible due to the presence of thick overburden in Nines Creek valley. No source could be identified on surface for the airborne anomaly.

Ground investigation of airborne conductors B and C identified exposures of black, carbonaceous shale along strike of the trace of airborne conductors (Map 3, Sheets 3 and 10).

7.3 Geophysics

Ground electromagnetic (UTEM) and magnetic surveys were carried out over a grid designed to define a coincident magnetic and electromagnetic conductor identified in a previous airborne geophysical survey. A total of 11.3 line-kilometers were surveyed by ground geophysical methods. Surveyed lines, spaced 100 metres apart, are shown on Map 4. Magnetometer readings were collected at 12.5 metre intervals and UTEM data was recorded at 25 metre intervals along grid lines. The survey equipment, procedures and data are presented in Appendix 1 of this report. The interpreted conductive and magnetic sources are presented in Map 4 of this report.

7.3.1 Ground Magnetic Survey

A linear magnetic high is observed extending the full length of the grid. The magnetic anomaly shows more high frequency character at the western end of the grid which is interpreted to be due the presence of magnetic rubble in the talus at this end of the grid. The location of the central axis of the magnetic source is shown in Map 4. Magnetic modeling indicates that the depth to the top of the body varies from about 275 metres near the centre of the grid to over 300 metres at the eastern end of the grid. The modeling also suggests that the source is dike-like, having a thickness of no less than 50 metres and probably no more than 200 metres, and dips steeply to the southwest (approximately 75°). It almost certainly represents a westward extension of the ultra-mafic Spy Sill seen further to the east connecting to the Bock's Brook intrusion to the west.

7.3.2 UTEM Geophysical Survey

The UTEM survey failed to detect any discrete highly conductive targets on the grid. A short strike length anomaly on the four western-most lines is interpreted to be a fault due to its apparent shallow depth of burial and poor conductivity (UTEM channel 7). However, the UTEM survey did define a broad, moderately conductive zone (UTEM channel 3), generally extending to the southwest beyond the ends of the survey lines, underlying almost the full length of the grid. The southern edge of the zone appears to have been detected on lines 193+00E to 196+00E, where it is coincident with a contact between sediments and gabbro. This southern contact anomaly develops the characteristics of an anomaly due to a discrete conductor further to the east on lines 197+00E to 199+00E, although it is more likely that this may be an effect of increasing overburden thickness there. The broad conductive zone is not as deeply buried and has a much greater areal extent than the magnetic source. The conductor may represent a more conductive

lithological unit lying to the southwest of the sill or possibly a thick wedge of conductive overburden in the Nines Creek valley.

7.4 Geochemistry

All analyses discussed in the following sections were performed at Chemex Labs in North Vancouver, British Columbia. Rock and silt sample locations are shown on Map 3, Sheet 3.

7.4.1 Rock Geochemical Survey

Three rock samples were collected during ground evaluation of airborne conductor C to obtain metal values and chemically characterize rock units. Samples were pulverized with a jumbo chrome steel ring mill to -150 mesh and analyzed by one or more of the following methods: multielement inductively coupled plasma (ICP) triple acid digestion (non-mineralized rocks), multielement inductively coupled plasma-atomic emission spectroscopy (ICP-AES) nitric-aqua-regia digestion (mineralized rocks), aqua-regia leach atomic absorption nickel analysis, and fire assay-ICP methods for precious metal analysis. Results are found in Appendix 3.

No anomalous base metal values were obtained in assay results. A sample of Maple Creek Gabbro (RX 331044) contains 64 ppm Ni, 94 ppm Cu, and 31 ppm Co. These results are consistent with the base metal chemistry of Maple Creek Gabbro as defined from previous work.

RX 331045, a sample of pyritic, siliceous float material locally contained up to 40% fracture-controlled sulphide mineralization. Pyrite is the dominant sulphide mineral, as assay results contained 15 ppm Cu, 35 ppm Ni, and 9.65% Fe. Gold and platinum-group-elements are below detection levels in the sample.

RX 331046 was collected from a carbonate and sulphide-bearing vein. The sample contains below-detection levels of gold and platinum-group-elements and low base metal values (45 ppm Cu and 35 ppm Ni).

7.4.2 Silt Geochemical Survey

A total of six silt samples were collected as part of ground follow-up of airborne conductor C. Silt samples were dried, sieved to -80 mesh, and analyzed by multielement nitric-aqua-regia leach ICP techniques. Precious metal analysis was performed by the ICP fluorescence package. Results are found in Appendix 5.

Silt samples contained up to 324 ppm Ni, 91 ppm Cu, 47 ppm Co, 10 ppb Pt, and 16 ppb Pd. The relatively low copper values suggest that the nickel may represent silicate nickel from olivine, rather than Ni-Cu sulphide mineralization. However, Pd values do appear elevated in comparison with samples collected in previous years. Geochemical results are believed to reflect the composition of a peridotite sill which outcrops north of the sampled area. No significant sulphide mineralization has been identified in the area.

8.0 CONCLUSIONS AND RECOMMENDATIONS

The trace of airborne conductor A was evaluated with ground magnetic and UTEM geophysical surveys. The discrete UTEM conductors correlate with fault projections and geologic contacts. The broad, moderately conductive zone is both shallower and wider than the magnetic body. The conductive zone is unlikely to have the same source as the magnetic anomaly and is not interpreted to represent a significant accumulation of Ni-Cu sulphides.

Carbonaceous rocks are interpreted as the source for airborne conductors B and C, hence they are of no further interest.

No further work on the property is recommended.

9.0 PERSONNEL

Names and addresses of Inco Limited personnel who participated in fieldwork on the property in 1997 are listed below.

Katherine Hattie
Geologist
2207 E 56th Avenue, #6, Anchorage, Alaska, 99507

Barry Power
Geological Assistant
13 Putney Place, Mount Pearl, Newfoundland, A1N 4P2

Ed Johnson
Field Assistant
Box 28, Burwash Landing, Yukon Territory, Y0B 1V0

Patrick McGowan
Geophysicist
1002-1616 Pendrill Street, Vancouver, British Columbia, V6C 1S8

10.0 COST STATEMENT**10.1 AEM Conductor A (Sheet 8)****KLU 3122-KLU 3123****KLU 3221-KLU 3223****KLU 3321-KLU 3323****KLU 3421-KLU 3422**Personnel

K. Hattie (Geologist)	\$200/day	x	13 days	2,600
B. Power (Geological Assistant)	\$120/day	x	10 days	1,200
E. Johnson (Field Assistant)	\$100/day	x	1 day	100
P. MacGowan (Geophysicist)	\$400/day	x	3 days	1,200
V. Fisher (Draftsman)	\$200/day	x	3 days	600
Personnel Total				5,700
Meals	\$37/man/day	x	38 man days	1,406
Accommodation	\$35/man/day	x	36 man days	1,260
Helicopter (Bell 206 Jetranger)	\$833/hour	x	32.2 hours	26,822.60
Line Cutting	12.1 line kilometers			5,000
UTEM and Ground Magnetometer Surveys	11.3 line kilometers			16,266.45
			TOTAL	\$56,455.05

10.2 AEM Conductor B (Sheet 10)

KLU 4412
KLU 4610

Personnel

K. Hattie (Geologist)	\$200/day	x	1 day	200
B. Power (Geological Assistant)	\$120/day	x	1 day	120
V. Fisher (Draftsman)	\$200/day	x	1 day	200
Personnel Total				520
Meals	\$37/man/day	x	2 man days	74
Accommodation	\$35/man/day	x	2 man days	70
Helicopter (Bell 206 Jetranger)	\$833/hour	x	1 hour	833
			TOTAL	\$1,497

10.3 AEM Conductor C (Sheet 3)**KLU 1810****KLU 1910**Personnel

K. Hattie (Geologist)	\$200/day	x	1 day	200
B. Power (Geological Assistant)	\$120/day	x	1 day	120
V. Fisher (Draftsman)	\$200/day	x	1 day	200
Personnel Total				520

Meals	\$37/man/day	x	2 man days	74
-------	--------------	---	------------	----

Accommodation	\$35/man/day	x	2 man days	70
---------------	--------------	---	------------	----

Helicopter (Bell 206 Jetranger)	\$833/hour	x	1.5 hours	1,249.50
---------------------------------	------------	---	-----------	----------

Analytical

Rock (preparation)	\$3.50/sample	x	3 samples	10.50
Rock (ICP)	\$9.00/sample	x	3 samples	27.00
Rock (Pt, Pd, Au)	\$13.50/sample	x	2 samples	27.00
Rock (Ni)	\$1.25/sample	x	1 sample	1.25
Sediment (preparation)	\$2.40/sample	x	6 samples	14.40
Sediment (ICP)	\$6.00/sample	x	6 samples	36.00
Sediment (Pt, Pd, Au)	\$13.50/sample	x	6 samples	81.00
Analytical Total				197.15

			TOTAL	\$2,110.65
--	--	--	--------------	-------------------

11.0 STATEMENT OF QUALIFICATIONS

I, Katherine Hattie, geologist, with business and residential addresses in Anchorage, Alaska, do hereby declare that:

1. I graduated from Mount Allison University, Sackville, New Brunswick, with a Bachelor of Science Degree in Geology in May of 1988 and an Honours Certificate in Geology in May of 1989.
2. I have practiced the profession of geology since 1989.
3. I personally supervised the work documented in this report.

Dated this 4th day of December, 1997, at Anchorage, Alaska.

Katherine J. Hattie

Katherine J. Hattie
Geologist

12.0 REFERENCES

- Bell, C., (1996):
Yukon Assessment Report on 1995 Geological and Geochemical Surveys on the Klu Property (115 G/2).
- Dodds, C.J. and Campbell, R.B. (1992):
Overview, Legend and Mineral Deposit Tabulations for Geological Survey of Canada Open Files 2188, 2189, 2190 and 2191.
- Geological Survey of Canada Open File Map 2188 (1992).
- Geological Survey of Canada Open File Map 381 (1976).
- Hulbert, L.J. (1997):
Geology and Metallogeny of the Kluane Mafic-Ultramafic Belt, Yukon Territory, Canada: Eastern Wrangellia - A New Ni-Cu-PGE Metallogenic Terrane. Geological Survey of Canada Bulletin 506.
- Keyser, H.J. (1987):
Yukon Assessment Report 92528 (115G/2).
- Read, P.B. and Monger, J.W.H. (1976):
Pre - Cenozoic Volcanic Assemblages of the Kluane and Alsek Ranges, Southwestern Yukon Territory, Unedited Report to accompany Geological Survey of Canada Open File Map 381.
- MacEy, M., McLoughlin, R.F. and Vincent, J.S. (1973):
Yukon Assessment Report 60154 (115G/2).

APPENDIX 1

UTEM & Magnetometer Surveys Logistics Report on the Klu Project

UTEM & MAGNETOMETER SURVEYS

Logistics Report

ON THE

KLU PROJECT

NINES CREEK AREA, N.T.S. 115G/2 CONGDON CREEK

YUKON TERRITORY

FOR

AMERICAN COPPER & NICKEL COMPANY LTD.

SURVEY BY

SJ GEOPHYSICS LTD.

November, 1997

REPORT BY
Zoran Dujakovic
Syd Visser P. Geo
SJ Geophysics Ltd.

TABLE OF CONTENTS

INTRODUCTION	1
DESCRIPTION OF UTEM SYSTEM.....	1
FIELD WORK.....	2
DATA PRESENTATION.....	3
APPENDIX I.....	1
STATEMENT OF QUALIFICATIONS	1
STATEMENT OF QUALIFICATIONS	2
APPENDIX II	3
LEGEND.....	3
APPENDIX III.....	4
PRODUCTION SHEETS	4
APPENDIX IV	5
A TIME DOMAIN EM SYSTEM MEASURING.....	5
THE STEP RESPONSE OF THE GROUND.....	5
APPENDIX V.....	6
DATA SECTIONS	6

INTRODUCTION

SJ Geophysics Ltd. was contracted by American Copper & Nickel Company Ltd., to conduct a large loop time domain electromagnetic (UTEM-3) and magnetometer survey on the Klu Project near Kluane National Park, Yukon Territory. The survey was completed between July 9th and July 13th, 1997.

The purpose of the survey was to search for massive sulfides and to aid in the mapping of local geology.

DESCRIPTION OF UTEM SYSTEM.

UTEM is an acronym for "University of Toronto ElectroMagnetometer". Dr. Y. Lamontagne (1975) developed the system while he was a graduate student of that University.

The following is a short description of the UTEM system used in the field. A paper (A time-domain EM system measuring the step response of the ground) by G.F. West, J.C. Macnae and Y. Lamontagne, giving a more complete description with an overview of interpretations is located in Appendix IV.

The field procedure consists of first laying out a large loop, which can vary in size from less than 100M X 100M to more than 2Km X 2Km, of single strand insulated wire and energizing it with current from a transmitter which is powered by a 2.2 kW motor generator. During a surface survey the lines are generally oriented perpendicular to one side of the loop and surveying can be performed both inside and outside the loop. For Borehole survey the sensor coil is placed down the borehole measuring the axial component of the electromagnetic field from a minimum of 2 separate loops.

The transmitter loop is energized with a precise triangular current waveform at a carefully controlled frequency (30.97 Hz for this survey). The receiver system includes a sensor coil and backpack portable receiver module, which has a digital recording facility. The time synchronization between transmitter and receiver is achieved through quartz crystal clocks in both units, which are accurate to about one second in 50 years.

The receiver sensor coil measures the vertical, horizontal, or axial magnetic component of the electromagnetic field and responds to its time derivative. Since the transmitter current waveform is triangular, the receiver coil will sense a perfect square

wave in the absence of geologic conductors. Electrical conductors who may be geologic or cultural in origin cause deviations from a perfect square wave. The receiver stacks any pre-set number of cycles in order to increase the signal to noise ratio.

The UTEM receiver gathers and records 10 channels of data at each station occupied. The higher number channels (7-8-9-10) correspond to short time or high frequency while the lower number channels (1-2-3) correspond to long time or low frequency. Therefore, poor or weak conductors will respond on channels 10, 9, 8, 7 and 6. Progressively better conductors will give responses on progressively lower number channels as well. For example, massive, highly conducting sulfides or graphite will produce a response on all ten channels.

FIELD WORK

The geophysical surveys were completed during the period of July 9th to 13th, 1997, which included four data acquisition and one demobilization day. The surveys were conducted under the supervision of the project geophysicist, Pat McGowan and the project geologist, Kathy Hattie. The geophysical crew consisted of John Ashenhurst (Technologist), Zoran Dujakovic (Geophysicist), Chris Gooliaff (Geologist) and Matthew Kowalczyk (Student).

The crew was flown by helicopter from Burwash Landing to the property every morning.

A GEM Systems GSM-19 portable high sensitivity proton magnetometer was used for the data acquisition. Diurnal variations were monitored using another GEM Systems GSM-19 portable high sensitivity proton magnetometer as base a station, which recorded at 30 seconds intervals. Magnetometer survey was performed at 12.5 m intervals along 100m spaced lines for a total of 11.275 Km.

Two UTEM receivers were used to survey from one transmitter setup to speed up the survey.

The surveys were completed July 12th, 1997 and the following day the crew was demobilized to Whitehorse.

DATA PRESENTATION

The Mag data are presented on the plan contour map of Total field magnetic, Plate G1.

The results of the UTEM survey are presented on 16 data sections (Appendix V).

Legends for the UTEM data sections are also attached (Appendix II).

In order to reduce the field data, the theoretical primary field of the loop must be computed at each station. The normalization of the data is follows:

a) For Channel 1:

$$\% \text{ Ch.1 anomaly} = (\text{Ch.1} - \text{PC}) \times 100 / \text{PT}$$

Where:

PC is the calculated primary field in the direction of the component from the loop at the occupied station

Ch.1 is the observed amplitude of Channel 1

PT is the calculated total field

b) For remaining channels (n = 2 to 9)

$$\% \text{ Ch.n anomaly} = (\text{Ch.n} - \text{Ch.1}) \times 100 / \text{Ni}$$

Where:

Ch.n is the observed amplitude of Channel n (2 to 9)

N is Ch1 for Ch1 normalized

N is PT for primary field normalized

I is the data station for continuous normalized (each reading normalized by different primary field)

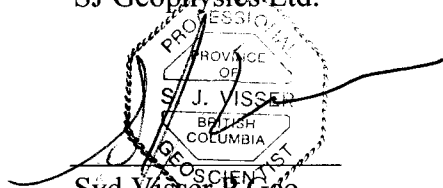
I is the station below the arrow on the data sections for point normalized (each reading normalized by the same primary field)

Subtracting channel 1 (Ch.1) from the remaining channels eliminates the topographic errors from all the data except channel 1.

If there is a response in channel 1 from a conductor then this value must be added to do a proper conductivity determination from the decay curves. Therefore channel 1 should not be subtracted indiscriminately.



Z. Dujakovic, Geophysicist
SJ Geophysics Ltd.



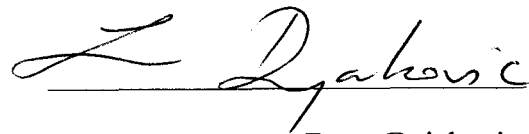
Syd Visser, P. Geo
S.J.V. Consulting Ltd.

APPENDIX I

STATEMENT OF QUALIFICATIONS

I, Zoran Dujakovic, of 7056 Waverley Ave., Burnaby in the Province of British Columbia, DO HEREBY CERTIFY:

- 1) THAT I am a graduate of the Belgrade University, Faculty of Mining and Geology - Geophysics Program with a Engineer of Geology degree in Geophysics.
- 2) THAT I have been engaged in mining and petroleum exploration since 1981.
- 3) THAT I am registered as a Engineer of Geology - Geophysics Program with the Chamber of Commerce of Serbia.



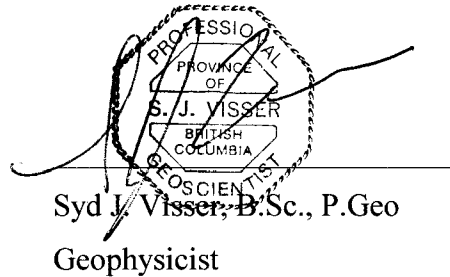
Zoran Dujakovic,

Geophysicist

STATEMENT OF QUALIFICATIONS

I, Syd J. Visser, of 11762 - 94th Avenue, Delta, British Columbia, hereby certify that,

- 1) I am a graduate from the University of British Columbia, 1981, where I obtained a B.Sc. (Hon.) Degree in Geology and Geophysics.
- 2) I am a graduate from Haileybury School of Mines, 1971.
- 3) I have been engaged in mining exploration since 1968.
- 4) I am a professional Geoscientist registered in British Columbia.



APPENDIX II

Legend

UTEM SYSTEM MEAN DELAY TIME		
Channel Number	Delay Time(msec)	Symbol
1	12.8	
2	6.4	\/
3	3.2	\/
4	1.6	□
5	0.8	∩
6	0.4	△
7	0.2	∇
8	0.1	×
9	0.05	△
10	0.025	◇

Base Frequency = 31 Hz

APPENDIX III

Production Sheets

Client : American Copper & Nickel Company Ltr Name : KLU PROJECT
Survey : UTEM & Mag N.T.S. : 115 G/2 Congdon Creek
Latitude : 61-11 N Longitude : 138-48 W
Survey Dates : 09/07/97 - 13/07/97 Magnetic Delineation : 26-05.5E (1997)
Project Geophysicist : Pat McGowan (PM) UTM's : NAD 83, GZD : 7 V
Project Geologist : Kathy Hattie (KH) Start Point - GRID : 19500E/10200N 1492m (altimeter), xxxx ft (map)
Inco Crew : Barry Power (BP) GPS #1 : 617227 6784530 1582m (300 readings)
Edward Johnson (EJ) GPS #2 : 617311 6784675 1539m (300 readings)
SJGL Crew : John Ashenhurst (JA) Start Point - UTM'S : 617267 6784602.5 1500m, 4921.26 ft
Zoran Dujakovic (ZD)
Matthew Kowalczyk (MK)
Chris Gooliaff (CG) Note : Elevations to be converted to feet for topo maps
Location : Nines Creek area, Yukon Territory
St. Elias Mountains, Klauane Range, Klauane Game Sanctuary (chopper access only)

Dy	Date	Whatc	Lp	Line	From	To	Rx 91	Rx 13	Wire,	Comments	
	1997	hadid	Hoo4	#	(E)	(N)	CI 10	CI#1	Mag	Other	
We	09-07	utem	Acnc Klu	1	19500	10205	9500	705	ZD/CG	JA/ZD MK/CG PM/EJ KH/BP	sunny, occ. cloudy, mild, cool breeze, 8 out + equip. in 3, loads, (only) lp#1 in, back edge by chopper, all lines extended 150m to north, read ~ 5 lines of 16, fixed flat on ford
		utem		1	19600	9500	10204	704	ZD/CG		UTEM: DAY = 3579m, TOTAL = 3,579m
		utem		1	19700	10201	9800	401	ZD/CG		
		utem		1	19400	10210	9500	710		JA/MK	
		utem		1	19300	9450	10221	771		JA/MK	
		utem		1	19200	10238	9950	288		JA/MK	
Th	10-07	utem	Acnc Klu	1	20000	10200	9500	700	ZD/MK		sunny, warm, cool breeze, tried to call Ed in morn, talked to machine briefly, read ~ 7.5 lines, ~3.5 to go + mag
		utem		1	19900	9600	10201	601	ZD/MK		UTEM: DAY = 5320m, TOTAL = 8,899m
		utem		1	19800	10202	9500	702	ZD/MK		
		utem		1	19700	9525	9800	275	ZD/MK		
		utem		1	19200	9950	9500	450		JA/CG	
		utem		1	19100	9500	10250	750		JA/CG	
		utem		1	19000	10250	9500	750		JA/CG	
		utem		1	18900	9500	10255	755		JA/CG	
		utem		1	18800	10262	9925	337		JA/CG	
Fr	11-07	utem	Acnc Klu	1	18800	9925	9500	425	ZD/MK	CG JA	overcast, cool, windy, called Ed in am, got grid file up to date, CG did mag all day with a bad cable - all data NFG - practice run
		utem		1	18700	9500	10243	743	ZD/MK		UTEM: DAY = 2586m, TOTAL = 11,485m PROJECT TOTAL = 11.485 km
		utem		1	18600	10218	9500	718	ZD/MK		MAG: DAY = 0 m, TOTAL = 0 m
		utem		1	18500	9500	10200	700	ZD/MK		

Sa 12-07	Mag	Acnc						ZD/MK	overcast, occ. sun, windy, cool, picked up lp, all mag complete, PM dif'l
	Mag	Klu	20000	10200	9600	600	CG	BP/JA	GPS'd lp corners, other points, base sta.'s mem. filled some data didn't
	Mag		19900	9600	10200	600	CG		process, JA on data, called Ed & Syd in eve, Syd out
	Mag		19800	10200	9525	675	CG		MAG: DAY = 11275.m, TOTAL = 11,275 m
	Mag		19700	9525	10200	675	CG		
	Mag		19600	10200	9500	700	CG		
	Mag		19500	9500	10200	700	CG		
	Mag		19400	10225	9500	725	CG		
	Mag		19300	9500	10225	725	CG		
	Mag		19200	10225	9500	725	CG		
	Mag		19100	9500	10250	750	CG		
	Mag		19000	10250	9500	750	CG		
	Mag		18900	9500	10250	750	CG		
	Mag		18800	10250	9500	750	CG		
	Mag		18700	9500	10250	750	CG		
	Mag		18500	10200	9500	700	CG		
	Mag		18600	9500	10200	700	CG		
Su 13-07	demob	Acnc						JA/ZD	mainly sunny, windy, mild, finished computer stuff by early aft, gave PM 3
		Klu						MK/CG	discs, drove to Whitehorse.

APPENDIX IV

A time domain EM system measuring the step response of the ground

A time-domain EM system measuring the step response of the ground

G. F. West*, J. C. Macnae*‡, and Y. Lamontagne‡

ABSTRACT

A wide-band time-domain EM system, known as UTEM, which uses a large fixed transmitter and a moving receiver has been developed and used extensively in a variety of geologic environments. The essential characteristics that distinguish it from other systems are that its system function closely approximates a step-function response measurement and that it can measure both electric and magnetic fields. Measurement of step rather than impulse response simplifies interpretation of data amplitudes, and improves the detection of good conductors in the presence of poorer ones. Measurement of electric fields provides information about lateral conductivity contrasts somewhat similar to that obtained by the gradient array resistivity method.

INTRODUCTION

This article describes the design of the UTEM system and its development at the Geophysics Laboratory of the University of Toronto by Y. Lamontagne and G. F. West from 1971 to 1979. UTEM is a wideband, time-domain, ground EM system with a step-function system response. It was designed to try to achieve the sensitivity and interpretability necessary to handle problems of deep exploration, conductive environments, and a variety of terrain conditions, in an economically viable manner. As with most EM systems, effective exploration for massive sulfide ores was the principal objective. The method was conceived in 1971, and the first UTEM I instrument was operational in 1972. It was an analog electronic system, and was used in a number of surveys which have been described by Lamontagne (1975). An improved UTEM II which incorporated a digital recording system was then designed and constructed at the University of Toronto with financial aid from a consortium of mining companies. It was first used in 1976. To fall 1980, about 1000 line-km had been surveyed with the system from 144 loops in 35 areas. UTEM III, which is a microprocessor-controlled system with expanded capabilities, is now produced commercially by Lamontagne Geophysics Ltd. Some of the field results obtained using the UTEM II system have been described in Lamontagne et al. (1977, 1980), Macnae (1977, 1980, 1981), Lodha (1977), and Podolsky and Slankis (1979). Data from all

three UTEM systems are identical insofar as geophysical characteristics are concerned. The differences affect only data noise levels and operational convenience. Some of the noise rejection features of UTEM III are discussed by Macnae et al. (1984).

THE UTEM SYSTEM

Design philosophy

UTEM uses a large, fixed, horizontal transmitter loop as its source. The field of the loop is mapped in the quasi-static zone with the receiver system; the vertical component of the magnetic field is always measured, and in some circumstances the horizontal magnetic and electric field components may be measured as well (Figure 1). The size of the transmitter loop depends on the prospecting problem; loops may range from about 2 km × 1 km in resistive terrain to 300 m × 300 m in a conductive area. Lines are typically surveyed to a distance of 1.5 to 2 times the loop dimensions.

The large loop transmitter-field mapping receiver configuration was chosen in order to give the system the deepest possible exploration for orebody sized conductors, without sacrificing the ability to resolve shallower structures (depth < 50 m). This dictates a very large transmitter moment, and makes an extended source desirable. The virtue of an extended source is that the coupling between the source and a receiver or the source and a nearby conductive zone is not so many orders of magnitude larger than the coupling to a distant receiver or deep target as is the case with a confined source.

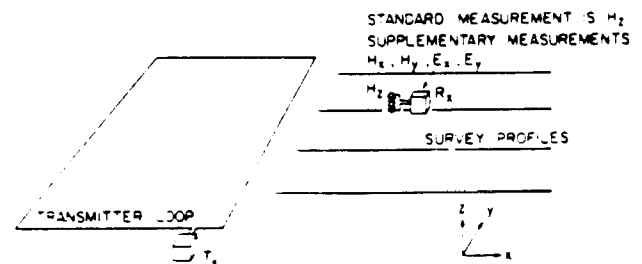


FIG. 1. Schematic layout of a UTEM survey.

Manuscript received by the Editor November 1983; revised manuscript received December 1983.

*Geophysics Lab., Dept. of Physics, Univ. of Toronto, Ont., Canada M5S 1A7.

‡Lamontagne Geophysics, 740 Spadina Ave., Toronto, Ont., Canada M5S 2J2.

© 1984 Society of Exploration Geophysicists. All rights reserved.

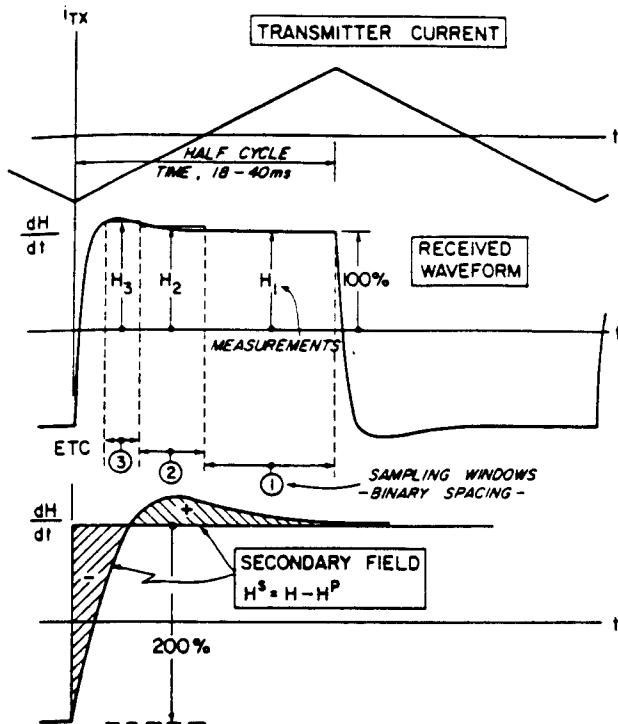


FIG. 2. Transmitted and received UTEM waveforms. Note that the measurement channels are numbered from the latest to the earliest. Sampling is repeated, with due regard to sign, in every half-cycle.

Given a large transmitter and a large T_x - R_x separation, it is inevitable that induction in extensive conductive overburden and in large formational conductors will contribute more to the response than with a small scale system. Also, as the separation becomes larger it becomes increasingly likely that the system will be responding to several nearby conductors at once. However, a fixed transmitter-moving receiver system offers a basis for separating the signal contributions from the various conductors and resolving the geometry of deep-seated conductors. At any time instant, the magnetic field of the current system induced in the ground is a potential field (within the quasi-static zone), and if it is mapped on a profile or over a surface, there is a firm theoretical basis for separating it into parts and estimating the current systems which caused it. When the transmitter and hence the eddy current system move for each observation, it is more difficult to find a theoretical basis for stripping of responses into component parts.

There are negative aspects to using a fixed transmitter method. In addition to the aforementioned enhancement of anomalies due to formational conductors, the transmitter can be positioned badly for induction in small plate-like conductors, and a large good conductor can screen a smaller, shorter time-constant conductor which lies behind it. For these reasons it may be desirable to have survey coverage from more than one transmitter location.

The UTEM II transmitter passes a low-frequency current of precise triangular waveform through the transmitter loop. The magnetic field is sensed with a coil, which responds to the time

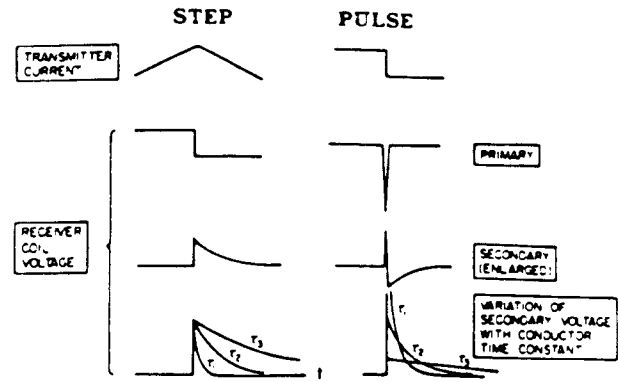


FIG. 3. Comparison of transient signals in step and pulse type systems.

derivative of the local magnetic field, so in "free space" a precise square-wave voltage would be induced in the receiver. In the presence of conductors the waveform is substantially distorted. The UTEM receiver measures this distortion by determining amplitudes at 10 delay times (actually, averages over time windows) which are spaced in a binary geometric progression between the waveform transitions. The sample scheme is shown in Figure 2. Note that the UTEM channel numbers are conventionally numbered in reverse order of time. This is because the latest time measurement often serves as a reference to which the other measurements are compared, whereas the number of earlier time measurements which can be made accurately may change if base period or instrument bandwidth is altered. The base frequency of the system is selectable, usually about 30 or 15 Hz (25 or 12.5 Hz in countries with 50 Hz power). A common practice is to set the base frequency (adjustable in 0.1 percent steps) about 0.5 Hz from a subharmonic of the power line in order that power line interference can be detected by slow beating in the data. The base frequency is usually set low enough that all ground response has nearly vanished by the end of the half-cycle. When this is the case, the UTEM system determines the step response of the ground in the time range $25\mu\text{s}$ to 12.8 ms (30 Hz base frequency).

Time-domain systems

Time-domain systems have some advantage over frequency-domain systems in that simultaneous measurement is easier to achieve over the whole spectrum and, at the same time, it is possible to check the phase synchronization of the transmitter and receiver time bases. Most time-domain systems employ an on-off type of transmitter current and confine all measurements to the off period, as this automatically separates the secondary from the primary field. However, when a coil is used as a sensor, the time derivative of the signal is observed. Thus, if the transmitter loop is energized with a step current, it is the impulse response of the ground which is observed.

When prospecting for conductive mineral deposits, it is generally more desirable for interpretation purposes to observe the step response than any other time response. The reason for this lies in the characteristics of eddy current decay. For the step

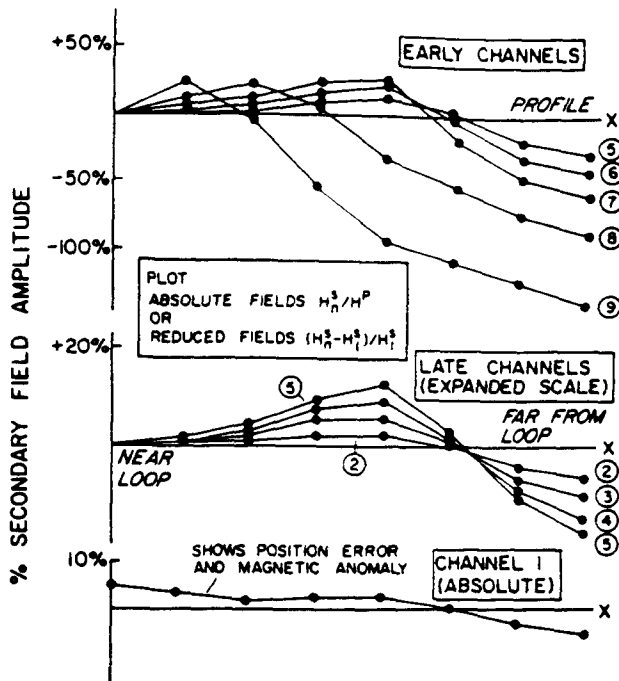


FIG. 4. Standard presentation of UTEM vertical component magnetic field data.

response, the early-time limit of response is identical to the frequency-domain inductive limit, and for a simple conductor in free space this is a function of geometry alone. For the impulse response, the early time limit is scaled from the step response limit by the inverse of the transient decay time constant (Figure 3). Thus, the decay rate must first be determined in order to interpret amplitude information in terms of geometry. This may present little difficulty in simple cases, but when complex or overlapping responses are observed it can be a serious problem. Also, even in the case of the step response, overburden anomalies which generally are of short time constant have early time amplitudes which are very much larger than the anomalies of target conductors with long time constant. Any further amplification caused by measuring the impulse rather than step response is clearly undesirable.

Although a system with a step response is usually desirable for interpretation purposes, the UTEM system is only one implementation of such a system. In fact a system using a magnetometer receiver with a square-wave transmitter instead of an induction coil (referred to as MSW system in the following sections) would have an identical system response. The foregoing rationale of the interpretational advantages of step response does not consider the other important factors which enter the design of actual systems such as signal-to-noise (S/N) efficiency and transmitter-sensor design constraints which in fact guide the choice of the actual transmitter waveform and sensor used. This is a complex topic discussed by Lamontagne et al. (1980). For example, the UTEM III system actually uses a modified triangular transmitter waveform and deconvolution in the receiver to improve its S/N performance but has a system response identical to the UTEM I and UTEM II systems (Macnae et al., 1984), i.e., a square-wave response. Thus the UTEM I/II systems, the conceptual MSW system, and the

UTEM III system all make identical measurements although they excite the ground differently. To avoid any confusion, discussions in this paper of actual induced current waveforms in the ground will be limited to the UTEM system with a purely triangular waveform and to the MSW system.

The sampling scheme of Figure 2 was chosen so that virtually all measuring time is utilized and time scaling of the measurements is permitted. In the frequency domain, inductive responses may be characterized by dimensionless parameters of the form

$$\theta_f = \sigma\mu\omega L^2,$$

which demonstrates that scale changes of conductivity, frequency or (length)² are equivalent to one another. The analogous parameter for the time domain is

$$\theta_t = \sigma\mu L^2/t.$$

In interpreting frequency-domain data, it is common to compare observed frequency response data with dimensionless model response data. This is convenient because it avoids the necessity of rescaling the model data for all frequencies and physical scale lengths that might be encountered in the field cases. The same sort of scaling is possible with time-domain data, but only if the system function of the apparatus is a pure discontinuity response. If this is not the case, for instance when the apparatus has a characteristic ramp shut-off time, model response curves cannot be rescaled in time to match field data as this would imply rescaling the shut-off time to a value different from that used by the apparatus.

To ensure that time scaling can readily be applied to data that have been sampled and averaged over a time window, it is also necessary that the window widths be proportional to time after the discontinuity. UTEM has such sampling. It should be noted that time scaling may only be applied to UTEM anomalous responses which are short enough so as to have vanished in the interval between the two successive transitions of the step which form the square wave.

Data presentation

Because the field intensity falls off rapidly with increasing distance from the transmitter loop, it is often desirable to normalize the secondary field observations in some manner. One suitable normalizing factor is the primary vertical magnetic field signal (H_1^3). If the positions of the transmitter loop and the receiver are known reasonably accurately, a calculated value of H_1^3 may be employed. If the ground response vanishes by late time, the channel 1 measurement is a direct measure of H_1^3 . Normal survey data plotting practice encompasses both procedures.

Figure 4 is an example of a standard plot of UTEM secondary vertical magnetic field data (H_1^3). Channel 1 is plotted as secondary field (Ch 1- H_1^3)/ H_1^3 (where H_1^3 is the calculated primary field) and all other channels are normalized to Ch 1 [(Ch n -Ch 1)/Ch 1] to correct for any position error in calculation of H^3 and also to remove the effect of induced magnetic anomalies (for further details see Lamontagne, 1975). The late channels on the example plot show a crossover type of anomaly, indicative of a concentration of (changing) induced current, as will be discussed. The amplitude variation with channel number indicates that these induced currents are decaying with

time. A small component of response appears to have persisted to Ch 1 and, for quantitative analysis, it should be remembered that the data reduction process will have caused subtraction of this amount from profiles of Ch 2-Chn. On the early-time channels, the migration of crossover location from one channel to another indicates that the secondary current flow at these times is not fixed in geometry, a characteristic which is indicative of an extensive conductor (here extensive overburden) rather than a localized conductor such as that responsible for the late time crossovers.

Since at any delay time, the secondary field is a potential field, interpretation of geometrically fixed current systems is best performed using absolute secondary fields normalized by the primary field intensity at a single point rather than continuously along the profile. Although only one case presented in this paper has this absolute or "point normalization," recent routine field practice is to point normalize all survey profiles exhibiting discrete anomalies, in order to simplify interpretation.

Horizontal magnetic field measurements may be made by

reorienting the receiver coil. Normalization is done using the vertical primary magnetic field (calculated or vertical Ch 1 measurement). Unfortunately, horizontal field measurements frequently suffer a somewhat higher noise level than vertical fields, due to the predominantly horizontal orientation of spheric interference.

The electric field waveform is, like the voltage from the coil sensor, a square wave if the ground is very resistive. It is distorted in much the same way as the coil signal when the ground is conductive. Electric field observations are usually plotted as E_i/E_T^p —the observed channel voltage between the electrodes divided by the maximum expected late time voltage between electrodes at the observation point in any horizontal direction, i.e., $E_T^p = (E_x^2 + E_y^2)^{1/2}$. "Expected" here refers to the electric field produced by a loop on a laterally uniform, resistive half-space. This normalization facilitates intercomparison of x and y component data. The geologic noise level in electric field data is usually high, so plotting on expanded scales is rarely justified. All channel data are usually plotted on the same axes, as shown in Figure 5.

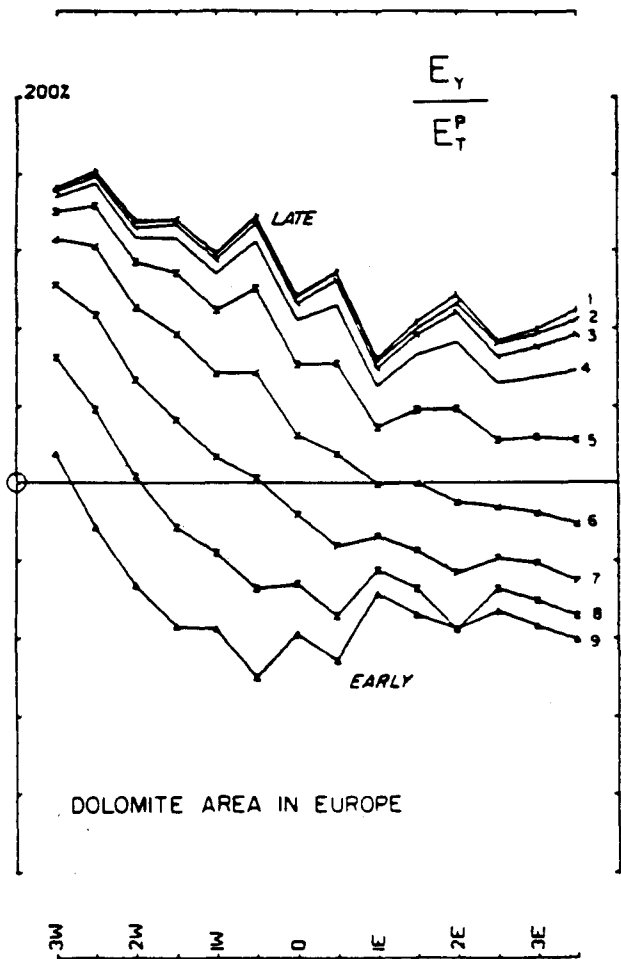


FIG. 5. Standard presentation of electric field data. The observed component is normalized to the total primary electric field of the transmitter loop.

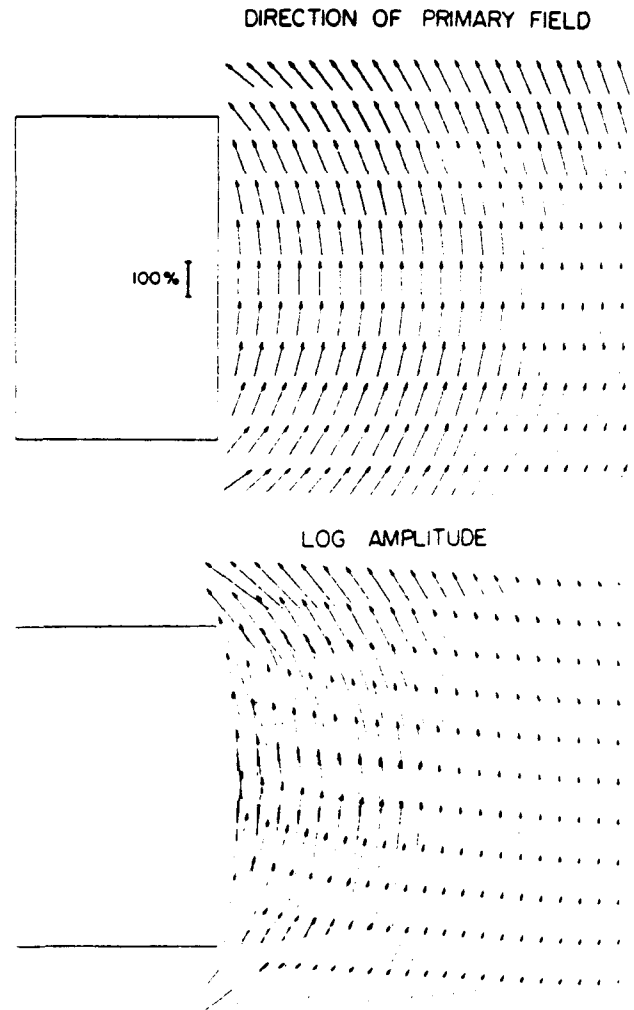


FIG. 6. Vector plots of late time electric field. (a) Direction information only. (b) Showing direction and intensity of the primary field.

The reference state for electric field data is usually described as a "laterally uniform, resistive half-space," rather than free space. By resistive is meant a case where all inductive transients have died out. The free-space electric field of a horizontal loop is horizontal, so introduction of a resistive half-space does not affect the field. However, for any other orientation of the transmitter loop or the earth-air interface, the free-space electric field will be directed across the interface and a strong distortion of the field will occur. Since the conductivity of air is virtually zero, the earth-air interface almost always has a high conductivity ratio, even if the earth is resistive in terms of induction. The charge which arises on the interface essentially doubles the vertical component of the E field in the air near the boundaries and annuls the vertical component in the ground. Thus the E field in the ground is (almost always) virtually horizontal. The nomenclature for the reference state serves to remind one that the earth-air interface has an important role in the physics of

the electric field and is always assumed to be present, but no lateral inhomogeneity or induction is permitted in the reference model.

The electric field of a heterogeneous, conductive earth does not normally become constant at late time, as the EM transients vanish. At the same time, the rate of change of magnetic field becomes constant. However, the observed late-time E limit is usually found to be different from the free-space or uniform resistive half-space value, due to lateral inhomogeneity of the earth's conductivity structure. The late-time electric field around a loop greatly resembles what might be seen in a gradient resistivity survey. The field weaves about, deflected around the more resistive areas and through the more conductive ones. A vector display of the late-time E field is an interesting reflection of the *relative* conductivity of various parts of the ground. It is impractical to plot the unnormalized E vectors, since the true field intensity falls off rapidly with increasing distance from the loop. The lengths of the plotted vectors are therefore proportioned to the normalized field of the loop, as for profile plots. Vector plots of the free-space field of a loop are shown in Figure 6. Examples of field data are given in the following section.

Errors caused by the presence of EM noise or by poor geometrical control are discussed for the magnetic (H) field case in Lamontagne (1975). For the electric (E) case, details of the measurement and sources of error are discussed in appendix G of Macnae (1981). As in the dc resistivity method, topographic features can seriously distort local electric fields, and local conductivity contrasts such as overburden patches and minor lithological changes can have quite large effects on the amplitude of measured E fields.

INTERPRETATION

We shall describe briefly the responses from a number of simple geologic models and how these can be identified and interpreted.

Layered earth responses

The problem of EM induction in a layered earth is very well treated in the literature, particularly for frequency-domain systems (e.g., Wait, 1962). Time-domain cases have also been studied for some specific problems, for example the infinite thin sheet was solved by Maxwell (1891) and the half-space response is discussed by Nabighian (1979). A general, layered earth solution for UTEM geometry and waveforms was given in Lamontagne (1975). Figure 7 shows three examples of computed responses for different layer conductivities. Figure 8 shows three examples of a thin layer at different depths. There are several common characteristics of layered earth responses. The shapes of the anomalous profiles are generally similar, becoming broader at later times. The migration of crossovers with time, with positive lobes toward the loop and negative lobes away from the loop, seems to indicate that the induced current system is migrating away from the loop. This is the type of behavior described by Nabighian (1979) as an expanding smoke ring.

If the UTEM system employed a magnetometer as receiver and a square current waveform in the transmitter, the smoke ring analogy would be exact, as the crossovers would indicate

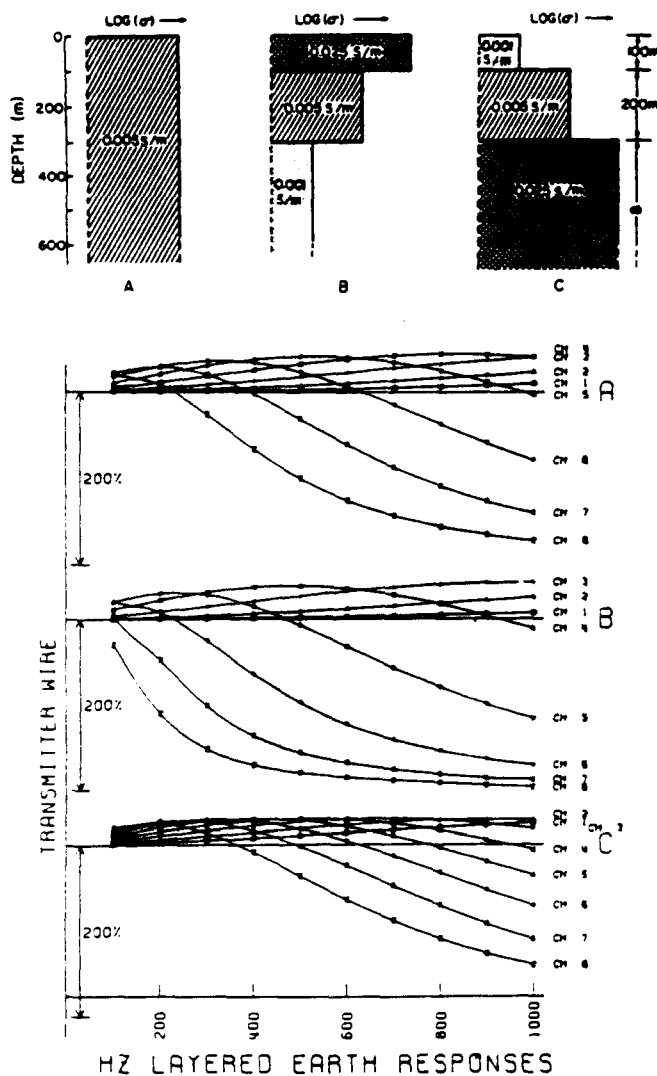


FIG. 7. UTEM layered earth response.

the position of the main current concentrations. However, the UTEM receiver is a coil which is sensitive only to dH/dt , and thus to the rate of change of induced and transmitter loop current. Thus the moving pattern of crossovers is actually indicating outward migration of changes in the induced current pattern. Toward the end of each half-cycle, the induced current system at any point in the survey area tends to a constant value, as indicated by the electric field measurements, but this steady current is invisible to the coil receiver.

When interpreting UTEM magnetic field data, it can often be simpler to think of the data in terms of the magnetometer receiver, square-wave transmitter current (MSW) analogy. Because the analogy is *exact* for a linear process like EM induction, there is no approximation in using it. It is very convenient to think of the field measurements of secondary signal at any delay time as describing the Biot-Savart magnetic field of a changing and decaying (analogous) induced current system. However, when electric field data are being analyzed and compared with magnetic field (dH/dt) data, it is necessary to revert to the true picture of the induced currents (or take a time derivative of the E data) to maintain a consistent relationship. UTEM magnetic field data are usually symbolized as H_{zi}^p (alphabetic subscript = component direction, superscript = p primary, s secondary, T total, numeric subscript = channel number) to accord with the magnetometer analogy; and in most discussions of simple induction, it is the time history of the *analogous* induced current which is described.

An important feature of layered earth H_z^p data is the early-time limit of continuously normalized H_{zi}^p/H_z^p data. If the ground is sufficiently conductive near the surface, the early-time secondary field data at points remote from the transmitter loop will approach -200 percent; i.e., one finds that the voltage in the receiver coil has had insufficient time to change from the steady value attained at the end of the previous half-cycle (Figure 2). This situation may be pictured in the magnetometer-square wave current analogy as an induced current system forming near the surface of the ground under the transmitter loop such as prevents the total (analogous) magnetic field from entering into the ground anywhere except very close to the transmitter wire. The -200 percent anomaly thus represents response at the inductive limit.

Finite thin plate in free space

A convenient modeling method for thin finite plate conductors in free space is the integral equation solution of Annan (1974). Annan computed the best set of polynomial eigenpotentials of order 4, and used these to represent the induced current flow in the plate as a sum of 15 "eigencurrents." The solution for the eigencurrents themselves is quite complicated, but needs only to be done once for a plate of given width to length ratio. After that, any induced current system can be described in terms of 15 coefficients in the eigenpotential summation. The secondary field at a receiver can then be simply computed in terms of these induced eigencurrents. One great advantage of Annan's method is that each eigencurrent has a frequency or time-domain response identical to a simple loop circuit. Thus the solution for a broad frequency range or many time windows is very easy to calculate. Routines for simple, interactive application of Annan's algorithms to a number of EM systems have been programmed by Dyck (Dyck et al., 1980).

Examples of type curves generated with Annan's solution may be found in Lodha (1977) and Lamontagne et al. (1980). Figure 9 shows the results of a set of computed UTEM type curves for the geometry shown in Figure 10. Also shown in Figure 10 is the geometry of the primary magnetic field, which controls the nature of induction in the plate. For the zero dip case, the primary field is mostly perpendicular to the plate. The induction in the plate tends to cancel this field at early times, leading to a negative H_z anomaly directly over the plate. Positive shoulders on each side show the secondary magnetic field of the "forward (analogous) current" near the front edge of the plate nearest the loop and the "reverse current" near the rear edge. The normalization scheme used in plotting this data is to divide the total secondary field by the calculated primary field at the measuring point. It has the undesirable effect of making asymmetric a secondary anomaly that is symmetric in terms of absolute amplitude by increasing the relative amplitude away from the loop. In fact, the absolute secondary amplitude of the positive shoulder near the loop is usually larger than the one on the side away from the loop. As the dip of the plate is increased, the positive shoulder moves away, and by the time a 30-degree dip is reached the reverse crossover is off the end of the plotted line. From dips of 30 to 135 degrees, the anomaly maintains a basic shape in the form of a simple crossover. The amplitude

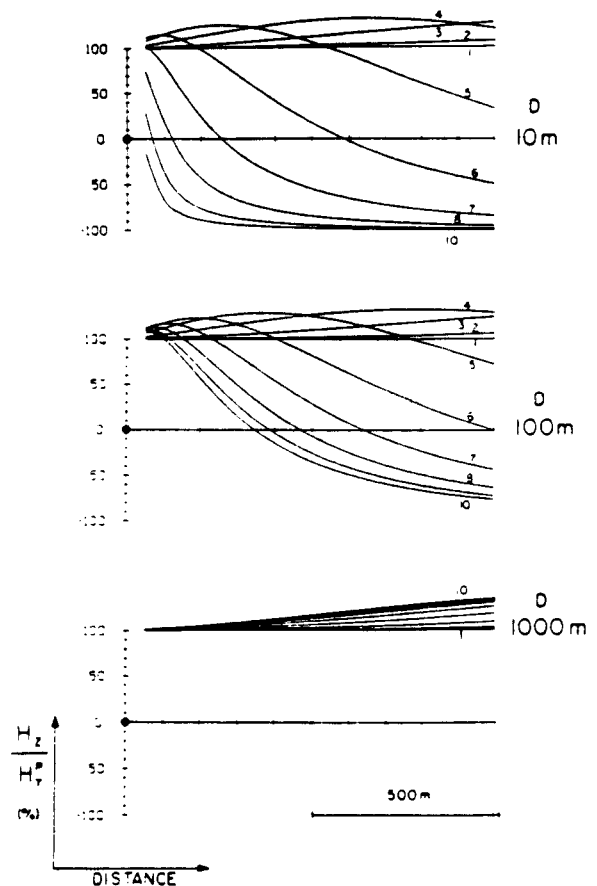


FIG. 8. H_z response of a thin horizontal sheet at various depths. The conductivity-thickness of the sheet is 2 S. The front of the transmitter loop is at the origin of coordinates.

does vary somewhat, however, being controlled by the primary field component normal to the plate which becomes a smaller and smaller fraction of the total field as the plate rotates from 30 to 150 degrees (Figure 10). The case at a dip of 150 degrees shows a very interesting behavior. The primary field can be seen to be *down* in the upper half of the plate and *up* in the lower half. The result of this is that the anomaly changes location and amplitude dramatically. For a very small plate, an anomaly could conceivably disappear completely. This phenomenon has been discussed by Bosschart (1964) for the Turam

method. For a large planar conductor, however, an anomaly is always present since a curving primary field must cut it somewhere, except in the special case when a vertical conductor is located directly under the center of a horizontal transmitting loop. The 165-degree dip case of Figure 9 shows a clear reverse crossover on the edge of the conductor far from the loop. The normal crossover is very small, due in part to the reduced induction at the near edge as shown in Figure 10, and also the large primary field used as a divisor for normalization.

The electric field anomaly generated by a plate conductor in

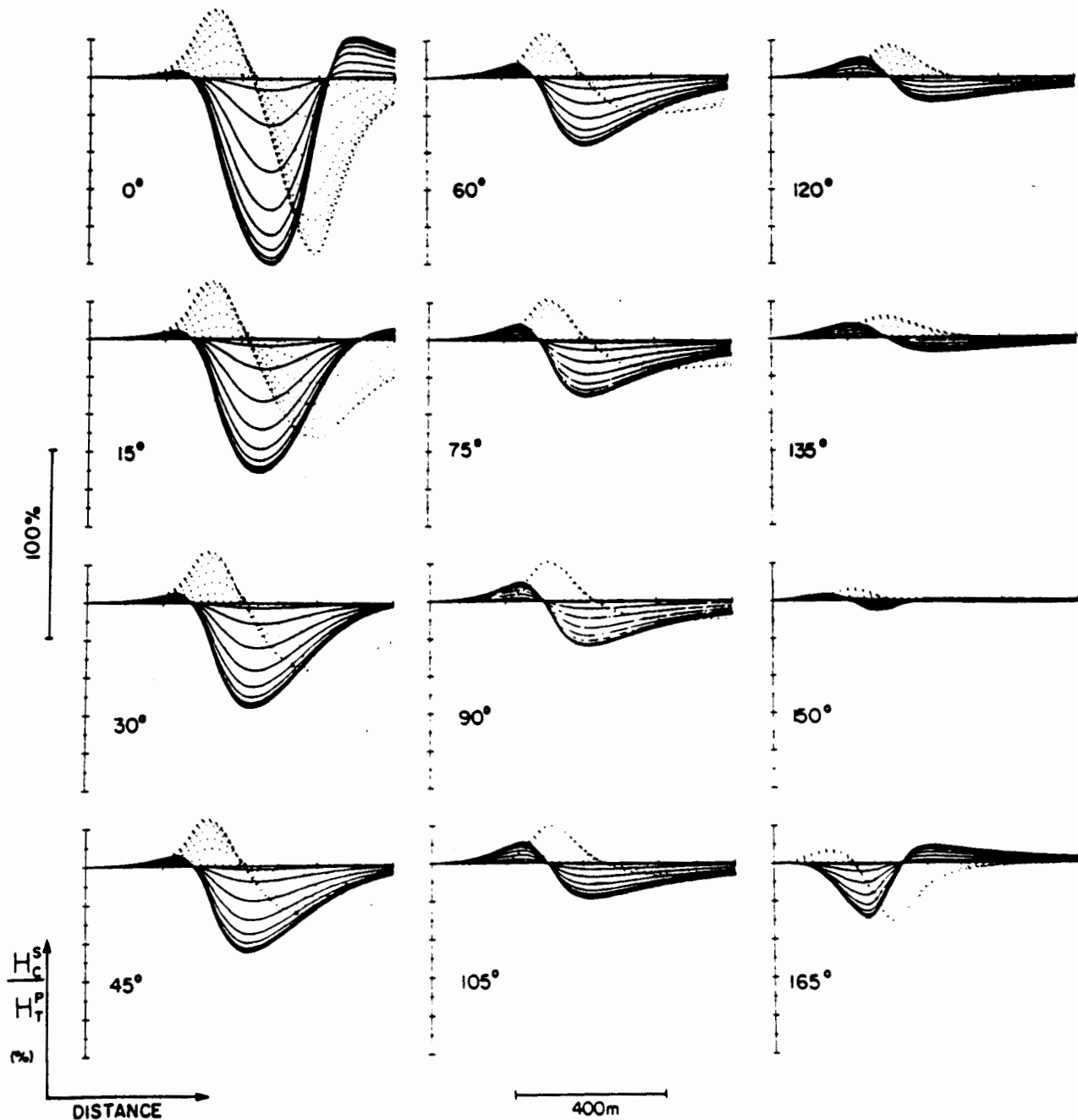


FIG. 9. UTEM H_z (solid) and H_x (dotted) profiles over a dipping plate (continuous normalization). (Geometry shown in Figure 10.)

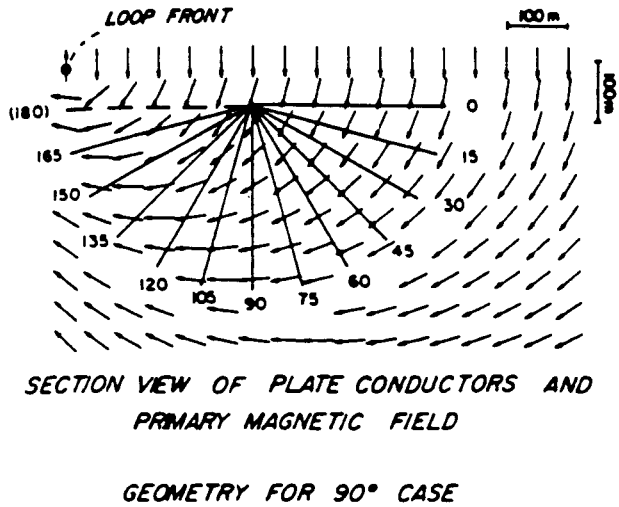


FIG. 10. Geometry and dimensions of the models shown in Figure 9. Also shown is the configuration of the primary field in the vicinity of the target conductor.

a resistive half-space is caused by charge on the plate as well as eddy currents flowing in it, and is affected by the earth-air interface. Annan's algorithm does not determine the charge distribution, so analog scale modeling methods were employed to produce type profiles. Figure 11 shows an example for a vertical plate. The longitudinal electric field is greatly reduced over the body at all times (i.e., there is a strong reduction in the late time limit). The dynamic (time-varying) part of the anomaly has the same time variation as the magnetic field but has a different geometrical pattern. The electric field is highly vulnerable to distortion by any conductivity contrast and the intensity of the static, late-limit anomaly over a conductor may therefore be reduced by any stratification between the conductor and the surface.

Other simple anomaly shapes

A set of simple schematic models is shown in Figure 12, for each of which the main features of the vertical magnetic field are sketched. The set of sketches was derived from quantitative scale model experiments by Lamontagne (1975). For the simple models illustrated where the host rock is completely non-conducting, the general anomaly shape for one body remains quite constant for the whole time range. The changes in anomaly from one channel to another are mostly in the amplitude and smoothness of the anomalies.

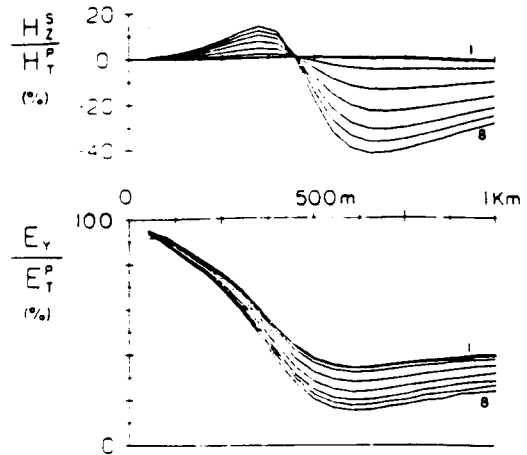


FIG. 11. Scale model UTEM secondary magnetic H_s and total electric E_s data over a vertical plate conductor.

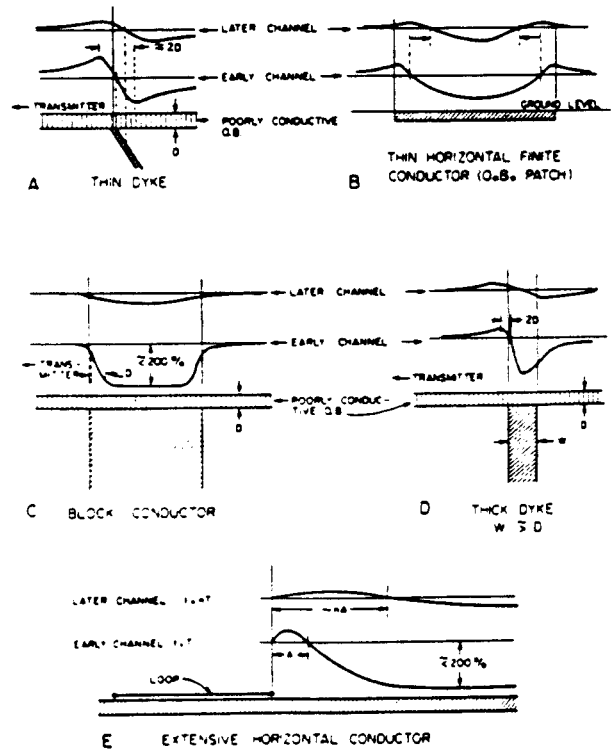
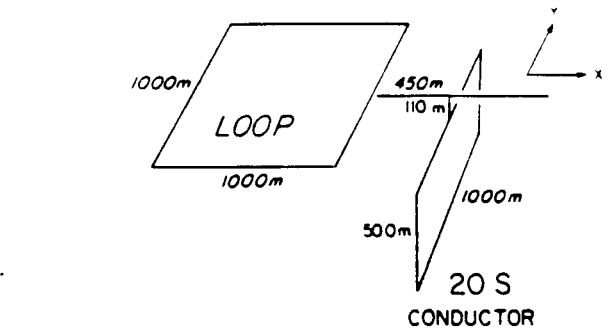


FIG. 12. The form of continuously normalized UTEM H_s anomalies over some simple shapes. All conductors are in free space.

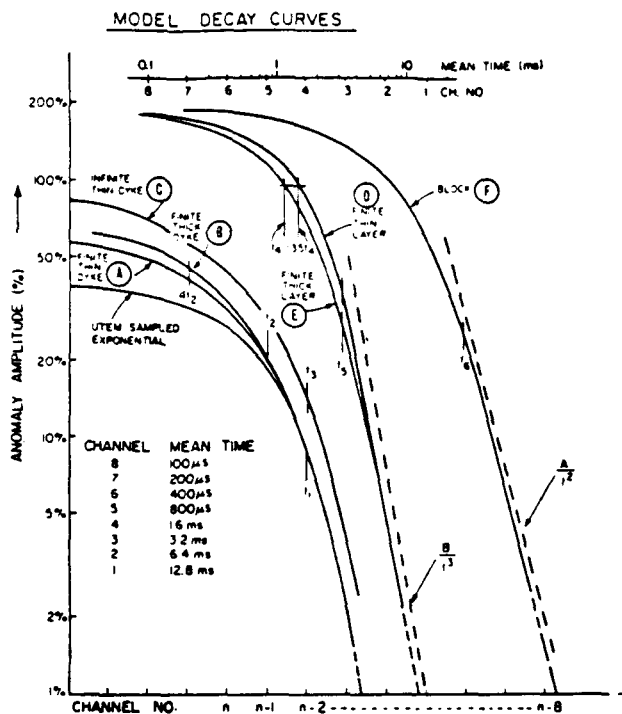


FIG. 13. The amplitude decay curves for the simple models of Figure 12. Mean sampling times are given for a base frequency of 30 Hz. The curve UTEM sampled exponential is a calculated function included for comparison. Lamontagne (1975) gives simple approximation formulas for interpreting target conductance from reference times t_1, \dots, t_6 determined by translational curve matching.

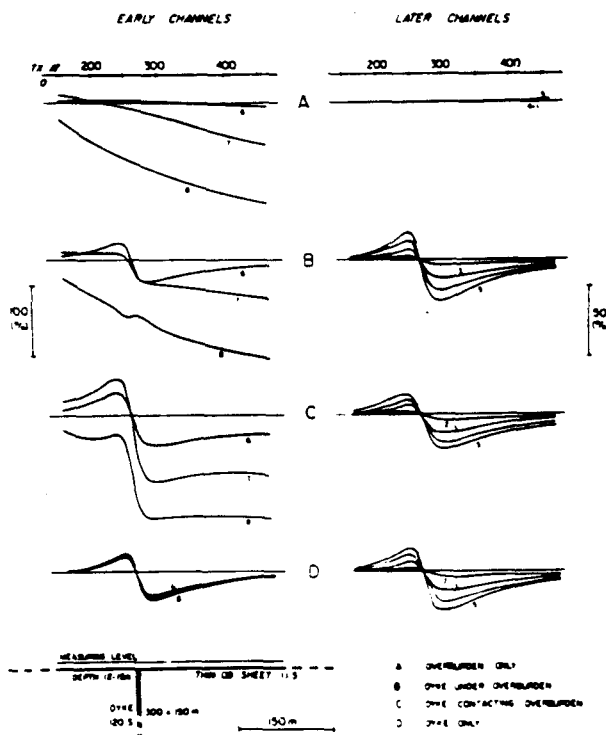


FIG. 14. Scale model UTEM H_z profiles over a conductive thin dike with overburden present.

Thin dike.—A conductive, steeply dipping body gives an H_z crossover shape similar to the plate model just discussed. The point where the anomaly changes sign indicates approximately the top edge of the conductor. The anomalies at later times tend to be broader and shifted slightly downdip from those at early times. The inductive decay rate of the anomalies will be discussed in a following section.

Surface horizontal finite conductor.—A thin horizontal conductor of limited dimensions (not extending under the loop) produces an anomaly consisting of a low over its central area, with large positive shoulders near its edge. The shoulders become rounded at later times and migrate towards the center of the conductor. Note that the thin horizontal plate shown in Figure 9 has a fairly deep location and thus the inward migration of the crossover points is less evident, although present.

Shallow block conductor.—This type of conductor produces a negative anomaly over its top having an amplitude of close to 200 percent at early times. An important characteristic of a block-like conductor is the absence of large positive flanking anomalies. The amplitude of the positive shoulders is less than 1/10 of the central negative, in contrast to the thin horizontal layer where the shoulders have amplitudes of order half the central negative. The sharpness of the crossovers at early time can be used as an indication of depth of burial. This type of anomaly is called a top anomaly and is due to a horizontal current pattern flowing around the top of the block.

Thick dike.—As might be expected, this is an intermediate case between a block and a thin dike where the width of a tabular body is of the same order as its depth of burial. In such cases the response is a combination of crossover and top anomaly due to vertical and horizontal current patterns, the top anomaly being more evident on the early-time channels and the crossover anomaly on later-time channels. The difference in decay rates results from the different scales of induced current flows, the top anomaly being controlled by the width of the dike, and the crossover by the depth extent.

Extensive horizontal conductors.—All the models with restricted lateral extent give rise to localized anomalies which simply change amplitude with time (approximately). The response of a very large conductor such as that shown in Figure 12e is included for comparison. In this case, the induced currents are not confined and they migrate horizontally with time.

Time response of simple free-space models.—Figure 13 shows example decay plots of log anomaly amplitude versus log time (channel number). The responses shown in Figure 13 are the UTEM sampled step responses that are only strictly valid for interpretation of actual field data when the observed anomalous response has effectively vanished at late times. Time scaling by lateral translation of the graphs is permitted for these cases, as previously discussed. The applicability of these time decays to interpretation is discussed by Lamontagne (1975), including the use of characteristic parameters to estimate conductance. A significant point to note is that simple induction in finite bodies eventually exhibits exponential decay at late time, whereas induction in infinite features takes the form of an inverse power law (Kaufman, 1978). Therefore, for models D, E, and F, the very late portion of the decay should ultimately show an exponential behavior if measured with sufficient sensitivity.

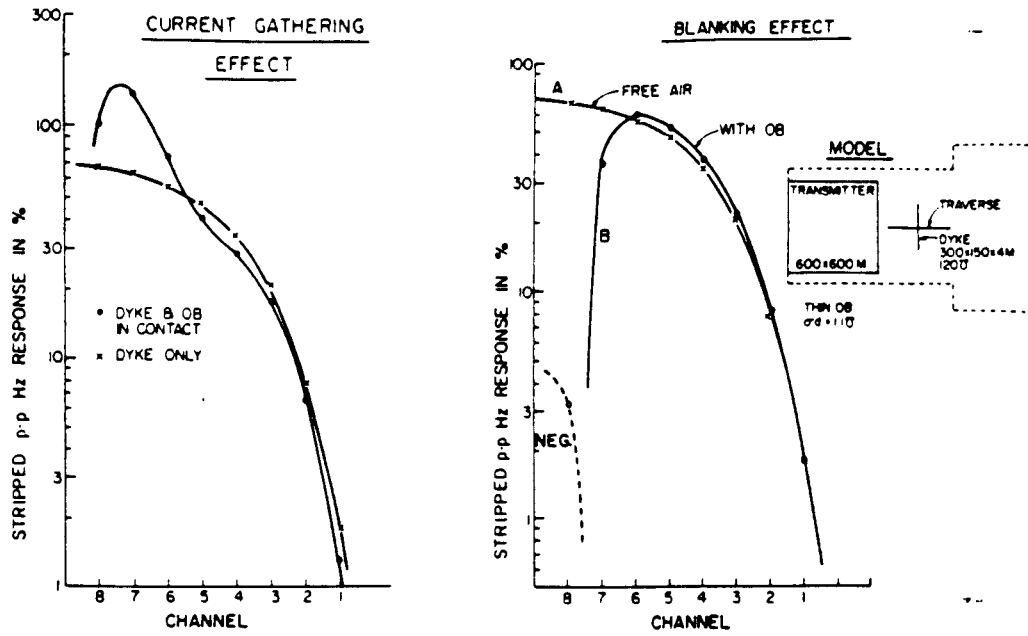


FIG. 15. Decay plots for the H_z^2 anomalies of Figure 14.

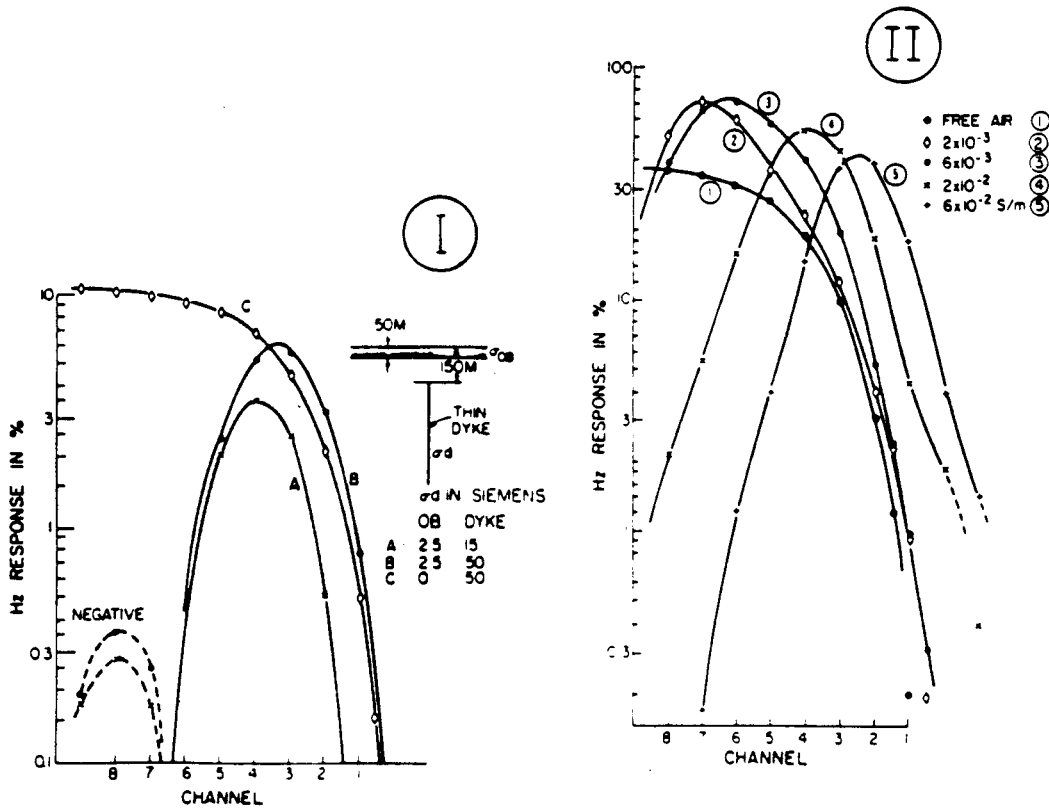


FIG. 16. Decay plots of H_z^2 anomalies over a thin dike (I) under a conductive overburden and (II) in a conductive half-space.

Overburden effects

We will restrict the discussion of overburden and host-rock effects to the case of a simple vertical finite dike conductive target, which was studied by Lamontagne (1975) using a scale model. Conductive overburden cover can modify the responses of underlying conductors in two main ways. Let us consider a dike target whose response in free space is given in Figure 14d. If overburden is now placed over this target conductor, the resultant response (Figure 14b) is not just the sum of the overburden and dike response. At early times it can be seen that there is very little response from the dike. This is because the magnetic field (MSW analogy) has not yet penetrated the overburden, and it leads to the name "overburden blanking" for this characteristic. At later times (Ch 6-1), when we can see from Figure 14a that the field has completely penetrated the overburden layer, the dike and overburden response (14b) is virtually indistinguishable from that of the dike alone (14d). The time decay pattern of the peak-to-peak amplitude of the crossover is plotted in Figure 15. It clearly shows the blanking effect of the overburden at early times (right-hand figure). The minute negative response at earliest time is present only when the

overburden extends under the loop, and appears to result from the complicated way in which the field first reaches the hidden target.

A second effect occurs when the dike is in conductive contact with the overburden. The results are quite different from those where the dike was not in contact (Figure 14c). In this case, regionally induced (analogous) current flow in the overburden has been "gathered" or "channeled" into the dike which is of higher conductivity. This accounts for the large-amplitude crossover anomalies at early times. Because the conductance of the dike greatly exceeds that of the overburden, the amount of current gathering is virtually independent of the dike's depth extent. The gathering effect at early times of just a "line conductor" remaining attached to the overburden after most of the dike was removed was found to be over 80 percent of that of the complete dike. At later times, when the (analogous) current flow in the overburden has migrated away (i.e., the real overburden current is no longer time-varying), the response is again almost identical to that of the dike alone. The time decay of the response is plotted on Figure 15, and in addition to the enhancement at early times a slight attenuation of the response at intermediate times can be seen.

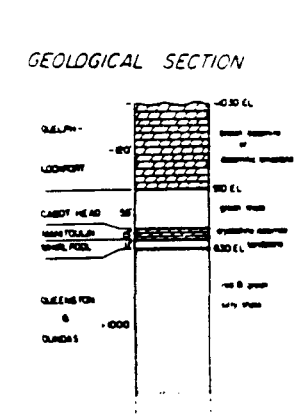
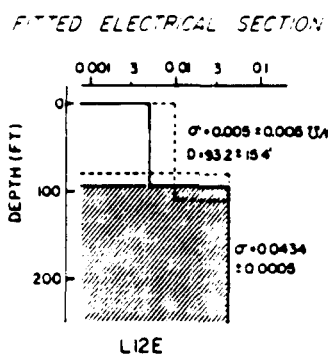
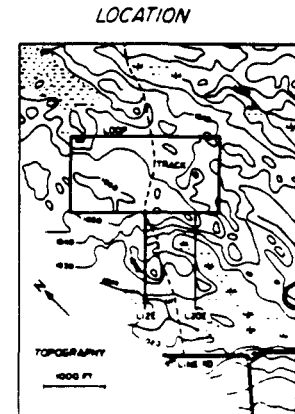
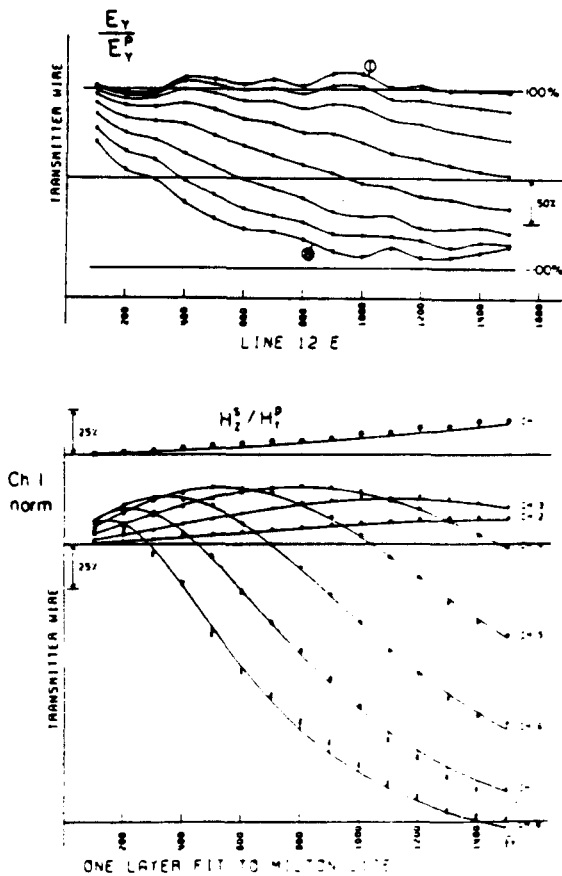


FIG. 17. Field example of E_y and H_z^2 data from a well-stratified earth. The electrical section was obtained from inversion of the H_z^2 data. The curves on the H_z^2 graph are the theoretical model; the points are the field data. The bottom axis is at -150 percent. The geologic section is from nearby gas drilling exploration.

Host rock effects

FIELD RESULTS

Figure 16 II shows the time variation in response of a 60 S vertical plate located in a half-space. The results were calculated by Lamontagne (1975) by Fourier transformation of the frequency-domain numerical modeling of Lajoie and West (1976). At early times the response is reduced from the free-air response: this corresponds to blanking by the conductive region above the target. At later times the response is enhanced indicating that the regional (analogous) current in the host rock is being gathered into the plate at these times. For poorly conducting host rock, the response at late times is close enough to the free-space response that simple interpretation of the target using a plate in free-space model is valid. For the higher host conductivities (case 4, 5) this is no longer the case.

Milton, Ontario

This area was surveyed to demonstrate what data from a conductive, well-stratified earth looks like. The area is one where 650 m of flat-lying Paleozoic sediments overlie the Precambrian basement. The predominant member of the stratigraphy is a uniform and thick sequence of shale. Other beds are mostly resistive calcareous and sandstone formations. The survey area is covered by a mixed forest and marshy streams, with occasional outcrops. The top of the bedrock is a dolomite formation which is everywhere more than 20 m thick. Topographic relief is minor (< 10 m), with occasional rough spots near outcrop. Overburden is probably less than 10 m every-

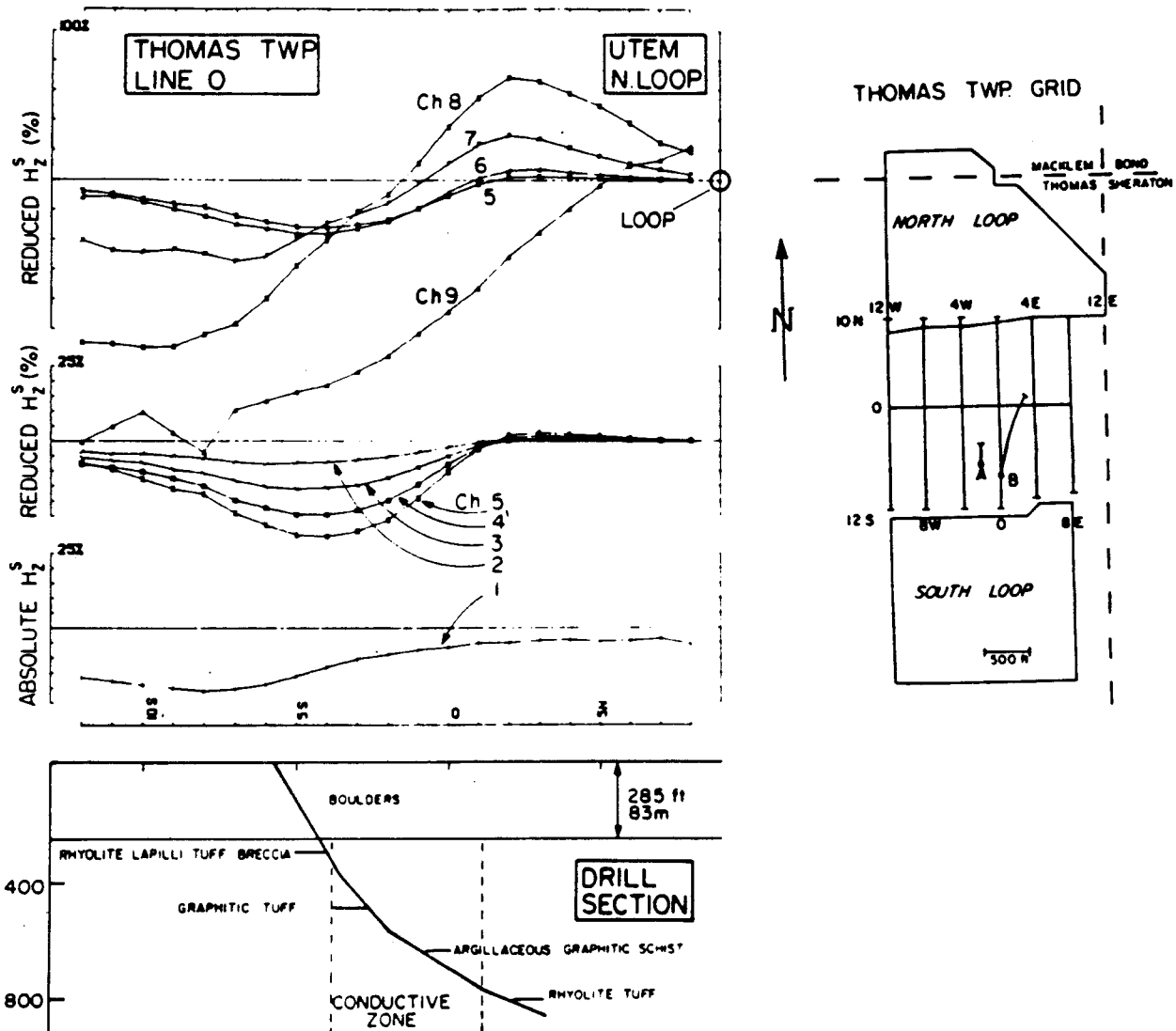


FIG. 18. A profile of H_2^S data from the north transmitter loop across the Thomas Twp test site. A map of the survey is included (different scale).

where and much less on average. It is mostly humus or thin glacial soil. Surface water is fresh, and likely quite resistive ($> 100 \Omega\text{m}$). Figure 17 shows some of the data with a layer and half-space model fitted to it by iterative minimization of squared error. Also shown is a stratigraphic section from a well a few kilometers distant. The dolomite layer is too resistive for its conductivity to be determined by data whose earliest time sample is at $100 \mu\text{s}$. (The survey was done with UTEM I.) At first glance, the data look just like that for any conductive earth, as the early-time data at the end of profiles have the usual strong negative anomaly, and there is a regular outward progression of crossovers as time progresses (decreasing channel number). However, the resistive surface layer does reveal itself in the limited approach of the early time curves to -200 percent anomaly. The convergence of E_z at late time to 100 percent of the primary field confirms the excellent lateral homogeneity of the site.

Thomas Township, Northern Ontario

This site has become an interesting test range for electrical methods, and a new grid has been cut and named the Night-hawk Lake geophysical test range. It is a graphitic zone that has many of the geometrical and electrical characteristics of a massive sulfide body. It is covered by 83 m of only moderately conductive overburden. It was found originally by airborne EM and has been intersected by two boreholes.

A UTEM II survey with 30 Hz base frequency was carried out on 6 lines of length 2200 ft and spacing 400 ft using transmitter loops to the north and south of the grid. Figure 18 shows a profile across the middle of the conductive zone.

At $50 \mu\text{s}$ (Ch 9), the regionally induced (analogous) current is only 500 ft from the loop. The field has not penetrated the overburden at the target site. From $100 \mu\text{s}$ to about $500 \mu\text{s}$ (Ch 8-6), a crossover response is observed over the target. At about

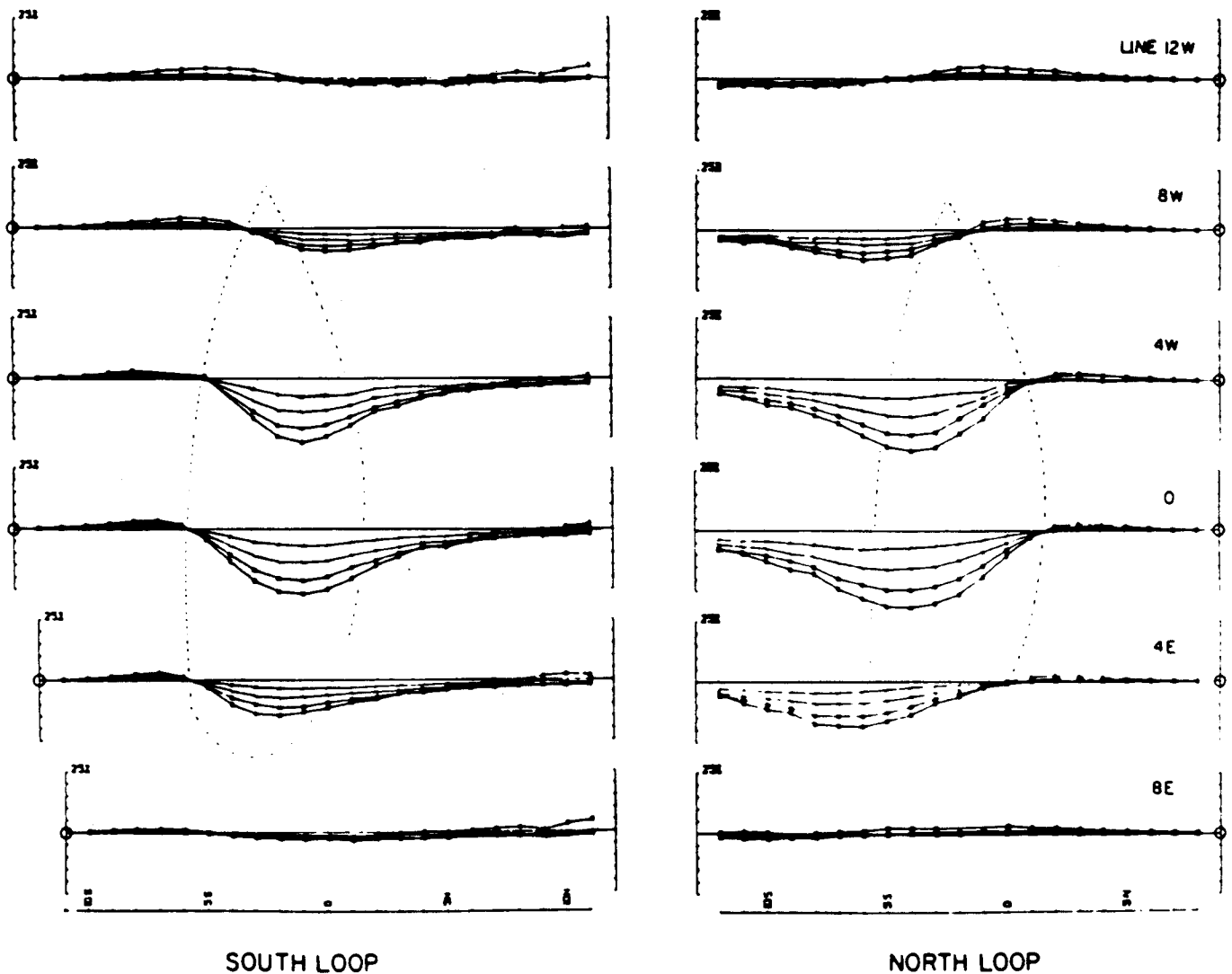


FIG. 19. Later time H_z profiles (Ch 5-2) outline the perimeter of the conductor.

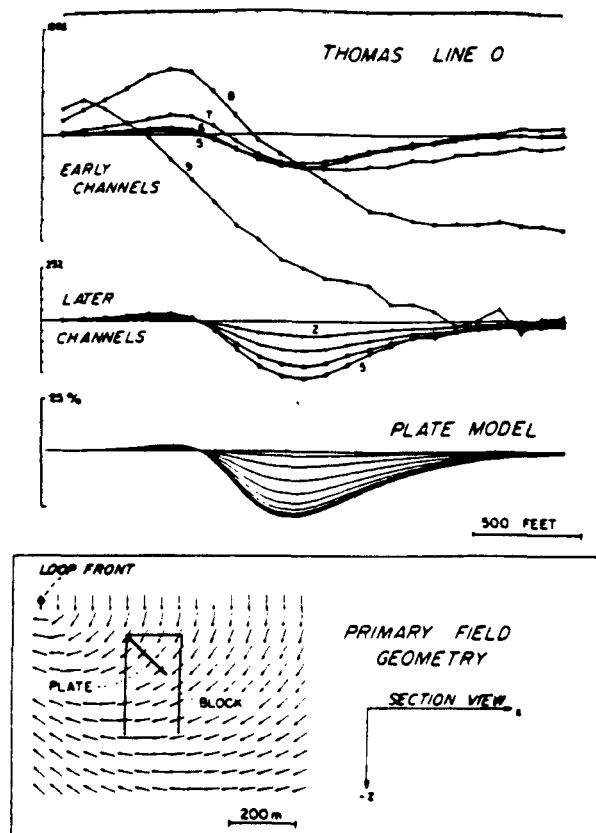


FIG. 20. Comparison of H_z^2 data from the south transmitter loop with a free-space plate model. The configuration of the primary field is also shown.

500 μ s the response changes to an asymmetric negative anomaly which decays much more slowly than the crossover response. The early-time crossover response is a current gathering or channeling anomaly where the (analogous) anomalous current flows along the length of the zone, while the longer time constant response is a local induction anomaly, where induced currents flow in a vortex within the target conductor.

Figure 19 shows a map of all the late-time profiles. They clearly delineate the edge of the target body. Figure 20 shows how a rectangular plate model can be found which models the observed results from one transmitter loop quite accurately, but which has to be rotated in order to match the results from the other loop. The late-time induced (analogous) current system in the actual conductor appears to be a tightly defined normal current in the front upper (near-loop) edge of the conductor with a more diffuse, return current deep in the rear of the body. A survey with the transmitter loop located on the other side of the body was similarly fitted by a plate dipping away from that loop, indicating the conductor to be a thick zone in which currents can flow in a variety of directions.

Electric fields were measured at the Thomas site. The late time vector map is shown in Figure 21, along with a rough numerical model. The conductive zone shows very clearly, although its edge is ill defined. Figure 22 shows a profile of the longitudinal component of electric field over the body. The field

intensity is almost constant from channel 6 onward, and the main feature of the response is the aforementioned broad reduction in the field strength over the conductor. It is helpful, when looking at E field profiles, to imagine a plot on the same axes of the negative of the observed channel 1 response. This is the value the field starts from at the half-cycle transition. Even as early as 50 μ s (Ch 9), the electric field has made most of its polarity reversal. In fact, between the loop to the target body it has overshoot, while from the target body outwards it is changing relatively slowly. The time changes in E are actually very similar to those in H . There are two dominant decay times, a short one corresponding to the overburden and the channeling target response (Ch 8-6) and a long one corresponding to the local induction response (Ch 5-1). Also, these two E -field responses have a different geometrical form corresponding with the different forms of the magnetic anomalies. The scaled up version of the E data in Figure 22 shows the slowly decaying anomaly. Considerable noise is apparent in the data at this magnification.

Bedrock conductor beneath overburden

Figure 23 shows the measured secondary H_z fields at a site in Australia. The slow outward migration of the early-time channels and the -200 percent early-time limit away from the transmitter loop are characteristics of the response of a near-surface conductive weathered layer. This layer has a total conductance of about 4 S.

Around station 210W a more local superimposed crossover anomaly is evident which is fixed in location. This feature is evident over a great strike length. When the visually estimated overburden response is stripped from the anomaly and the peak-to-peak crossover response is plotted on a decay plot (Figure 26), the characteristics of early time blanking, time delay, and enhancement are clearly displayed. Corresponding to the model data of Figure 16, the early time blanking attenuates the local anomaly as the (analogous) magnetic field has not had time to penetrate the weathered layer. At intermediate times (Ch 5, 4) the response lies above a fitted free-space, half-plane conductor decay curve. This is partly an amplitude enhancement from current gathering and partly due to a small delay in time while the (analogous) magnetic field penetrates the near-surface conductor. It is not clear whether any of the L400S response can be identified as due to local induction. Nevertheless, the plotted induction curve for a half-plane in free space serves as a useful reference and establishes an upper limit on the conductance of the feature (7S in this case).

On two survey lines about 1 km away, the same local feature is observed, but the response has changed to one of longer time constant. As shown in Figure 24, a clear response persists through channels 2 and 1. These data are replotted with "point normalization" on Figure 25 to show the absolute secondary field. Absolute normalization preserves the true anomaly shape, but has the disadvantage of scaling up strongly those anomalies which lie near the transmitter. The stripped peak-to-peak response is plotted in decay form in Figure 26 and clearly shows the difference in time constant at the two locations.

The increase in time constant seen on line 600N is very significant, since little change is seen in the background response and only a lesser change in the blanking time. It indicates that the L600N late-time response is due to local induc-

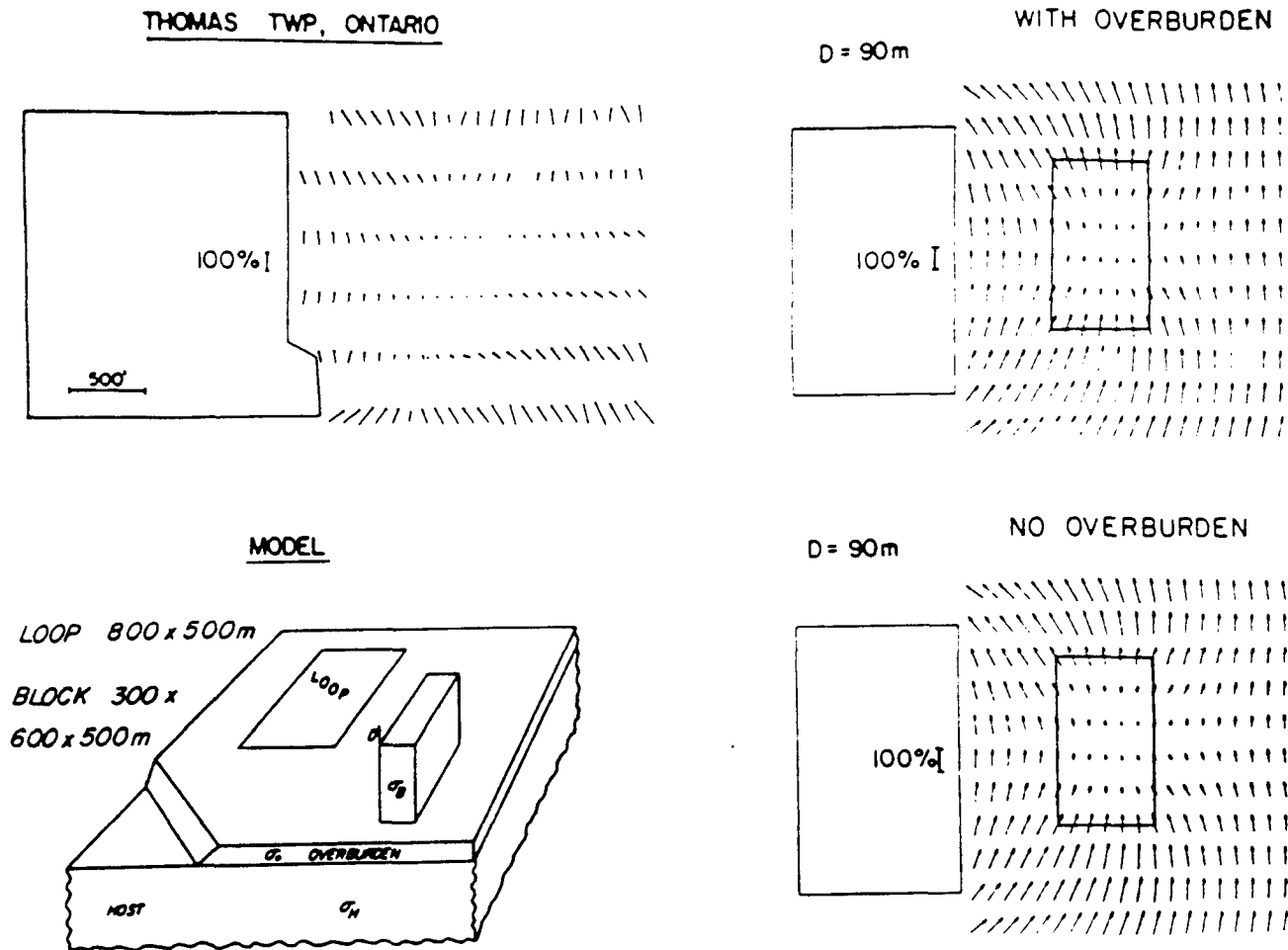


FIG. 21. Vector map of the late-time E field at Thomas Twp. A block model is included for comparison. The example is for a case where $\sigma_B \gg \sigma_O \gg \sigma_H \gg \sigma_{AIR}$.

tion. Model fitting of the decay, taking into account the limited strike extent of the long time constant response, leads to an interpretation of this feature as a local thickening of the half-plane conductor. The local conductance needed to produce the longer time constant is 120 S in contrast to the 7 S maximum of the rest of the bedrock conductor.

Drilling indicated that the extensive conductor was a 50 m thick calc-silicate zone containing both carbonates and sulfide lenses within a talc-sericite host. The locally more conductive part consisted chiefly of nearly massive noneconomic sulfides.

CONCLUSIONS

Experience with UTEM demonstrates that a wideband, time-domain EM system which measures the step response of the ground is electronically feasible and practical. Considerable field and modeling experience has shown that it is simple to use the amplitude information from such a system to aid significantly in interpretation. In our opinion the step response has a

significant advantage over the impulse response for detection and interpretation of good conductors in the presence of poorer ones. Electric field data measured with the system can provide independent information about lateral conductivity contrasts and may be a useful aid in interpretation.

ACKNOWLEDGMENTS

Development of the UTEM system and its interpretational capability was funded from a number of sources. UTEM I was developed with support from the National Research Council of Canada. UTEM II instrumentation was supported by UMEX Ltd., Texasgulf Inc., and Cominco Ltd., with interpretational studies funded by a consortium of companies consisting of Aquitaine, Asarco, Cominco, Geoterrex, Gulf Minerals, Inco, Newmont, Noranda, Phelps Dodge, Selco, Shell Canada Resources, Texasgulf, and Umex. Graduate students, Y. Lamontagne, G. Lodha, J. Macnae, and M. Vallée, who worked on the project received stipendary and computing support from the

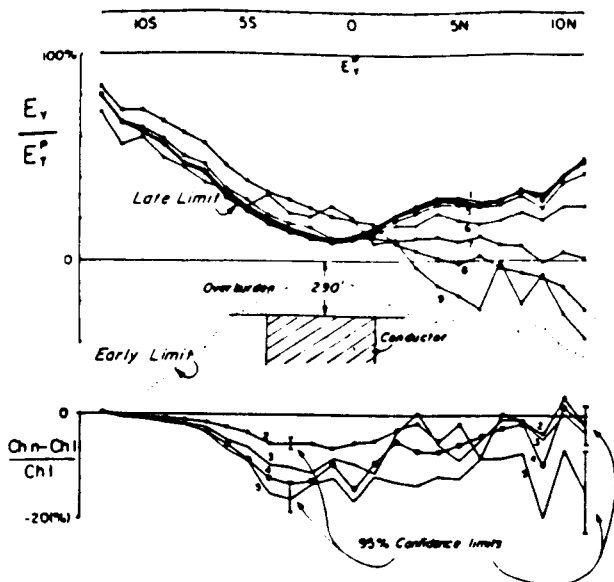


FIG. 22. Thomas Twp E_z data for line 0 from the south transmitter loop. The expanded scale data on the lower axes show that a very weak dynamic E field anomaly is associated with the main H_z^2 late time response (Ch 5-1).

Natural Sciences and Engineering Research Council of Canada and the University of Toronto. All this assistance is gratefully acknowledged. We also thank an anonymous reviewer for a very careful, helpful review.

REFERENCES

Annan, A. P., The equivalent physical method for electromagnetic scattering analysis and its geophysical application: Ph.D. thesis, Memorial Univ. of Newfoundland.

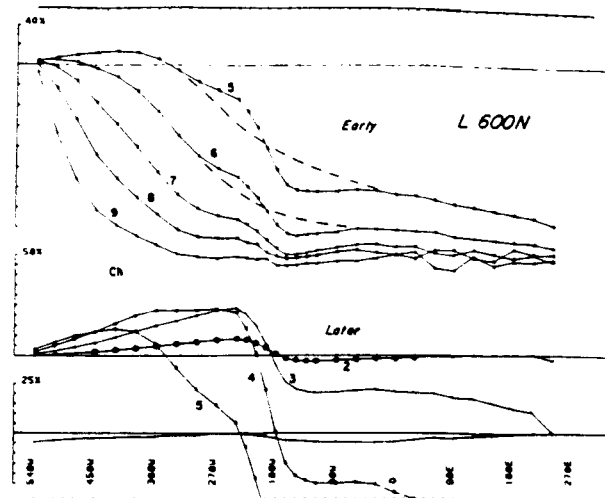


FIG. 24. H_z^2 data on line 600N 1 km away from the previous figure showing a time decay of the local anomaly lasting to much later times. Remeasurement of the profile at 13 Hz gave virtually identical profiles (shifted one channel) with no visible Ch 1 anomaly.

Boschart, R. A., 1964, Analytical interpretation of fixed source electromagnetic data: Doctoral thesis, Univ. of Delft.
 Dyck, A. V., Bloore, M., and Vallée, M. A., 1980, User manual for programs PLATE and SPHERE: Res. in Appl. Geophys. 14, Geophys. Lab. Dept. of Physics, Univ. of Toronto.
 Kaufman, A., 1978, Frequency and transient responses of electromagnetic fields created by currents in confined conductors: Geophysics, v. 43, p. 1002-1010.
 Lajoie, J., and West, G. F., 1976, The electromagnetic response of a conductive inhomogeneity in a layered earth: Geophysics, v. 41, p. 1133-1156.
 Lamontagne, Y., 1975, Applications of wide-band, time domain EM

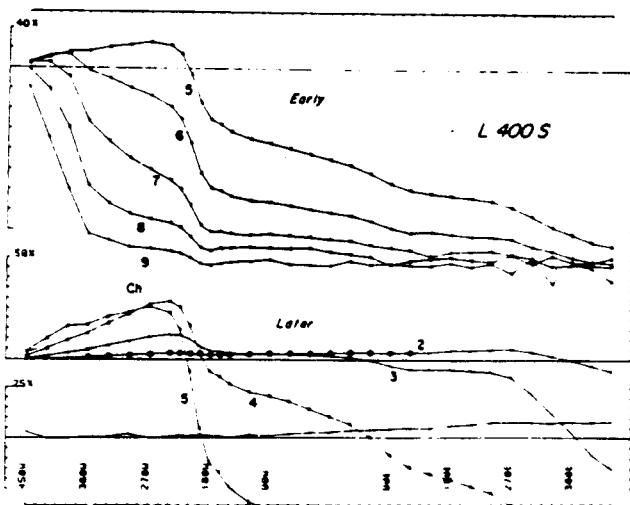


FIG. 23. H_z^2 data from New South Wales showing the migrating crossovers of the overburden near the loop and a local anomaly around station 210 W. (Survey frequency 26 Hz.)

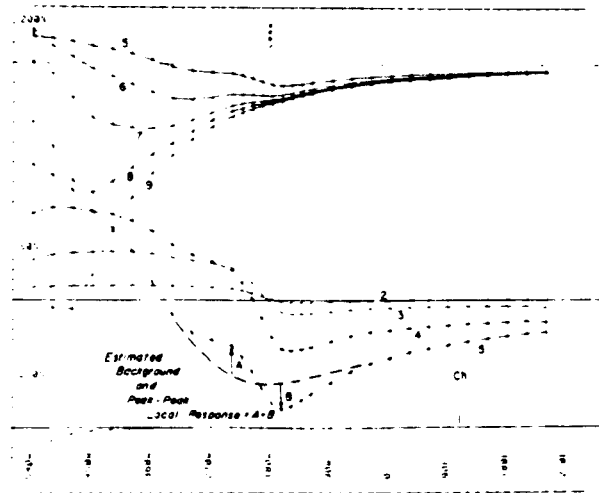


FIG. 25. Point normalized H_z^2 from line 600N. The local secondary fields have been normalized to the constant primary field at station 210W and show stripped peak-to-peak local anomaly amplitude is estimated.

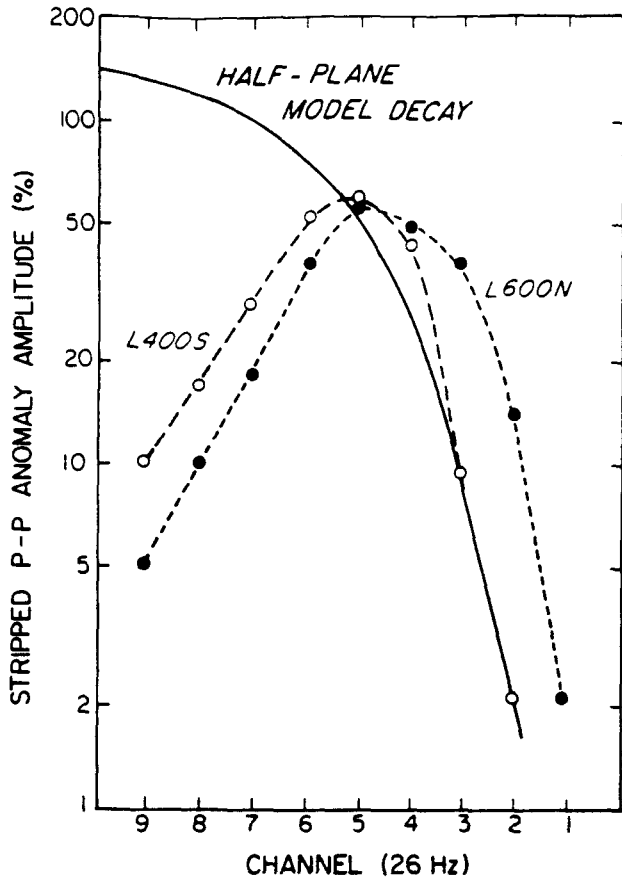


FIG. 26. Amplitude decay plot of stripped anomaly on lines 400S and 600N of the New South Wales survey.

measurements in mineral exploration: Ph.D. thesis, Univ. of Toronto; available as Res. in Appl. Geophys. 7, Geophys. Lab., Univ. of Toronto.

Lamontagne, Y., Lodha, G. L., Macnae, J. C., and West, G. F., 1977, Towards a deep penetration EM system: Paper presented at 79th annual meeting of the Can. Inst. of Min. and Metall., Ottawa, April; published in Bull. Austral. Soc. Expl. Geophys., v. 9, 1978.

— 1980, UTEM, "Wideband Time-domain EM Project 1976-8, Reports 1-5"; Res. in Appl. Geophys. 11, Geophys. Lab., Dept. of Physics, Univ. of Toronto.

Lodha, G. L., 1977, Time domain and multifrequency electromagnetic responses in mineral prospecting: Ph.D. thesis, Univ. of Toronto; available as Res. in Appl. Geophys. 8, Geophys. Lab., Dept. of Physics, Univ. of Toronto.

Macnae, J. C., 1977, The response of UTEM to a poorly conducting mineralized environment: M.Sc. thesis, Univ. of Toronto.

— 1980, The Cavendish test site: a UTEM survey plus a compilation of other ground geophysical data: Res. in Appl. Geophys. 12, Geophys. Lab., Dept. of Physics, Univ. of Toronto.

— 1981, Geophysical prospecting with electrical fields from an inductive source: Ph.D. thesis, Dept. of Physics, Univ. of Toronto, 279 p.; available as Res. in Appl. Geophys., 18, Geophys. Lab., Univ. of Toronto.

Macnae, J. C., Lamontagne, Y., and West, G. F., 1984, Noise processing techniques for time-domain E.M. systems: Geophysics, v. 49, this issue, p. 934-948.

Maxwell, J. C., 1891, A treatise on electricity and magnetism: London, Clarendon Press, v. 2, 500 p.

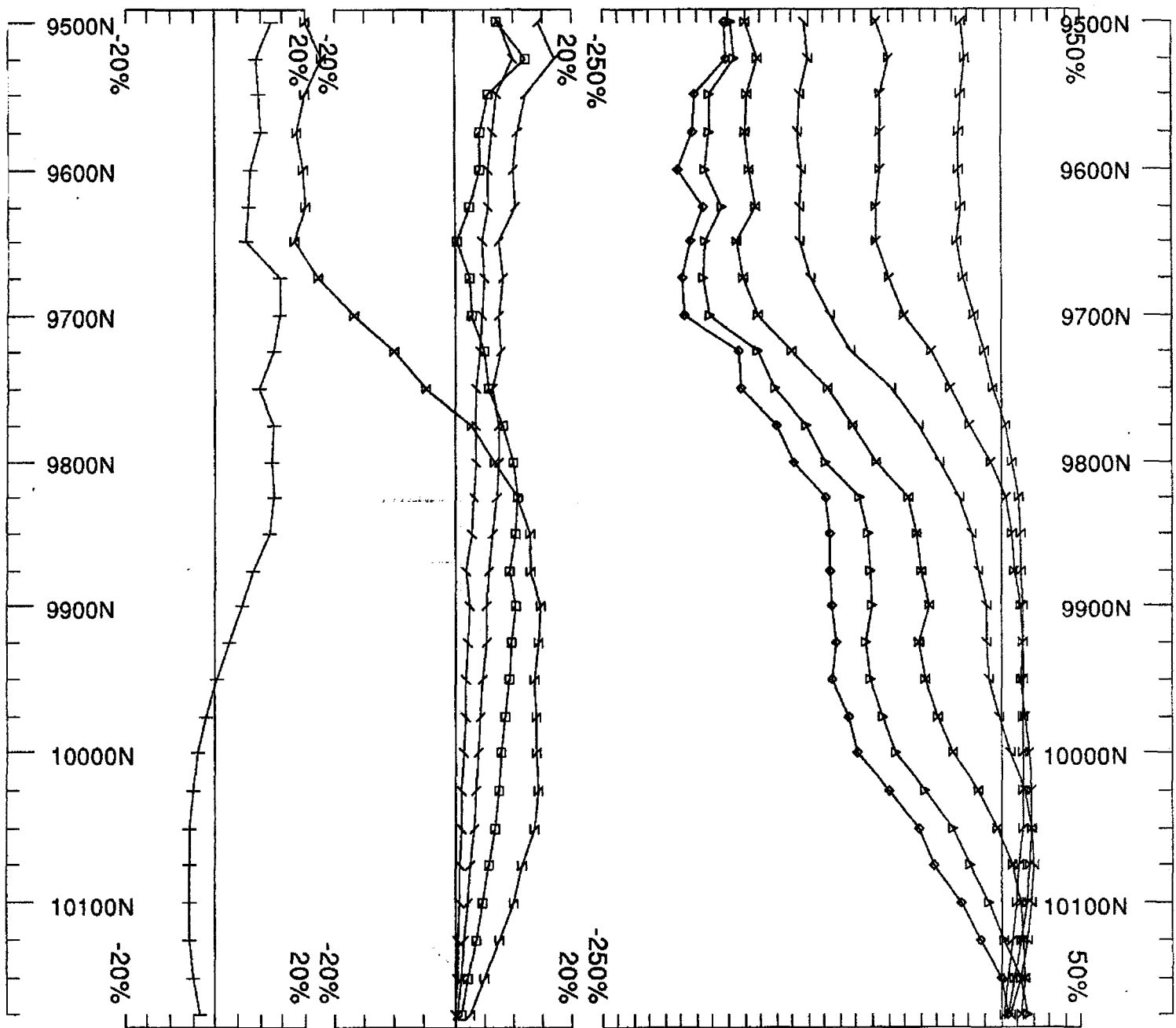
Nabighian, M. N., 1979, Quasi-static transient response of a conducting half-space—An approximate representation: Geophysics, v. 44, p. 1700-1705.

Podolsky, G., and Slankis, J., 1979, Izok Lake deposit, Northwest Territories, Canada. A geophysical case history: in Geophysics and Geochemistry in the search for metallic ores: P. J. Hood, ed., Econ. Geol. rep. 31, Geol. Survey of Canada.

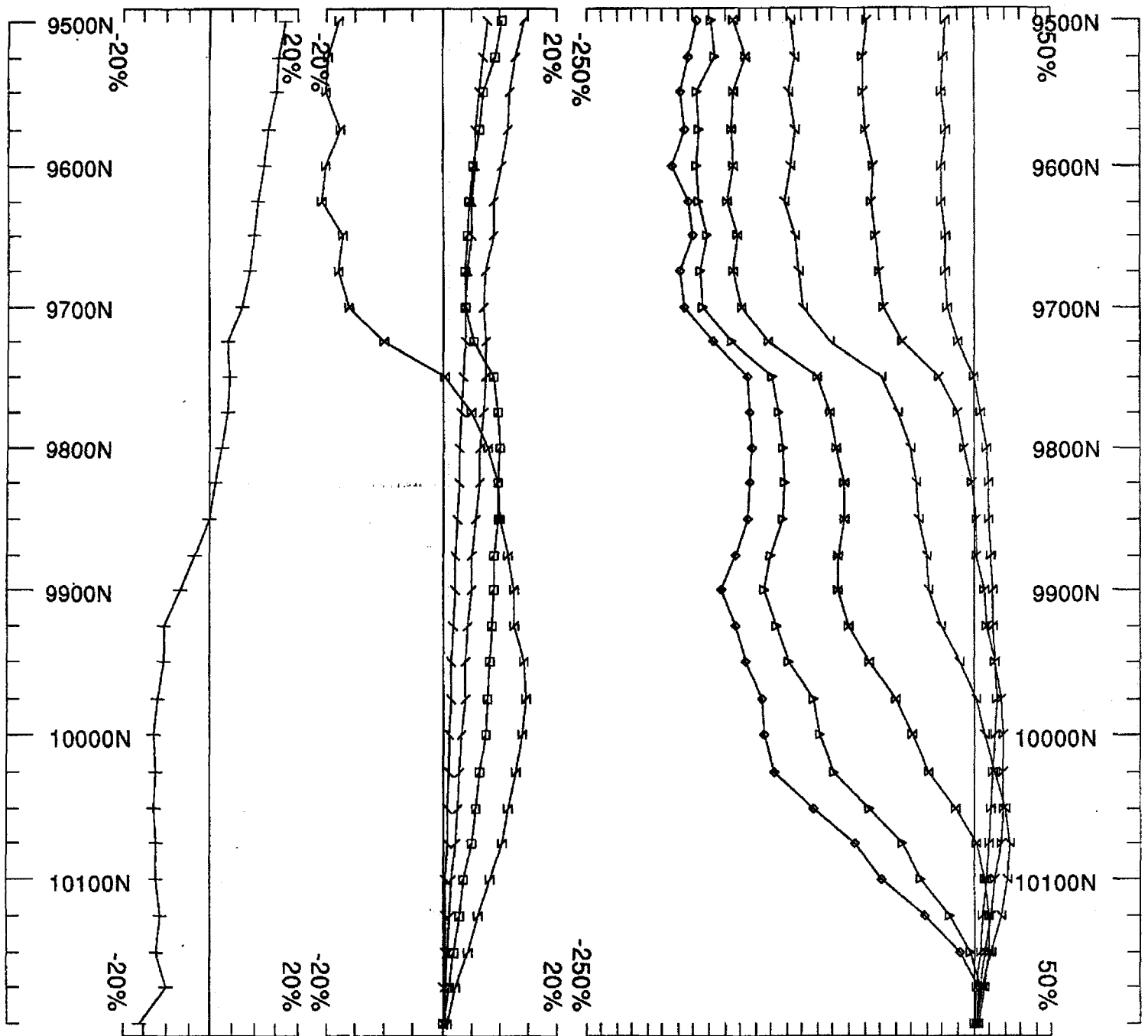
Wait, J. R., 1962, Electromagnetic waves in stratified media: New York, MacMillan Co.

APPENDIX V

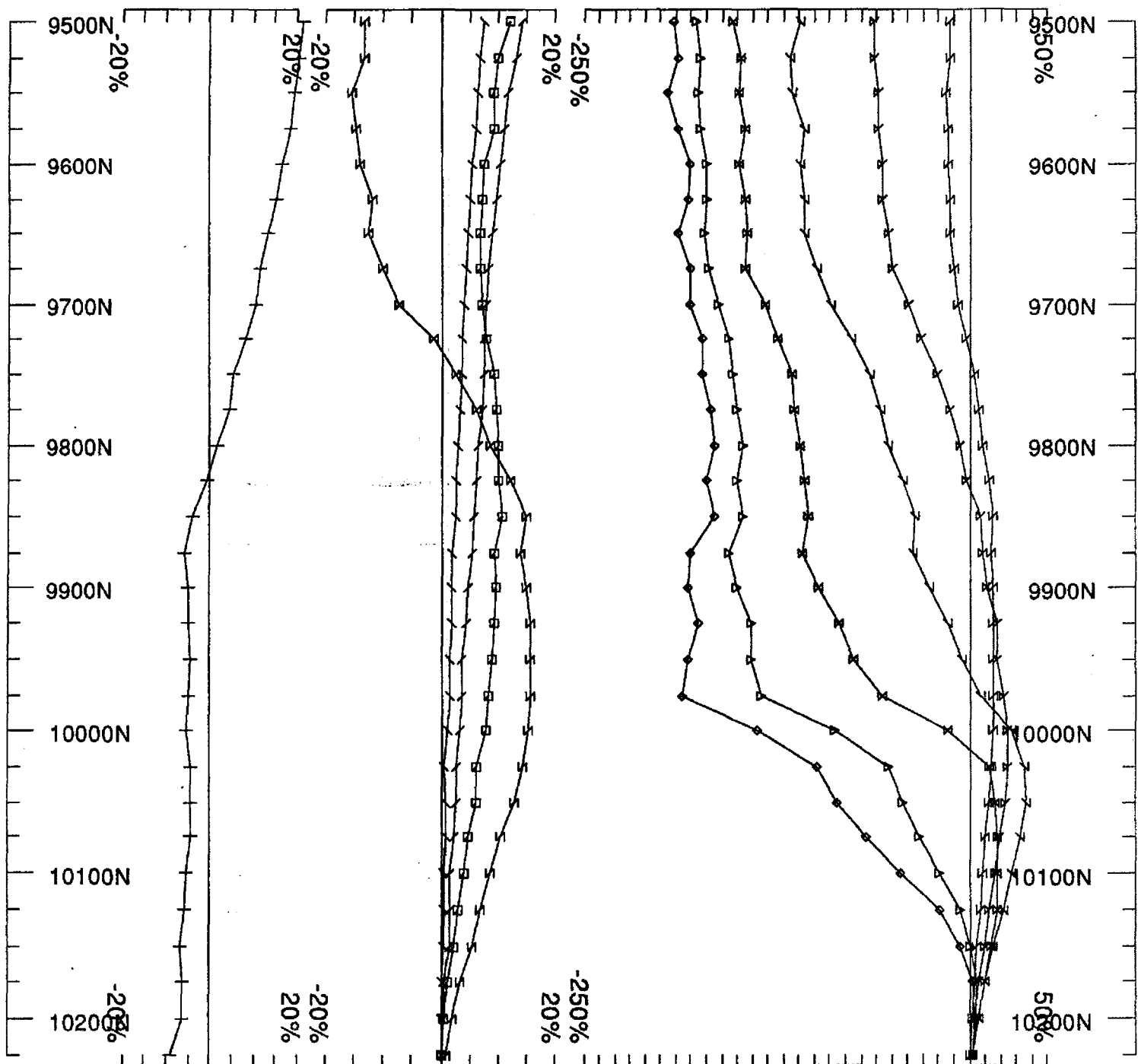
Data Sections



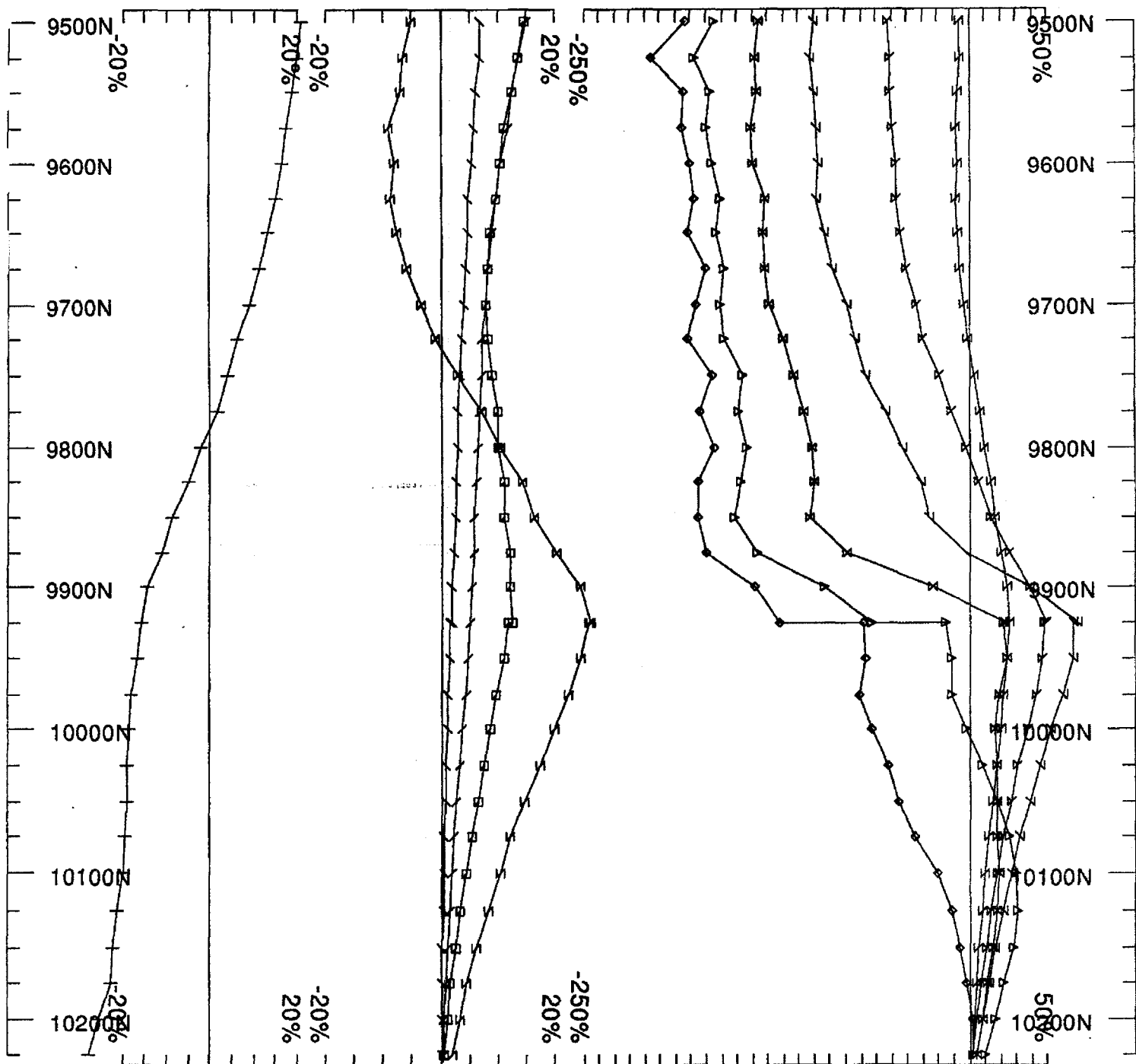
Loop: 1	Secondary, (Chn - Ch1)/ Hpl	UTEM Survey at: KLU PROJECT	
Line: 18500E	Contin. Norm at depth of 0 m	For: AMERICAN COPPER & NICKEL CO. LTD	
Compt: Hz	Base Freq. 30.974 Hz	SJ GEOPHYSICS LTD.	Job U9705
			Surveyed : 11/7 Reduced : 12/7 Plotted : 19/11/



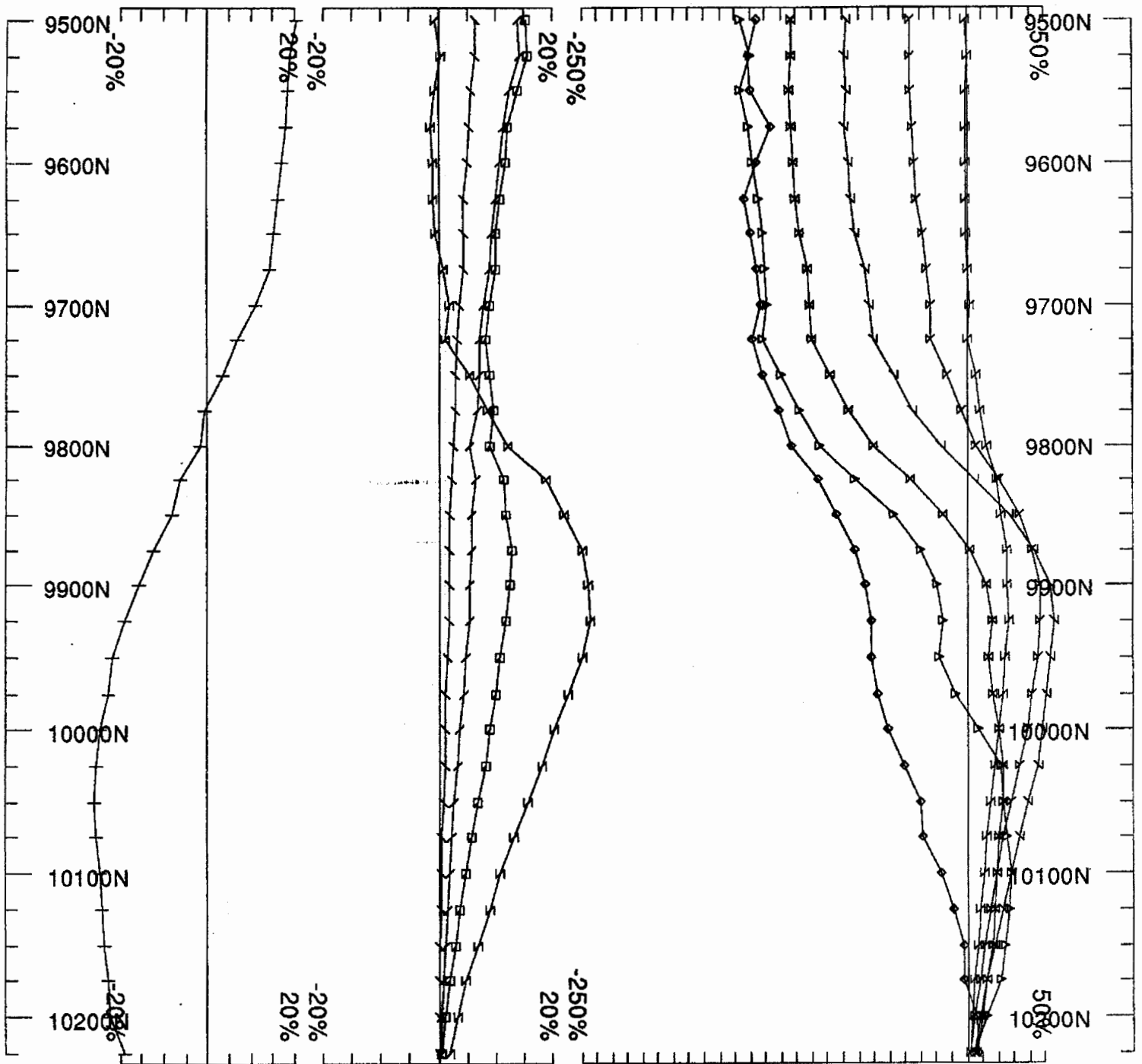
Loop: 1	Secondary, (Chn - Ch1)/ Hp	UTEM Survey at: KLU PROJECT	
Line: 18600E	Contin. Norm at depth of 0 m	For: AMERICAN COPPER & NICKEL CO. LTE	
Compt: Hz	Base Freq. 30.974 Hz	SJ GEOPHYSICS LTD.	
		Job U9705	Surveyed : 11/7 Reduced : 12/7 Plotted : 19/11/81



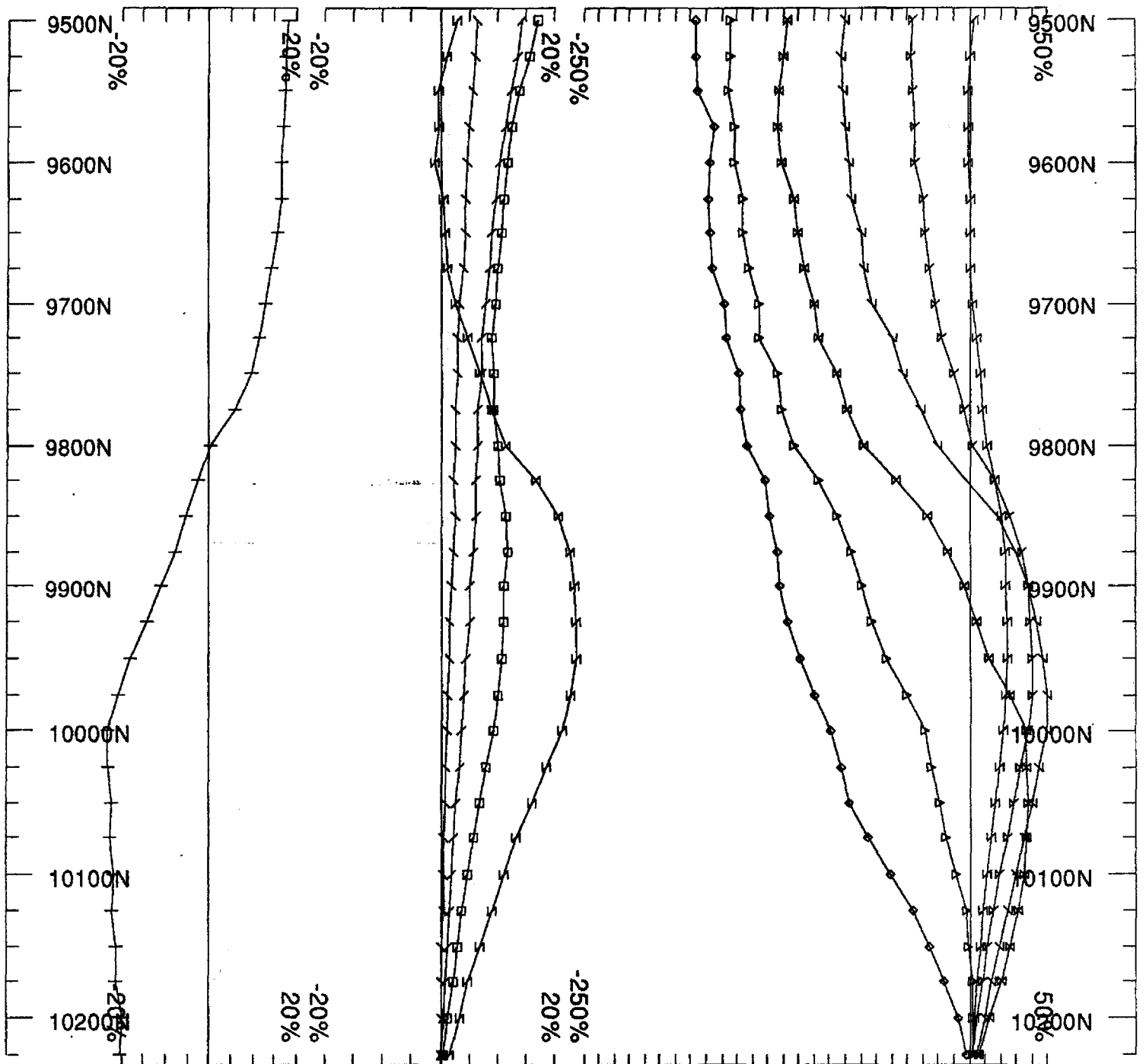
Loop: 1	Secondary, (Chn - Ch1)/ Hp	UTEM Survey at: KLU PROJECT	
Line: 18700E	Contin. Norm at depth of 0 m	For: AMERICAN COPPER & NICKEL CO. LTD	
Compt: Hz	Base Freq. 30.974 Hz	SJ GEOPHYSICS LTD.	Job U9705
			Surveyed : 11/7 Reduced : 12/7 Plotted : 19/11/8



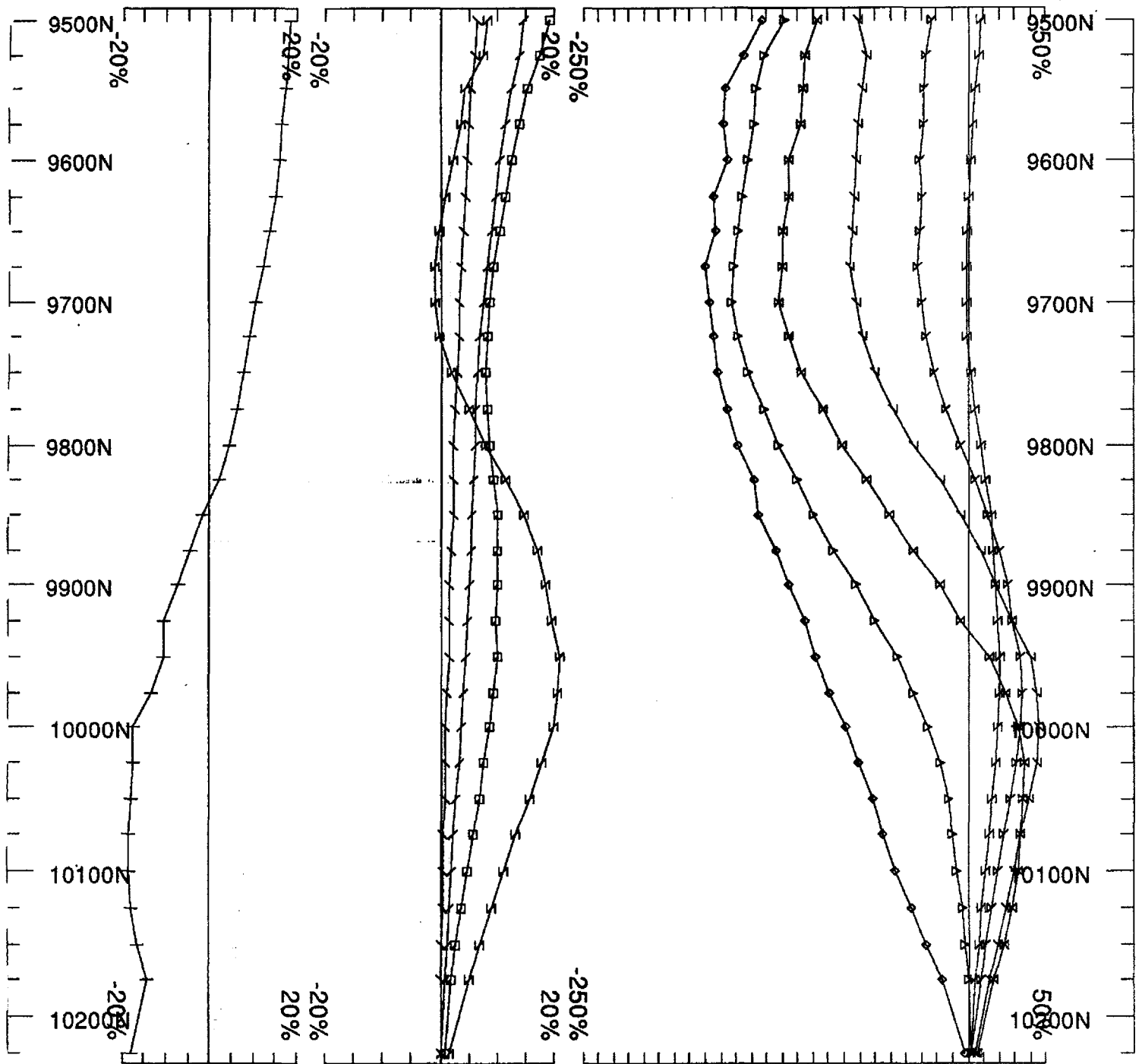
Loop: 1	Secondary, (Chn - Ch1)/ Hp	UTEM Survey at: KLU PROJECT	
Line: 18800E	Contin. Norm at depth of 0 m	For: AMERICAN COPPER & NICKEL CO. LTD	
Compt: Hz	Base Freq. 30.974 Hz	SJ GEOPHYSICS LTD.	
		Job	Plotted : 19/11/
		U9705	



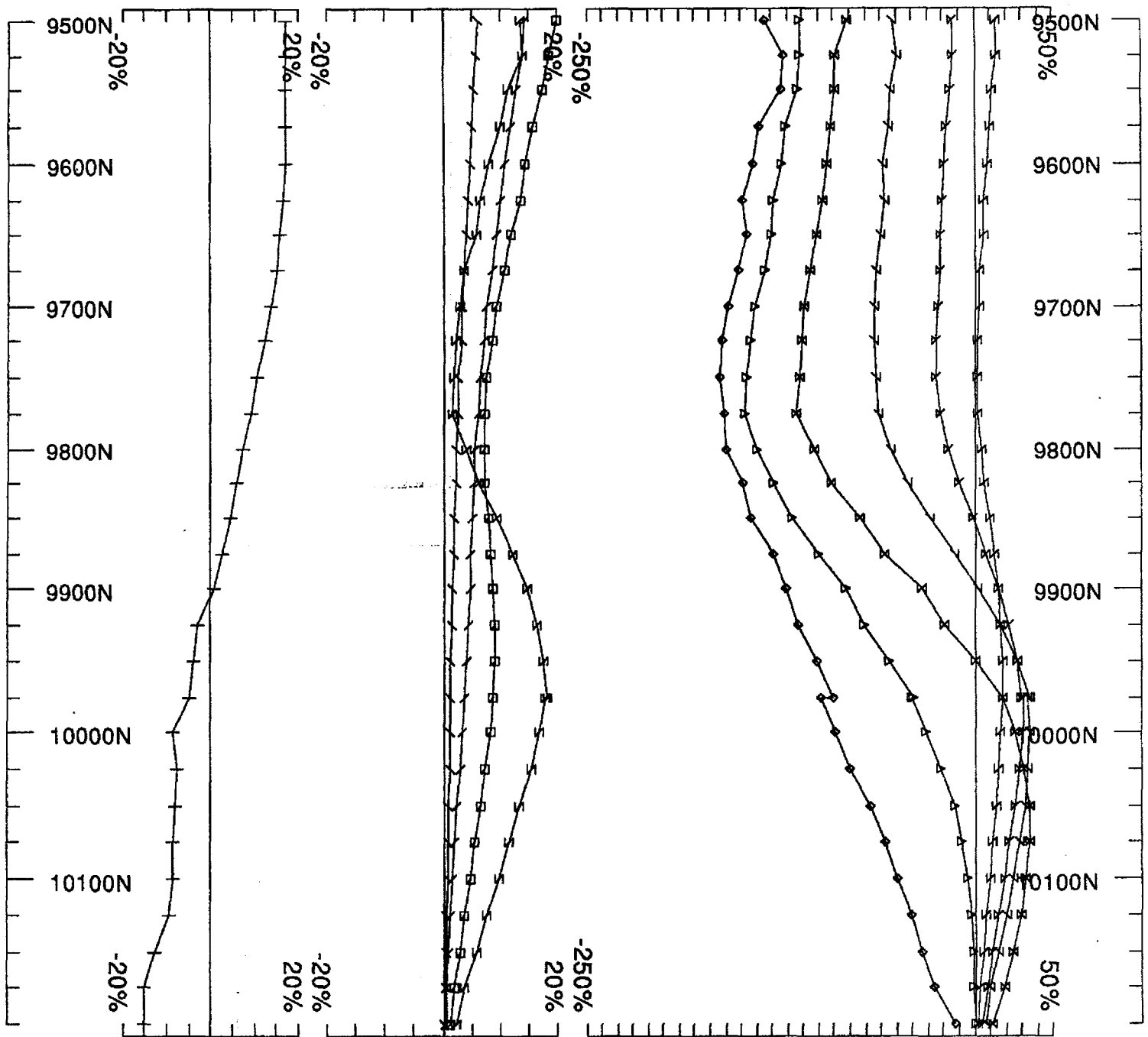
Loop: 1	Secondary, (Chn - Ch1)/ Hp	UTEM Survey at: KLU PROJECT	
Line: 18900E	Contin. Norm at depth of 0 m	For: AMERICAN COPPER & NICKEL CO. LTD	
Compt: Hz	Base Freq. 30.974 Hz	SJ GEOPHYSICS LTD.	
		Job U9705	Surveyed : 10/7 Reduced : 11/7 Plotted : 19/11/7



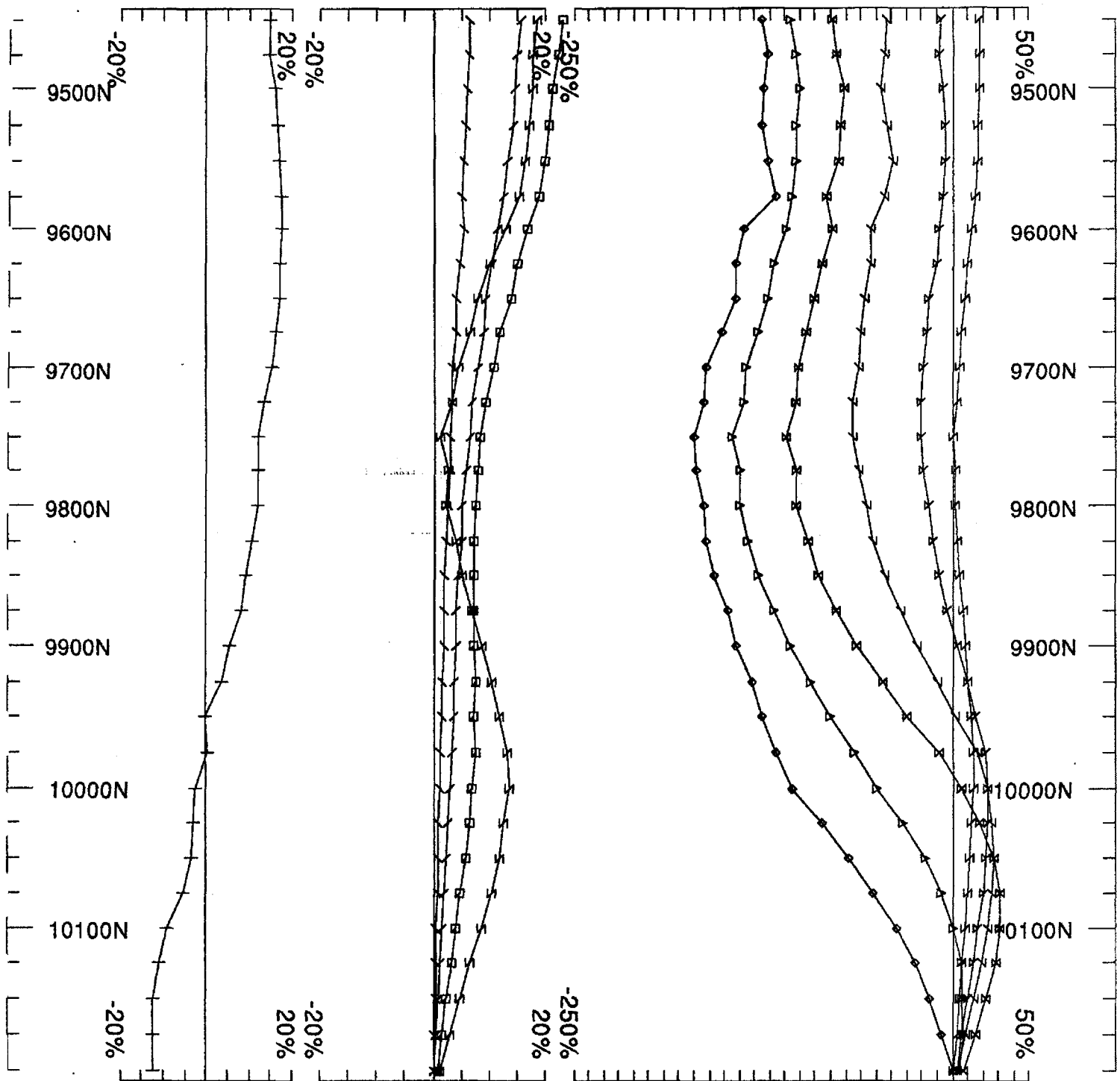
Loop: 1	Secondary, (Chn - Ch1)/ Hp	UTEM Survey at: KLU PROJECT	
Line: 19000E	Contin. Norm at depth of 0 m	For: AMERICAN COPPER & NICKEL CO. LTD	
Compt: Hz	Base Freq. 30.974 Hz	SJ GEOPHYSICS LTD.	
		Job U9705	Surveyed: 10/7 Reduced: 11/7 Plotted: 19/11/7



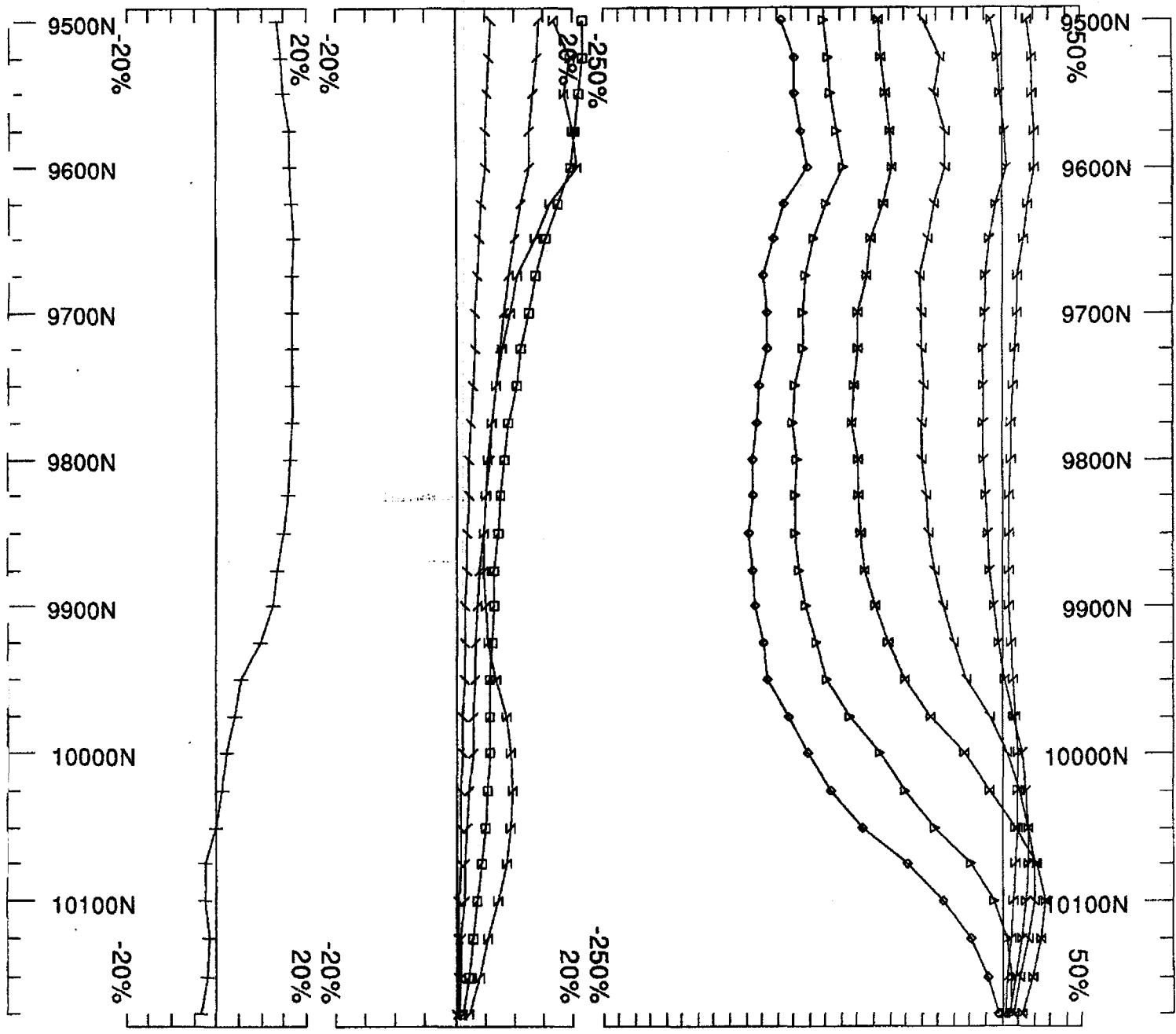
Loop: 1 Line: 19100E Compt: Hz	Secondary, (Chn - Ch1)/ Hp Contin. Norm at depth of 0 m Base Freq. 30.974 Hz	UTEM Survey at: KLU PROJECT For: AMERICAN COPPER & NICKEL CO. LTD SJ GEOPHYSICS LTD. Job U9705 Surveyed : 10/7 Reduced : 11/77 Plotted : 19/11/81
--------------------------------------	---	--



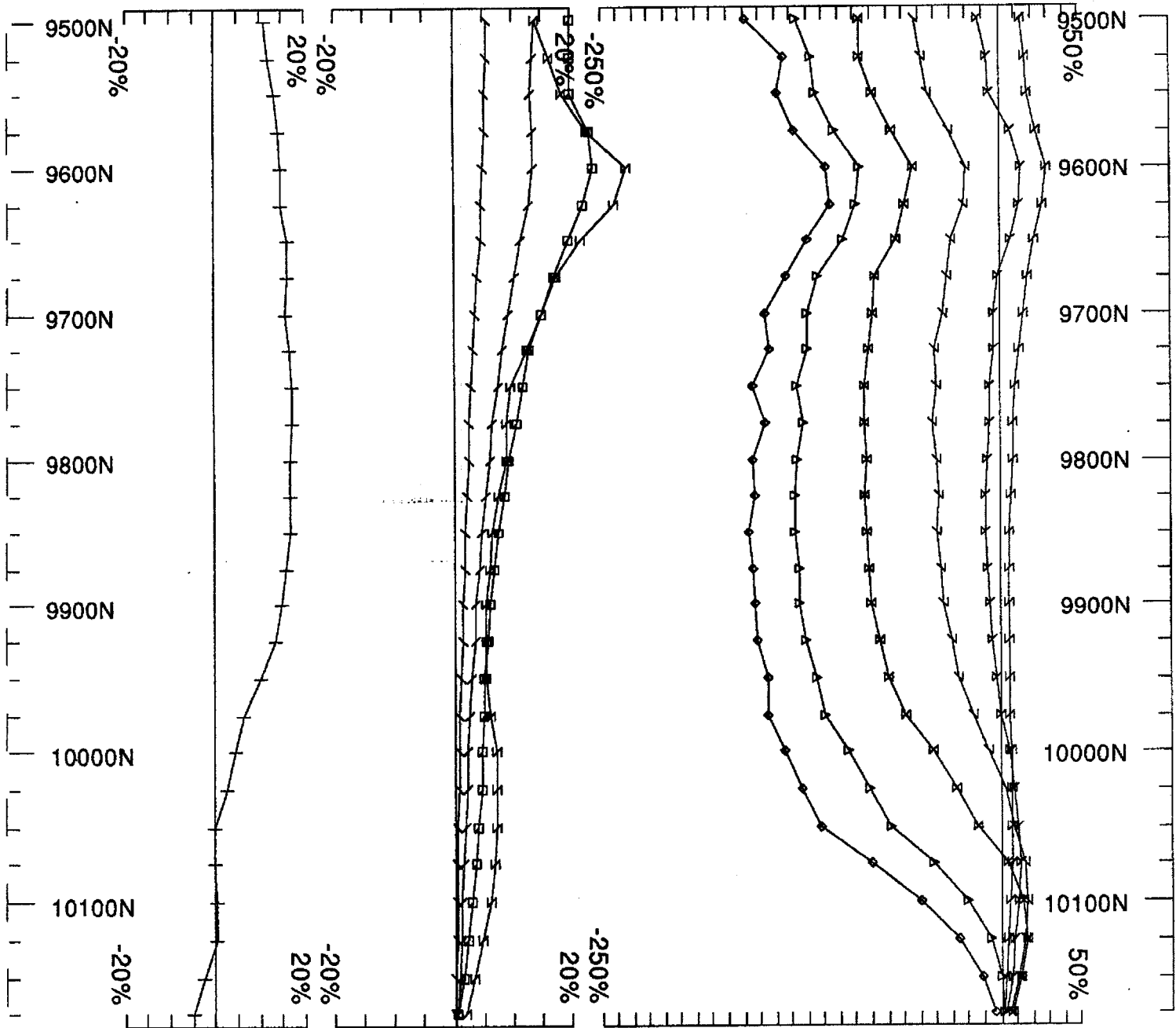
Loop: 1	Secondary, (Chn - Ch1)/ Hp	UTEM Survey at: KLU PROJECT	
Line: 19200E	Contin. Norm at depth of 0 m	For: AMERICAN COPPER & NICKEL CO. LTD	
Compt: Hz	Base Freq. 30.974 Hz	SJ GEOPHYSICS LTD.	
		Job U9705	Surveyed: 9/7/8 Reduced: 9/7/8 Plotted: 19/11/8



Loop: 1	Secondary, (Chn - Ch1)/ Hp	UTEM Survey at: KLU PROJECT	
Line: 19300E	Contin. Norm at depth of 0 m	For: AMERICAN COPPER & NICKEL CO. LTD	
Compt: Hz	Base Freq. 30.974 Hz	SJ GEOPHYSICS LTD.	
		Job U9705	Surveyed : 9/7/8 Reduced : 11/77 Plotted : 19/11/8



Loop: 1 Line: 19400E Compt: Hz	Secondary, (Chn - Ch1)/ Hp Contin. Norm at depth of 0 m Base Freq. 30.974 Hz	UTEM Survey at: KLU PROJECT For: AMERICAN COPPER & NICKEL CO. LTD SJ GEOPHYSICS LTD. Job U9705 Surveyed : 9/7/ Reduced : 11/7/ Plotted : 19/11/
--------------------------------------	---	--

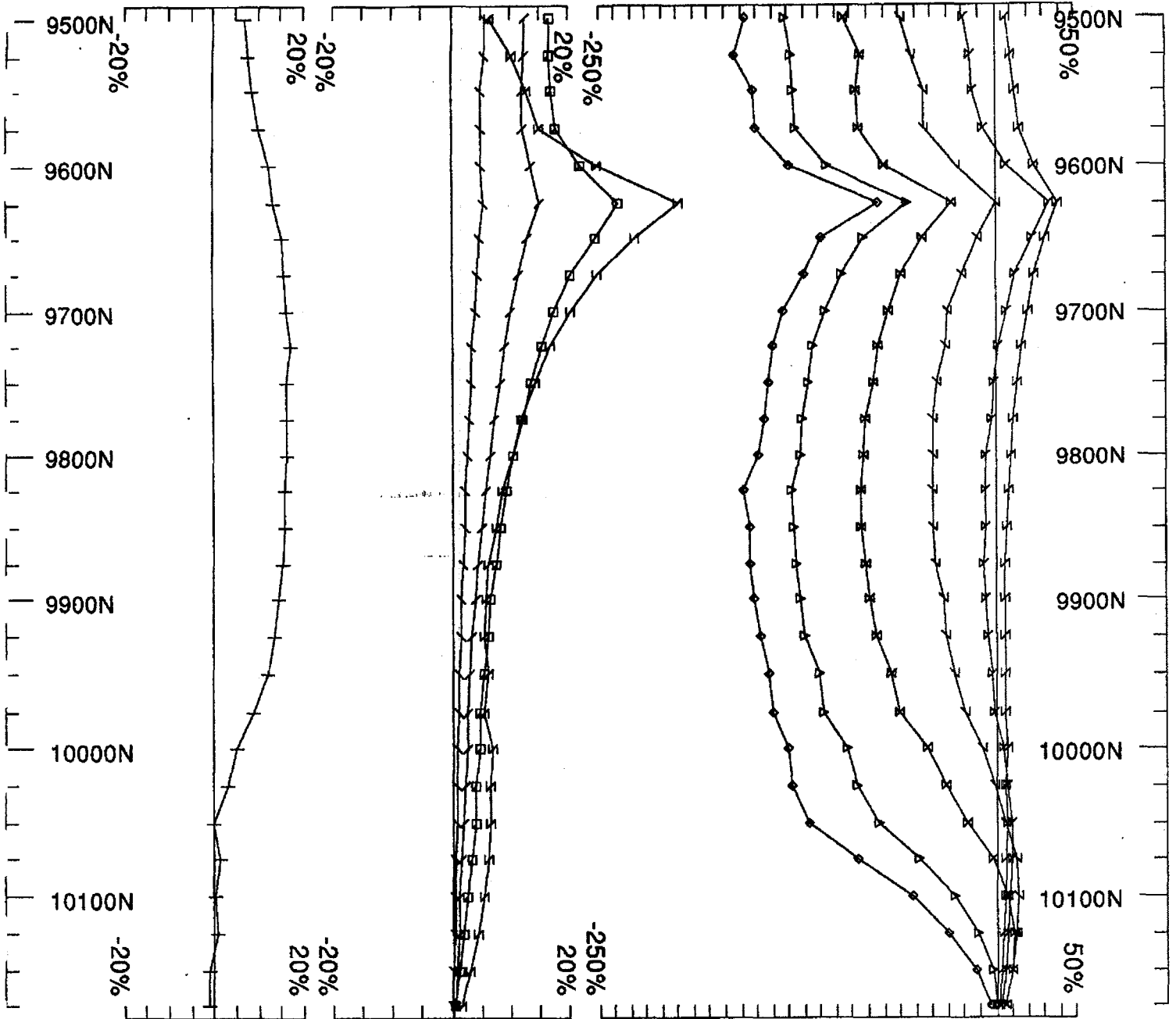


Loop: 1
 Line: 19500E
 Compt: Hz

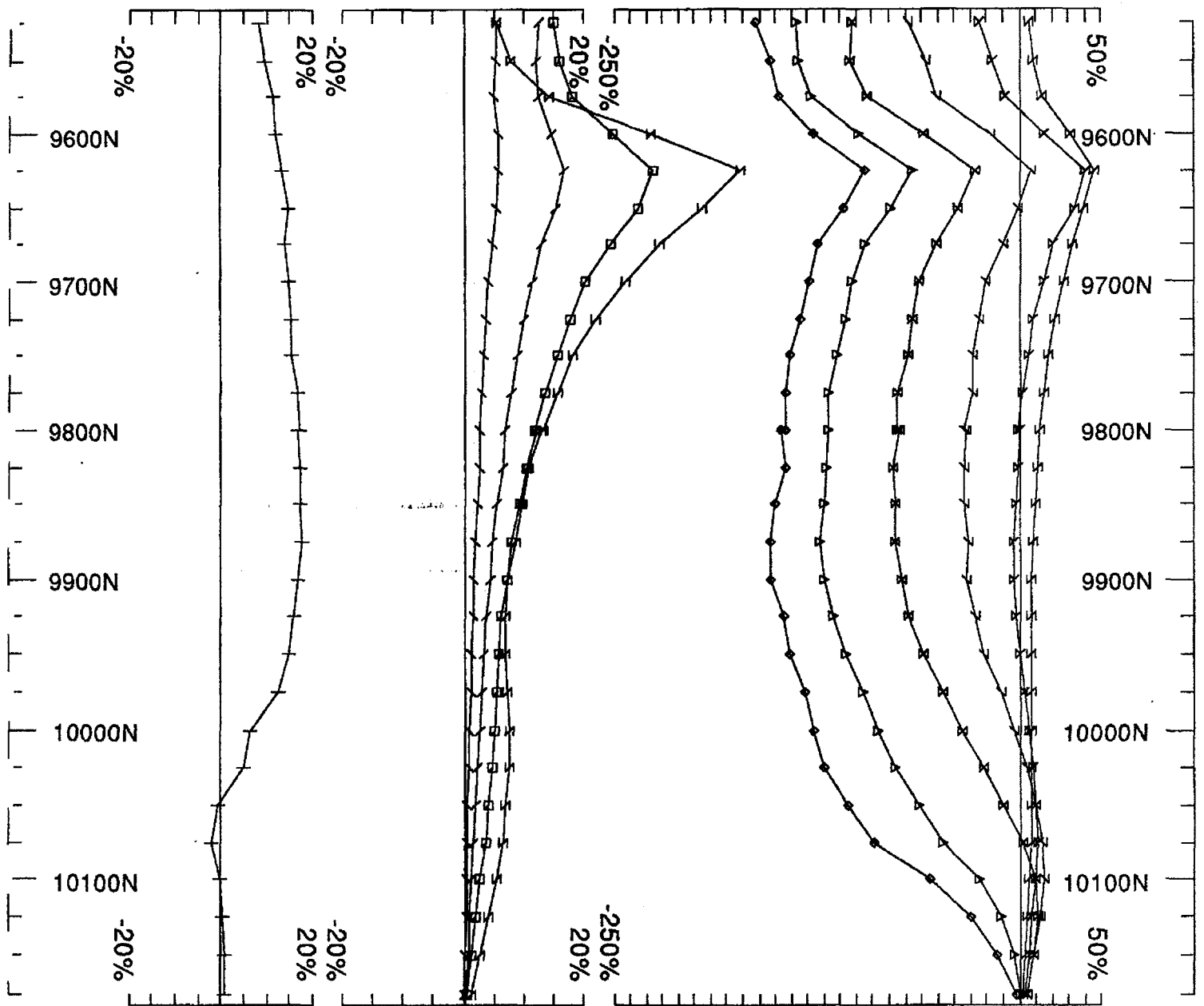
Secondary, (Chn - Ch1)/|Hp|
 Contin. Norm at depth of 0 m
 Base Freq. 30.974 Hz

UTEM Survey at: KLU PROJECT
For: AMERICAN COPPER & NICKEL CO. LTD
SJ GEOPHYSICS LTD.

Job U9705
 Surveyed : 9/7/8
 Reduced : 11/7/8
 Plotted : 19/11/8



Loop: 1	Secondary, (Chn - Ch1)/ Hp	UTEM Survey at: KLU PROJECT	
Line: 19600E	Contin. Norm at depth of 0 m	For: AMERICAN COPPER & NICKEL CO. LTD	
Compt: Hz	Base Freq. 30.974 Hz	SJ GEOPHYSICS LTD.	
		Job U9705	Surveyed : 9/7/ Reduced : 11/7/ Plotted : 19/11/

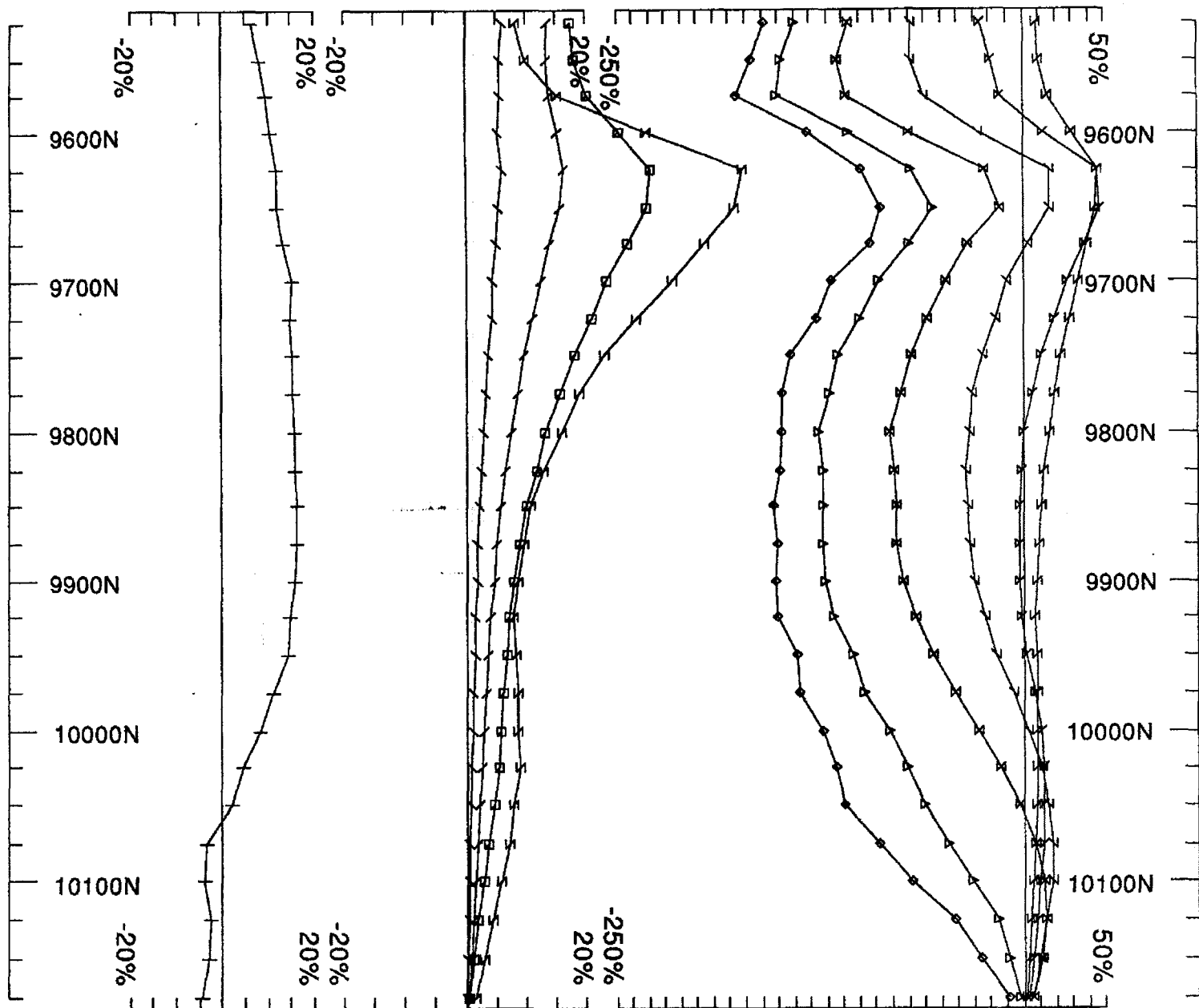


Loop: 1
 Line: 19700E
 Compt: Hz

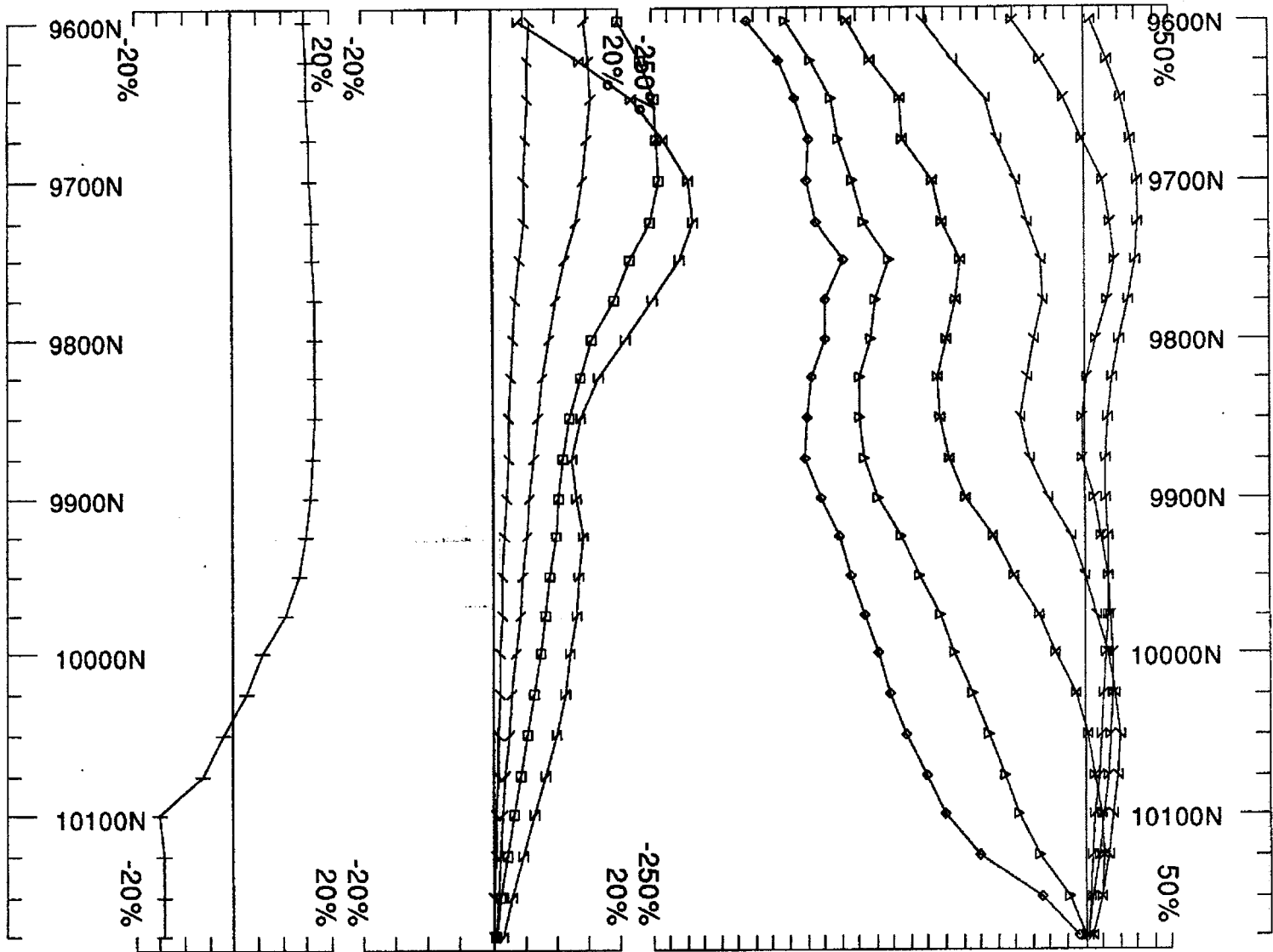
Secondary, (Chn - Ch1)/|Hp|
 Contin. Norm at depth of 0 m
 Base Freq. 30.974 Hz

UTEM Survey at: KLU PROJECT
For: AMERICAN COPPER & NICKEL CO. LTD
SJ GEOPHYSICS LTD.

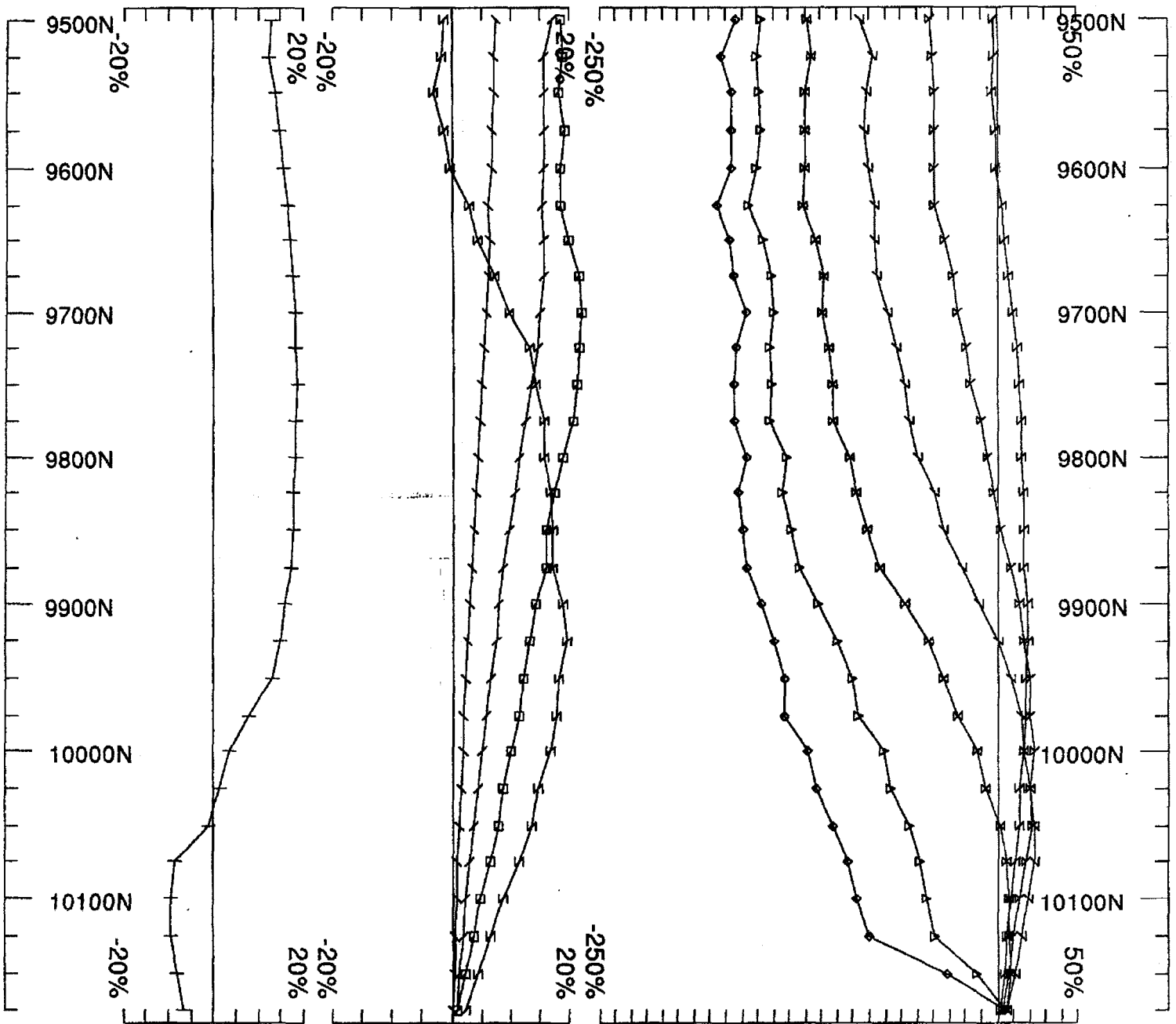
Job U9705
 Surveyed: 9/7/8
 Reduced: 9/7/8
 Plotted: 19/1/8



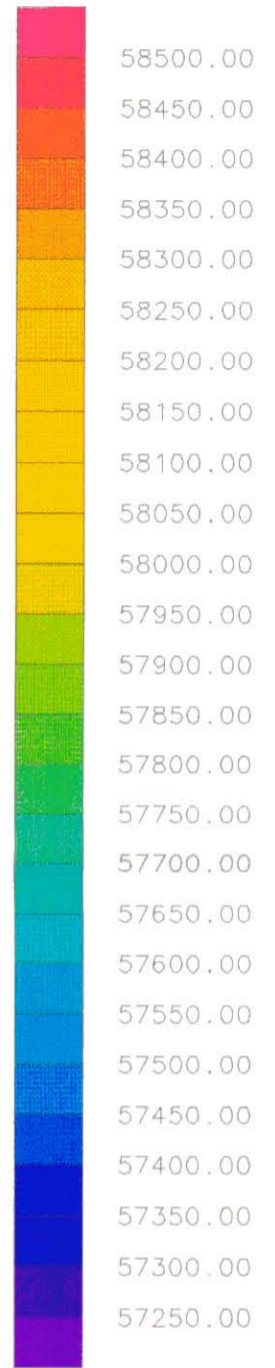
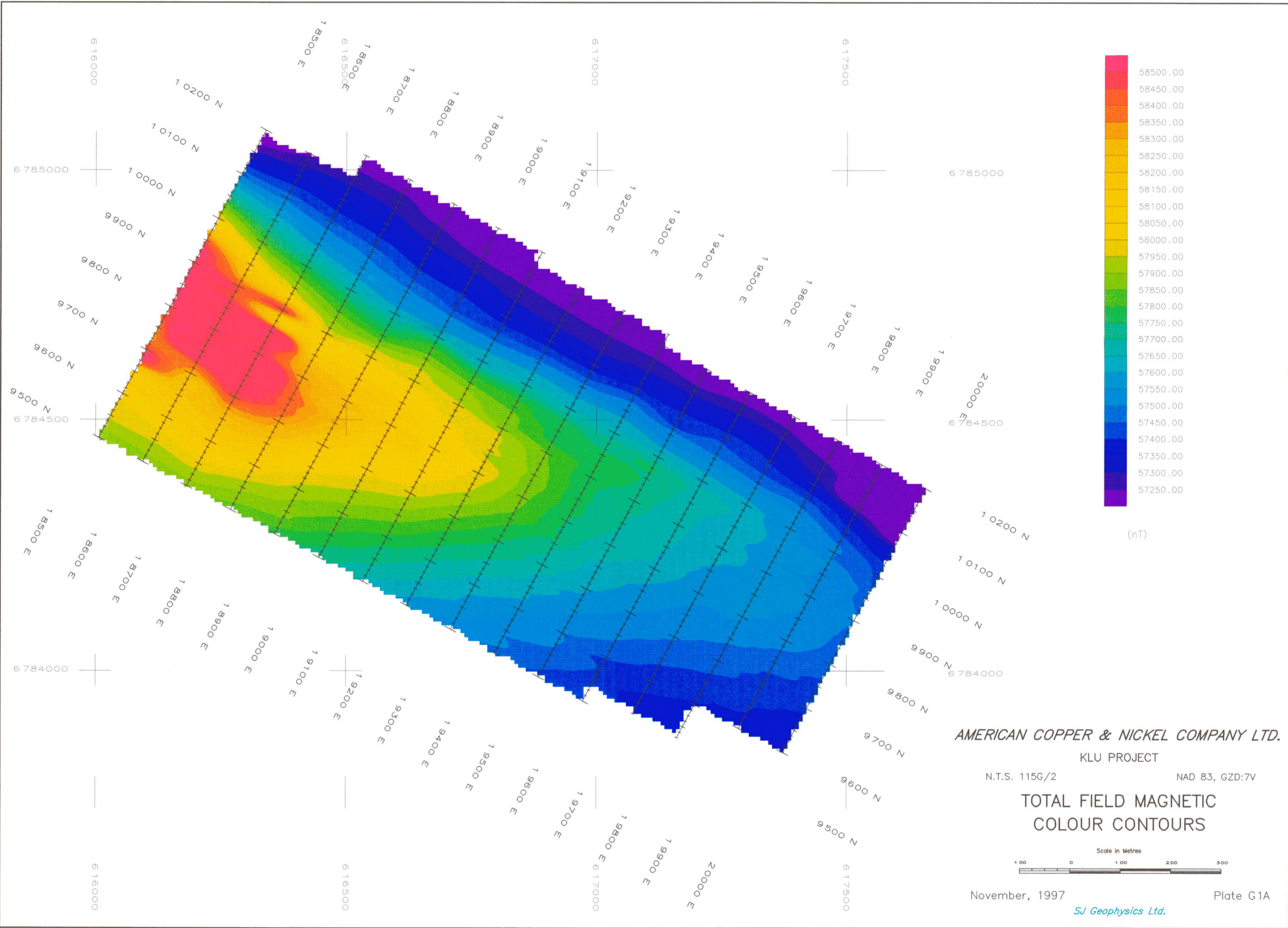
Loop: 1	Secondary, (Chn - Ch1)/ Hp	UTEM Survey at: KLU PROJECT	
Line: 19800E	Contin. Norm at depth of 0 m	For: AMERICAN COPPER & NICKEL CO. LTI	
Compt: Hz	Base Freq. 30.974 Hz	SJ GEOPHYSICS LTD.	
		Job U9705	Surveyed : 10/7 Reduced : 11/7 Plotted : 19/11/



Loop: 1	Secondary, (Chn - Ch1)/ Hp	UTEM Survey at: KLU PROJECT	
Line: 1990E	Contin. Norm at depth of 0 m	For: AMERICAN COPPER & NICKEL CO. LTD	
Compt: Hz	Base Freq. 30.974 Hz	SJ GEOPHYSICS LTD.	
		Job U9705	Surveyed : 10/7 Reduced : 11/7 Plotted : 19/11/8



Loop: 1	Secondary, (Chn - Ch1)/ Hp	UTEM Survey at: KLU PROJECT	
Line: 20000E	Contin. Norm at depth of 0 m	For: AMERICAN COPPER & NICKEL CO. LTE	
Compt: Hz	Base Freq. 30.974 Hz	SJ GEOPHYSICS LTD.	
		Job U9705	Surveyed : 10/7 Reduced : 11/7/ Plotted : 19/11/



(nT)

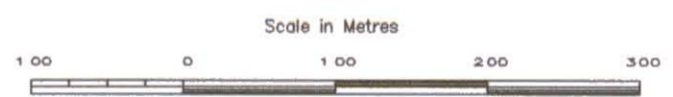
AMERICAN COPPER & NICKEL COMPANY LTD.

KLU PROJECT

N.T.S. 115G/2

NAD 83, GZD:7V

TOTAL FIELD MAGNETIC
COLOUR CONTOURS



November, 1997

Plate G1A

SJ Geophysics Ltd.

093786 DWG 05

DIAND - YUKON REGION, LIBRARY

APPENDIX 2

Rock Sample Descriptions

1997 KLUANE PROPERTY ROCK SAMPLES

RX #	Location	NTS Sheet	UTM Coordinates		Sample Type	Rock Description
			Easting	Northing		
331044	Anomaly C	115 G/2	618450	6775830	Grab	Maple Creek Gabbro? Gray, medium grained. Blocky outcrop. Trace pyrrhotite.
331045	Anomaly C	115 G/2	618120	6775450	Grab	Very light gray, siliceous, pyritic, vuggy. Up to 40% fracture-related pyrite.
331046	Anomaly C	115 G/2	617620	6775870	Grab	Discontinuous calcite vein in gabbro with 7% disseminated pyrite.

APPENDIX 3

Rock Sample Analytical Results



Chemex Labs, Inc.

Analytical Chemists * Geochemists * Registered Assayers

994 Glendale Ave., Unit 3, Sparks
Nevada, U.S.A. 89431
PHONE: 702-356-5395 FAX: 702-355-0179

To: AMERICAN COPPER & NICKEL CO.

4400 BUSINESS PARK BLVD., BLDG. B, STE. 48
ANCHORAGE, ALASKA
99503-7118

A9736548

Comments: ATTN: GREG BEISCHER CC: KATHERINE HATTIE

CERTIFICATE

A9736548

(QQS) - AMERICAN COPPER & NICKEL COMPANY, INC.

Project: 66556
P.O. #: 665568597-02

Samples submitted to our lab in Anchorage, AK
This report was printed on 20-AUG-97.

SAMPLE PREPARATION

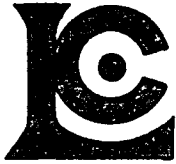
CHEMEX CODE	NUMBER SAMPLES	DESCRIPTION
1388	1	Ring 600 g to approx -150 mesh
226	1	0-3 Kg crush and split
3202	1	Rock - save entire reject
285	1	ICP - HF digestion charge

ANALYTICAL PROCEDURES

CHEMEX CODE	NUMBER SAMPLES	DESCRIPTION	METHOD	DETECTION LIMIT	UPPER LIMIT
8	1	Ni ppm: HNO3-aqua regia digest	AAS-BKGD CORR	1	10000
578	1	Ag ppm: 24 element, rock & core	AAS	0.2	100.0
573	1	Al %: 24 element, rock & core	ICP-AES	0.01	25.0
565	1	Ba ppm: 24 element, rock & core	ICP-AES	10	10000
575	1	Be ppm: 24 element, rock & core	ICP-AES	0.5	1000
561	1	Bi ppm: 24 element, rock & core	ICP-AES	2	10000
576	1	Ca %: 24 element, rock & core	ICP-AES	0.01	25.0
562	1	Cd ppm: 24 element, rock & core	ICP-AES	0.5	500
563	1	Co ppm: 24 element, rock & core	ICP-AES	1	10000
569	1	Cr ppm: 24 element, rock & core	ICP-AES	1	10000
577	1	Cu ppm: 24 element, rock & core	ICP-AES	1	10000
566	1	Fe %: 24 element, rock & core	ICP-AES	0.01	25.0
584	1	K %: 24 element, rock & core	ICP-AES	0.01	10.00
570	1	Mg %: 24 element, rock & core	ICP-AES	0.01	15.00
568	1	Mn ppm: 24 element, rock & core	ICP-AES	5	10000
554	1	Mo ppm: 24 element, rock & core	ICP-AES	1	10000
583	1	Na %: 24 element, rock & core	ICP-AES	0.01	10.00
564	1	Ni ppm: 24 element, rock & core	ICP-AES	1	10000
559	1	P ppm: 24 element, rock & core	ICP-AES	10	10000
560	1	Pb ppm: 24 element, rock & core	AAS	2	10000
582	1	Sr ppm: 24 element, rock & core	ICP-AES	1	10000
579	1	Ti %: 24 element, rock & core	ICP-AES	0.01	10.00
572	1	V ppm: 24 element, rock & core	ICP-AES	1	10000
556	1	W ppm: 24 element, rock & core	ICP-AES	10	10000
558	1	Zn ppm: 24 element, rock & core	ICP-AES	2	10000

The results of this assay were based solely upon the content of the sample submitted. Any decision to invest should be made only after the potential investment value of the claim or deposit has been determined based on the results of assays of multiple samples of geologic materials collected by the prospective investor or by a qualified person selected by him/her and based on an evaluation of all engineering data which is available concerning any proposed project

Statement required by Nevada State Law NRS 519



Chemex Labs, Inc.

Analytical Chemists * Geochemists * Registered Assayers
994 Glendale Ave., Unit 3, Sparks
Nevada, U.S.A. 89431
PHONE: 702-356-5395 FAX: 702-355-0179

To: AMERICAN COPPER & NICKEL CO.

4400 BUSINESS PARK BLVD., BLDG. B, STE. 48
ANCHORAGE, ALASKA
99503-7118

Project : 66556
Comments: ATTN: GREG BEISCHER CC: KATHERINE HATTIE

Page Number :1-A
Total Pages :1
Certificate Date: 20-AUG-97
Invoice No. :19736548
P.O. Number :665568597-0
Account :KQS

CERTIFICATE OF ANALYSIS A9736548

SAMPLE	PREP CODE	Ni ppm	Ag ppm AAS	Al % (ICP)	Ba ppm (ICP)	Be ppm (ICP)	Bi ppm (ICP)	Ca % (ICP)	Cd ppm (ICP)	Co ppm (ICP)	Cr ppm (ICP)	Cu ppm (ICP)	Fe % (ICP)	K % (ICP)	Mg % (ICP)
RX331044	1388 226	64	< 0.2	7.00	670	< 0.5	< 2	5.14	0.5	31	340	94	5.62	1.68	4.02

CERTIFICATION: Hatt Bichler



Chemex Labs, Inc.

Analytical Chemists * Geochemists * Registered Assayers

994 Glendale Ave., Unit 3, Sparks
Nevada, U.S.A. 89431
PHONE: 702-356-5395 FAX: 702-355-0179

To: AMERICAN COPPER & NICKEL CO.

4400 BUSINESS PARK BLVD., BLDG. B, STE. 48
ANCHORAGE, ALASKA
99503-7118

Project : 66556

Comments: ATTN: GREG BEISCHER CC: KATHERINE HATTIE

Page Number :1-B

Total Pages :1

Certificate Date: 20-AUG-97

Invoice No. :19736548

P.O. Number :665568597-0

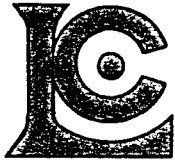
Account :KQS

CERTIFICATE OF ANALYSIS

A9736548

SAMPLE	PREP CODE		Mn ppm (ICP)	Mo ppm (ICP)	Na % (ICP)	Ni ppm (ICP)	P ppm (ICP)	Pb ppm AAS	Sr ppm (ICP)	Ti % (ICP)	V ppm (ICP)	W ppm (ICP)	Zn ppm (ICP)			
RX331044	1388	226	960	1	1.76	81	320	< 2	186	0.48	250	< 10	64			

CERTIFICATION: *Hatt H. Beischer*



Chemex Labs, Inc.

Analytical Chemists * Geochemists * Registered Assayers
 994 Glendale Ave., Unit 3, Sparks
 Nevada, U.S.A. 89431
 PHONE: 702-356-5395 FAX: 702-355-0179

To: AMERICAN COPPER & NICKEL CO.

4400 BUSINESS PARK BLVD., BLDG. B, STE. 48
 ANCHORAGE, ALASKA
 99503-7118

A9736549

Comments: ATTN: GREG BEISCHER CC: KATHERINE HATTIE

CERTIFICATE **A9736549**

(QOS) - AMERICAN COPPER & NICKEL COMPANY, INC.

Project: 66556
 P.O.#: 665568597-03

Samples submitted to our lab in Anchorage, AK
 This report was printed on 18-AUG-97.

SAMPLE PREPARATION		
CHEMEX CODE	NUMBER SAMPLES	DESCRIPTION
1388	2	Ring 600 g to approx -150 mesh
226	2	0-3 Kg crush and split
3202	2	Rock - save entire reject
233	2	Assay AQ ICP digestion charge

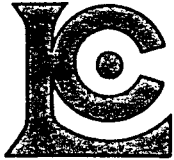
* NOTE 1:

The 32 element ICP package is suitable for trace metals in soil and rock samples. Elements for which the nitric-aqua regia digestion is possibly incomplete are: Al, Ba, Be, Ca, Cr, Ga, K, La, Mg, Na, Sr, Ti, Tl, W.

ANALYTICAL PROCEDURES

CHEMEX CODE	NUMBER SAMPLES	DESCRIPTION	METHOD	DETECTION LIMIT	UPPER LIMIT
975	2	Au ppb: ICP-fluorescence package	FA-ICP-AFS	2	10000
976	2	Pt ppb: ICP-Fluorescence package	FA-ICP-AFS	5	10000
977	2	Pd ppb: ICP-fluorescence package	FA-ICP-AFS	2	10000
4001	2	Ag ppm : A30 ICP package	ICP-AES	1	200
4002	2	Al %: A30 ICP package	ICP-AES	0.01	15.00
4003	2	As ppm: A30 ICP package	ICP-AES	10	50000
4004	2	Ba ppm: A30 ICP package	ICP-AES	20	200000
4005	2	Be ppm: A30 ICP package	ICP-AES	5	100
4006	2	Bi ppm: A30 ICP package	ICP-AES	10	50000
4007	2	Ca %: A30 ICP package	ICP-AES	0.01	30.0
4008	2	Cd ppm: A30 ICP package	ICP-AES	5	1000
4009	2	Co ppm: A30 ICP package	ICP-AES	5	50000
4010	2	Cr ppm: A30 ICP package	ICP-AES	10	20000
4011	2	Cu ppm: A30 ICP package	ICP-AES	5	50000
4012	2	Fe %: A30 ICP package	ICP-AES	0.01	30.0
4013	2	Hg ppm: A30 ICP package	ICP-AES	10	10000
4014	2	K %: A30 ICP package	ICP-AES	0.01	20.0
4015	2	Mg %: A30 ICP package	ICP-AES	0.01	30.0
4016	2	Mn ppm: A30 ICP package	ICP-AES	10	50000
4017	2	Mo ppm: A30 ICP package	ICP-AES	5	50000
4018	2	Na %: A30 ICP package	ICP-AES	0.01	20.0
4019	2	Ni ppm: A30 ICP package	ICP-AES	5	50000
4020	2	P ppm: A30 ICP package	ICP-AES	100	10000
4021	2	Pb ppm: A30 ICP package	ICP-AES	5	50000
4022	2	Sb ppm: A30 ICP package	ICP-AES	10	10000
4023	2	Sc ppm: A30 ICP package	ICP-AES	5	10000
4024	2	Sr ppm: A30 ICP package	ICP-AES	5	10000
4025	2	Ti %: A30 ICP package	ICP-AES	0.01	10.00
4026	2	Tl ppm: A30 ICP package	ICP-AES	20	10000
4027	2	U ppm: A30 ICP package	ICP-AES	20	10000
4028	2	V ppm: A30 ICP package	ICP-AES	20	50000
4029	2	W ppm: A30 ICP package	ICP-AES	20	10000
4030	2	Zn ppm: A30 ICP package	ICP-AES	5	50000

The results of this assay were based solely upon the content of the sample submitted. Any decision to invest should be made only after the potential investment value of the claim or deposit has been determined based on the results of assays of multiple samples of geologic materials collected by the prospective investor or by a qualified person selected by him/her and based on an evaluation of all engineering data which is available concerning any proposed project
 Statement required by Nevada State Law NRS 519



Chemex Labs, Inc.

Analytical Chemists * Geochemists * Registered Assayers

994 Glendale Ave., Unit 3, Sparks
Nevada, U.S.A. 89431
PHONE: 702-356-5395 FAX: 702-355-0179

To: AMERICAN COPPER & NICKEL CO.

4400 BUSINESS PARK BLVD., BLDG. B, STE. 48
ANCHORAGE, ALASKA
99503-7118

Project : 66556

Comments: ATTN: GREG BEISCHER CC: KATHERINE HATTIE

Page Number :1-A

Total Pages :1

Certificate Date: 18-AUG-97

Invoice No. :19736549

P.O. Number :665568597-0

Account :KQS

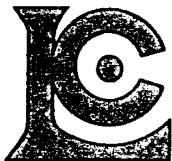
CERTIFICATE OF ANALYSIS

A9736549

SAMPLE	PREP CODE		Au	Pt	Pd	Ag	Al	As	Ba	Be	Bi	Ca	Cd	Co	Cr	Cu	Fe	Hg	K	Mg	Mn
			ppb AFS	ppb AFS	ppb AFS	ppm	%	ppm	ppm	ppm	ppm	ppm	%	ppm	ppm	ppm	ppm	%	ppm	%	%
RX331045	1388	226	< 2	< 5	< 2	< 1	0.37	40	460	< 5	< 10	0.09	< 5	< 5	< 10	15	9.65	< 10	0.18	0.05	60
RX331046	1388	226	< 2	< 5	< 2	< 1	2.76	< 10	200	< 5	< 10	2.23	< 5	35	70	45	6.32	< 10	0.09	2.97	490

CERTIFICATION:

Hanti Buchler



Chemex Labs, Inc.

Analytical Chemists * Geochemists * Registered Assayers
994 Glendale Ave., Unit 3, Sparks
Nevada, U.S.A. 89431
PHONE: 702-356-5395 FAX: 702-355-0179

To: AMERICAN COPPER & NICKEL CO.

4400 BUSINESS PARK BLVD., BLDG. B, STE. 48
ANCHORAGE, ALASKA
99503-7118

Project: 66556

Comments: ATTN: GREG BEISCHER CC: KATHERINE HATTIE

Page Number : 1-B
Total Pages : 1
Certificate Date: 18-AUG-97
Invoice No. : 19736549
P.O. Number : 665568597
Account : KQS

CERTIFICATE OF ANALYSIS

A9736549

SAMPLE	PREP		Mo	Na	Ni	P	Pb	Sb	Sc	Sr	Ti	Tl	U	V	W	Zn
	CODE		ppm	%	ppm	ppm	ppm	ppm	ppm	ppm	%	ppm	ppm	ppm	ppm	ppm
RX331045	1388	226	< 5	0.05	35	< 100	45	< 10	< 5	5	< 0.01	< 20	< 20	< 20	< 20	30
RX331046	1388	226	< 5	0.08	35	600	< 5	< 10	10	35	0.35	< 20	< 20	140	20	35

CERTIFICATION:

Hatt Biehler

APPENDIX 4

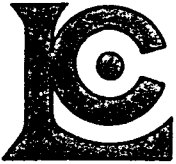
Silt Sample Descriptions

1997 KLUANE PROPERTY SILT SAMPLES

SX #	Location	Sample Type	NTS Sheet	UTM Coordinates		Sample Description
				Easting	Northing	
167301	Anomaly C	Silt	115 G/2	618250	6775440	Stream 4 m wide, fine sediment accumulation in eddy.
167302	Anomaly C	Silt	115 G/2	618230	6775340	Stream 3 m wide, moderate flow.
167303	Anomaly C	Silt	115 G/2	618085	6775610	Stream 4 m wide, moderate to rapid current.
167304	Anomaly C	Silt	115 G/2	617900	6775730	Stream 5 m wide, rapid current, gentle grade.
167305	Anomaly C	Silt	115 G/2	618020	6775740	Stream 1 m wide.
167306	Anomaly C	Silt	115 G/2	617680	6775820	Stream 4 m wide, rapid flow.

APPENDIX 5

Silt Sample Analytical Results



Chemex Labs, Inc.

Analytical Chemists • Geochemists • Registered Assayers

994 Glendale Ave., Unit 3,
Nevada, U.S.A.

Sparks
89431

PHONE: 702-356-5395 FAX: 702-355-0179

To: AMERICAN COPPER & NICKEL CO.

4400 BUSINESS PARK BLVD., BLDG. B, STE. 48
ANCHORAGE, ALASKA
99503-7118

A9736547

Comments: ATTN: GREG BEISCHER CC: KATHERINE HATTIE

CERTIFICATE

A9736547

(KQS) - AMERICAN COPPER & NICKEL COMPANY, INC.

Project: 66556
P.O. #: 665568597-01

Samples submitted to our lab in Anchorage, AK
This report was printed on 15-AUG-97.

SAMPLE PREPARATION

CHEMEX CODE	NUMBER SAMPLES	DESCRIPTION
241	6	RUSH: Dry, sieve to -80 mesh
202	6	save reject
229	6	ICP - AQ Digestion charge

* NOTE 1:

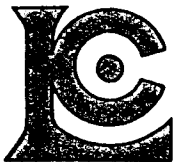
The 32 element ICP package is suitable for trace metals in soil and rock samples. Elements for which the nitric-aqua regia digestion is possibly incomplete are: Al, Ba, Be, Ca, Cr, Ga, K, La, Mg, Na, Sr, Ti, Tl, W.

ANALYTICAL PROCEDURES

CHEMEX CODE	NUMBER SAMPLES	DESCRIPTION	METHOD	DETECTION LIMIT	UPPER LIMIT
975	6	Au ppb: ICP-fluorescence package	FA-ICP-AFS	2	10000
976	6	Pt ppb: ICP-Fluorescence package	FA-ICP-AFS	5	10000
977	6	Pd ppb: ICP-fluorescence package	FA-ICP-AFS	2	10000
2118	6	Ag ppm: 32 element, soil & rock	ICP-AES	0.2	100.0
2119	6	Al %: 32 element, soil & rock	ICP-AES	0.01	15.00
2120	6	As ppm: 32 element, soil & rock	ICP-AES	2	10000
2121	6	Ba ppm: 32 element, soil & rock	ICP-AES	10	10000
2122	6	Be ppm: 32 element, soil & rock	ICP-AES	0.5	100.0
2123	6	Bi ppm: 32 element, soil & rock	ICP-AES	2	10000
2124	6	Ca %: 32 element, soil & rock	ICP-AES	0.01	15.00
2125	6	Cd ppm: 32 element, soil & rock	ICP-AES	0.5	100.0
2126	6	Co ppm: 32 element, soil & rock	ICP-AES	1	10000
2127	6	Cr ppm: 32 element, soil & rock	ICP-AES	1	10000
2128	6	Cu ppm: 32 element, soil & rock	ICP-AES	1	10000
2150	6	Fe %: 32 element, soil & rock	ICP-AES	0.01	15.00
2130	6	Ga ppm: 32 element, soil & rock	ICP-AES	10	10000
2131	6	Hg ppm: 32 element, soil & rock	ICP-AES	1	10000
2132	6	K %: 32 element, soil & rock	ICP-AES	0.01	10.00
2151	6	La ppm: 32 element, soil & rock	ICP-AES	10	10000
2134	6	Mg %: 32 element, soil & rock	ICP-AES	0.01	15.00
2135	6	Mn ppm: 32 element, soil & rock	ICP-AES	5	10000
2136	6	Mo ppm: 32 element, soil & rock	ICP-AES	1	10000
2137	6	Na %: 32 element, soil & rock	ICP-AES	0.01	5.00
2138	6	Ni ppm: 32 element, soil & rock	ICP-AES	1	10000
2139	6	P ppm: 32 element, soil & rock	ICP-AES	10	10000
2140	6	Pb ppm: 32 element, soil & rock	ICP-AES	2	10000
2141	6	Sb ppm: 32 element, soil & rock	ICP-AES	2	10000
2142	6	Sc ppm: 32 elements, soil & rock	ICP-AES	1	10000
2143	6	Sr ppm: 32 element, soil & rock	ICP-AES	1	10000
2144	6	Ti %: 32 element, soil & rock	ICP-AES	0.01	5.00
2145	6	Tl ppm: 32 element, soil & rock	ICP-AES	10	10000
2146	6	U ppm: 32 element, soil & rock	ICP-AES	10	10000
2147	6	V ppm: 32 element, soil & rock	ICP-AES	1	10000
2148	6	W ppm: 32 element, soil & rock	ICP-AES	10	10000
2149	6	Zn ppm: 32 element, soil & rock	ICP-AES	2	10000

The results of this assay were based solely upon the content of the sample submitted. Any decision to invest should be made only after the potential investment value of the claim or deposit has been determined based on the results of assays of multiple samples of geologic materials collected by the prospective investor or by a qualified person selected by him/her and based on an evaluation of all engineering data which is available concerning any proposed project

Statement required by Nevada State Law NRS 519



Chemex Labs, Inc.

Analytical Chemists * Geochemists * Registered Assayers

994 Glendale Ave., Unit 3, Sparks
Nevada, U.S.A. 89431
PHONE: 702-356-5395 FAX: 702-355-0179

To: AMERICAN COPPER & NICKEL CO.

4400 BUSINESS PARK BLVD., BLDG. B, STE. 48
ANCHORAGE, ALASKA
99503-7118

Project: 66556
Comments: ATTN: GREG BEISCHER CC: KATHERINE HATTIE

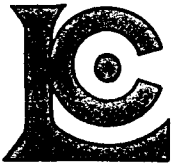
Page Number : 1-A
Total Pages : 1
Certificate Date: 15-AUG-97
Invoice No. : 19736547
P.O. Number : 665568597-0
Account : KQS

CERTIFICATE OF ANALYSIS A9736547

SAMPLE	PREP CODE		Au ppb	Pt ppb	Pd ppb	Ag ppm	Al %	As ppm	Ba ppm	Be ppm	Bi ppm	Ca %	Cd ppm	Co ppm	Cr ppm	Cu ppm	Fe %	Ga ppm	Hg ppm	K %	La ppm
			AFS	AFS	AFS																
SX167301	241	202	< 2	< 5	10	1.0	1.08	12	190	< 0.5	< 2	2.17	2.5	18	44	54	3.65	< 10	< 1	0.09	10
SX167302	241	202	< 2	< 5	20	< 0.2	0.95	< 2	190	< 0.5	< 2	4.07	0.5	40	164	76	5.62	< 10	< 1	0.03	< 10
SX167303	241	202	< 2	< 5	16	< 0.2	1.01	< 2	200	< 0.5	< 2	4.29	0.5	42	167	76	5.19	< 10	< 1	0.03	< 10
SX167304	241	202	< 2	< 5	16	0.2	1.05	6	250	< 0.5	< 2	4.41	0.5	43	169	79	5.16	< 10	< 1	0.03	< 10
SX167305	241	202	< 2	< 5	6	0.2	0.82	< 2	80	< 0.5	< 2	1.52	0.5	13	24	21	3.37	< 10	< 1	0.04	10
SX167306	241	202	< 2	10	16	0.2	1.22	10	310	< 0.5	< 2	4.48	0.5	47	192	91	5.93	< 10	< 1	0.04	< 10

CERTIFICATION:

Hatt Biechler



Chemex Labs, Inc.

Analytical Chemists * Geochemists * Registered Assayers
 994 Glendale Ave., Unit 3, Sparks
 Nevada, U.S.A. 89431
 PHONE: 702-356-5395 FAX: 702-355-0179

To: AMERICAN COPPER & NICKEL CO.

4400 BUSINESS PARK BLVD., BLDG. B, STE. 48
 ANCHORAGE, ALASKA
 99503-7118

Page Number : 1-B
 Total Pages : 1
 Certificate Date: 15-AUG-97
 Invoice No. : 19736547
 P.O. Number : 665568597-0
 Account : KQS

Project : 66556

Comments: ATTN: GREG BEISCHER CC: KATHERINE HATTIE

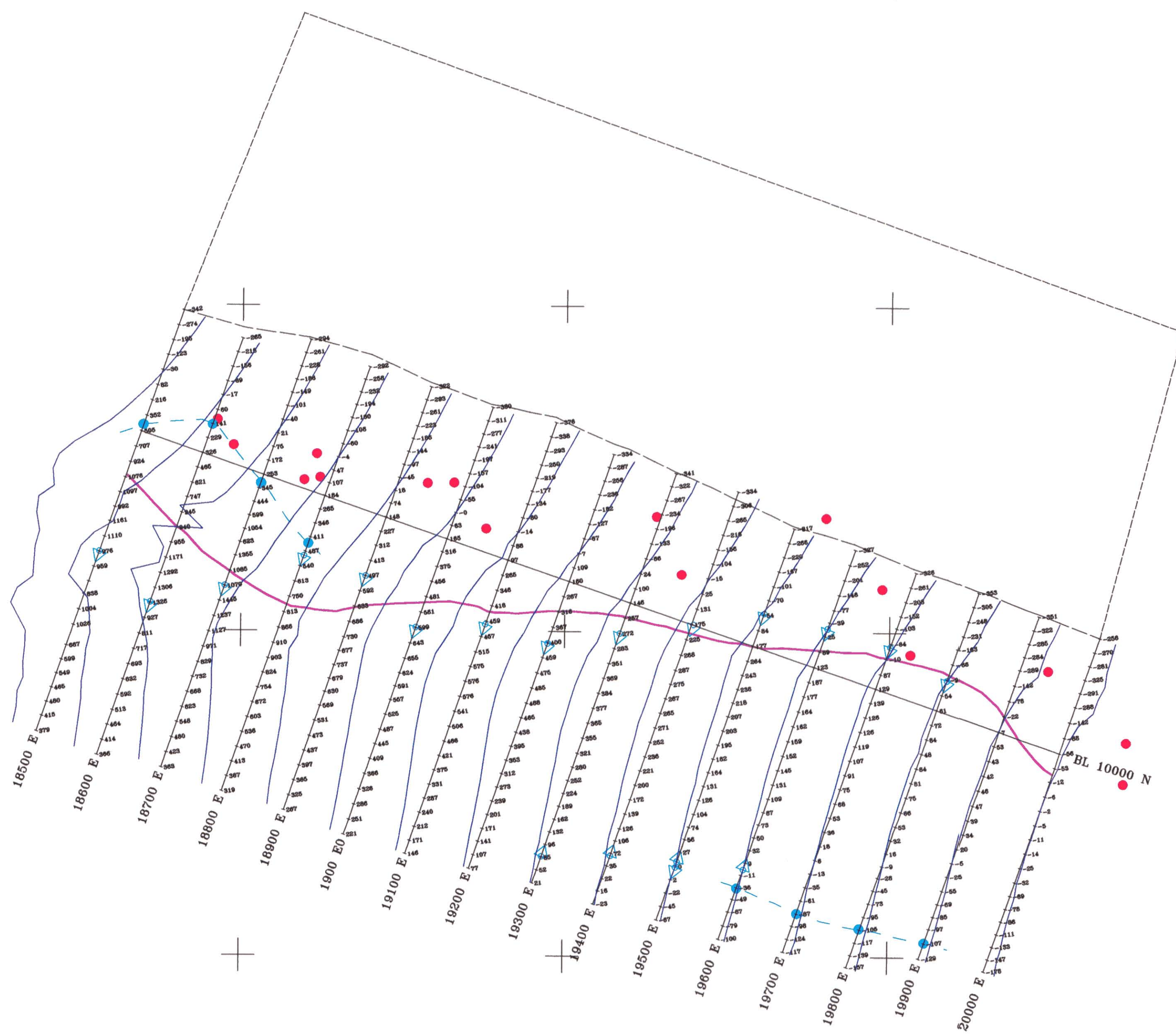
CERTIFICATE OF ANALYSIS

A9736547

SAMPLE	PREP CODE		Mg	Mn	Mo	Na	Ni	P	Pb	Sb	Sc	Sr	Ti	Tl	U	V	W	Zn
			%	ppm	ppm	%	ppm	ppm	ppm	ppm	ppm	ppm	%	ppm	ppm	ppm	ppm	ppm
SX167301	241	202	0.99	650	4	0.01	67	1200	4	< 2	7	66	0.03	< 10	< 10	68	< 10	198
SX167302	241	202	4.40	855	1	< 0.01	281	390	< 2	< 2	7	45	0.05	< 10	< 10	70	< 10	84
SX167303	241	202	4.38	940	1	< 0.01	295	480	2	< 2	8	48	0.04	< 10	< 10	65	< 10	92
SX167304	241	202	4.44	975	1	< 0.01	299	490	4	< 2	8	50	0.04	< 10	< 10	68	< 10	96
SX167305	241	202	1.01	975	1	< 0.01	25	1620	< 2	< 2	6	31	0.12	< 10	< 10	72	< 10	88
SX167306	241	202	4.57	975	1	< 0.01	324	580	< 2	< 2	9	57	0.07	< 10	< 10	85	< 10	110

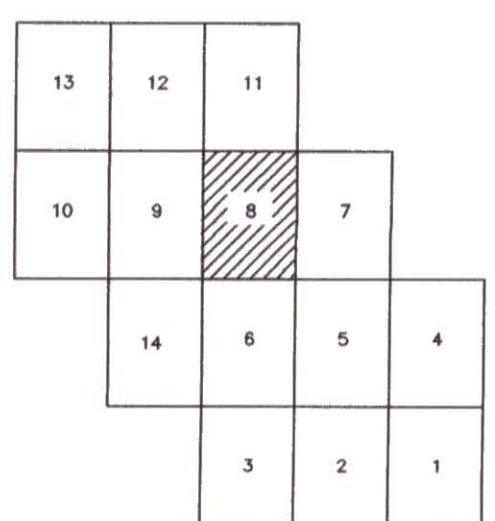
CERTIFICATION:

Hatt Buehler



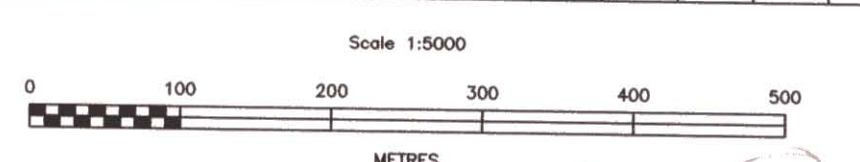
093726

SHEET 8



Contour Interval = 100 feet

- 1996 AEM Conductor
- Discrete UTEM Conductor
- ◆ Broad UTEM Conductor Showing Conductive Edge
- Trace of Magnetic Body
- Profiles of Total Magnetic Intensity (plotted and posted with respect to station with 57500nT baselevel)
- UTEM Loop
- Grid Line

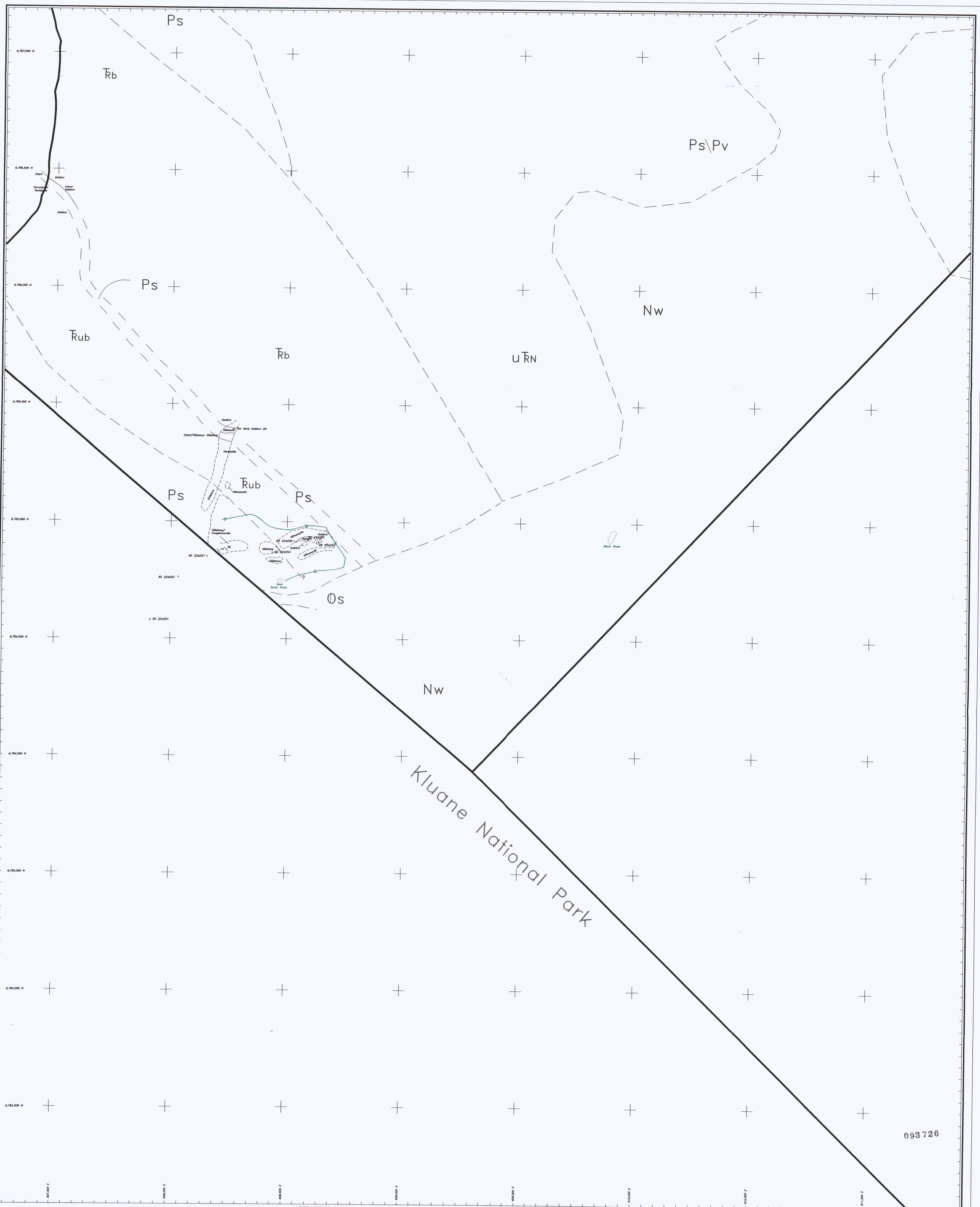


INCO EXPLORATION
 Anchorage AK
 4400 Business Park Blvd.
 Suite 48
 99503

Project: KLU PROJECT Area: KLUANE LAKE, YUKON TERRITORY

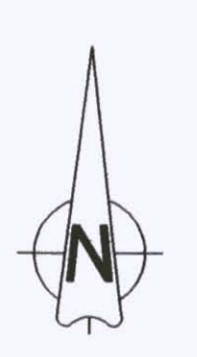
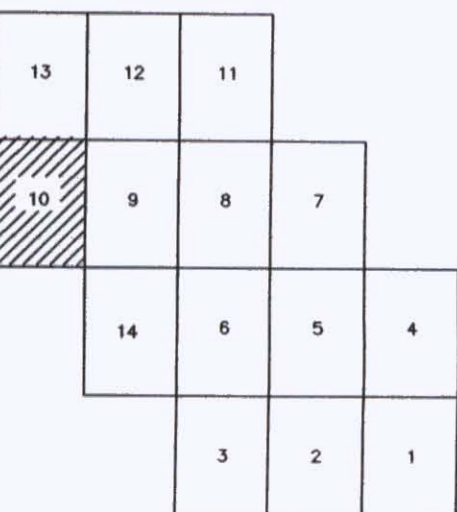
GROUND MAGNETIC & UTEM SURVEY RESULTS

Compiled by: C. Bell, S. Cosselman, K. Hattie	Supervisor: K. Hattie	Date drawn: Sept 08, 1997
Drawn by: Victor Fisher	Revised by:	Revised: Nov 19, 1997
Scale: 1:5000	N.T.S. 1:150/2	File: KLUsheet08.dwg
		Map 4



093726

SHEET 10



Contour Interval = 100 feet

1997 mapping indicated in green.

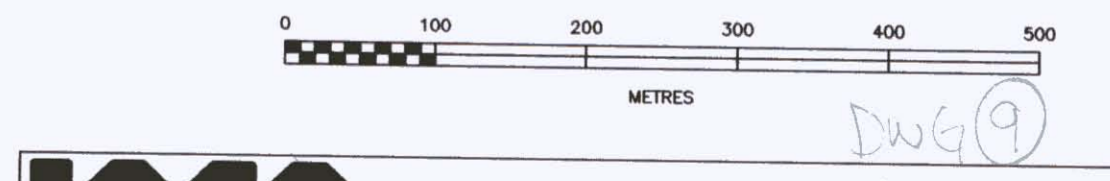
STRATIFIED ROCKS

Tertiary (Miocene - Pliocene)	
Nw	Wrangell Lava (undivided) Basalt to Andesite flows, minor white to yellow felsic pyroclastics and flows
Tertiary (Oligocene)	
Os	Amphitheatre Formation Yellow-buff to gray-buff sandstone, pebbly sandstone, pyroclastic conglomerate
Upper Triassic - Cretaceous	
UTr	Dark gray phyllite, minor greywacke and conglomerate
Upper Triassic	
UTr	McCarty Formation White to creamy-white gypsum and anhydrite
UTr	Chilton and Nizna Formations Massive light gray limestone, limestone breccia, and dark gray well bedded limestone
UTr	Nikolai Formation Dark green and maroon amygdaloidal to massive basaltic and andesitic flows, locally interbedded with buff breccia, siltstone, pillow lava and conglomerate occur at base

INTRUSIVE ROCKS

Lower Permian	
Ps	Hassen Creek Formation This bedded altheous argillite, siltstone, shale, greywacke, conglomerate, local thin basalt flows
Ps	Hassen Creek Formation Buff to gray bioclastic limestone
Pennsylvanian	
Pv	Sitation Creek Formation Andesite to basaltic tuffs and flows
Tertiary (Miocene)	
IMF	Wrangell Plutonic Suite Buff to creamy-white granodiorite, diorite, gabbro dykes and sills, fine grained
IMd	Brook's Brook Sill Light buff-gray biotite diorite, medium grained
Triassic	
Rb	Maple Creek Gabbro Gabbro and anorthositic gabbro sills, medium grained
Rb	Kluane-type Ultramafic Pyroxenite, feldspathic peridotite sills with minor pyroxenite and dunite, medium grained
Rb	Kluane-type chilled gabbro Gray medium grained to fine grained locally Marginal Gabbro

•	Silt Sample Locations
X	Rock Sample Locations
—	fault
///	bedding (vertical, inclined)
///	cleavage (vertical, inclined)
///	foliation
///	lineation
///	shearing (vertical, inclined)
///	jointing
—	outcrop boundary
—	contact (defined, assumed)
—	traverse path showing direction of travel
—	property and park boundaries



INCO EXPLORATION

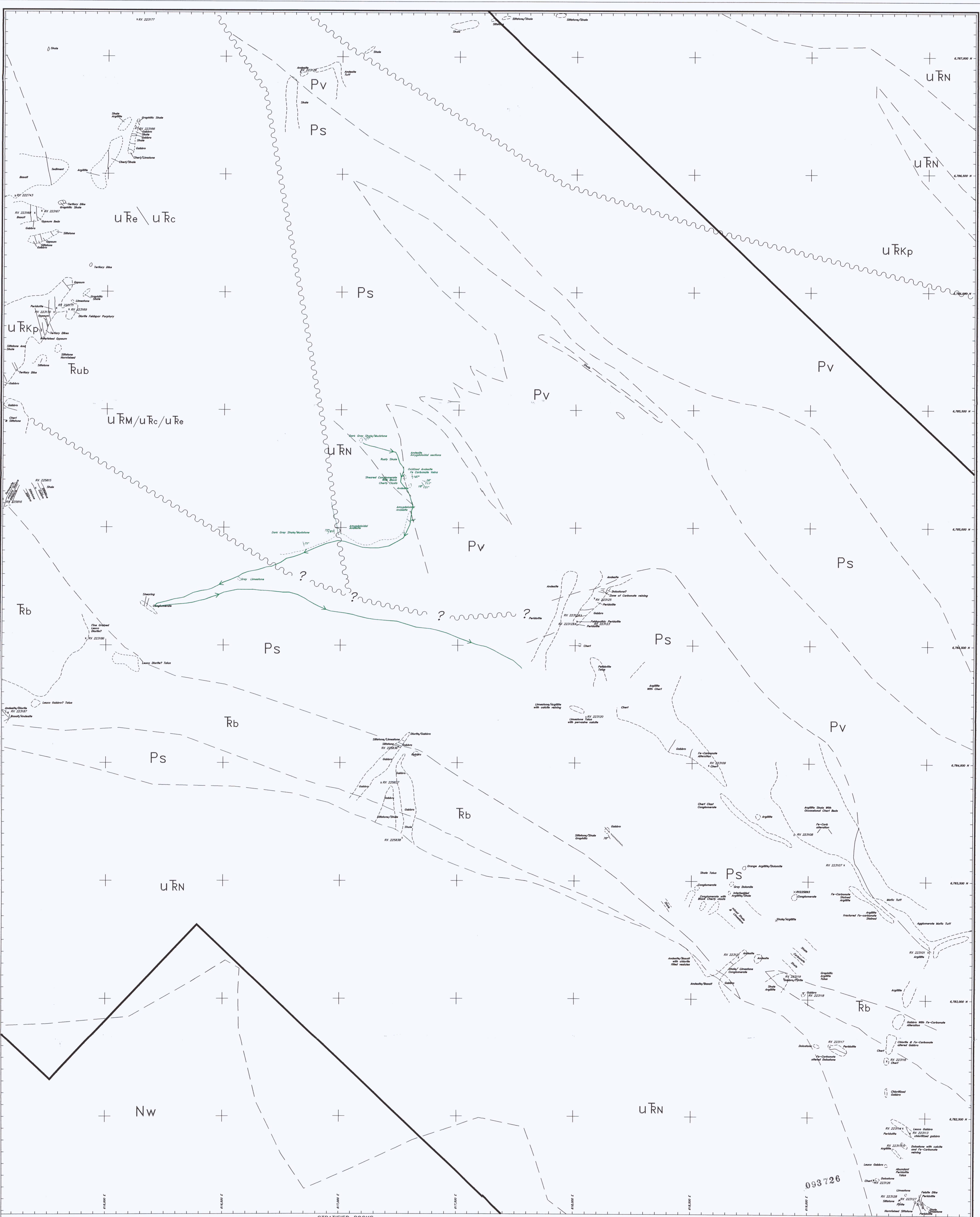
Project: KLU PROJECT Area: KLUANE LAKE, YUKON TERRITORY

GEOLOGY AND SAMPLE LOCATIONS

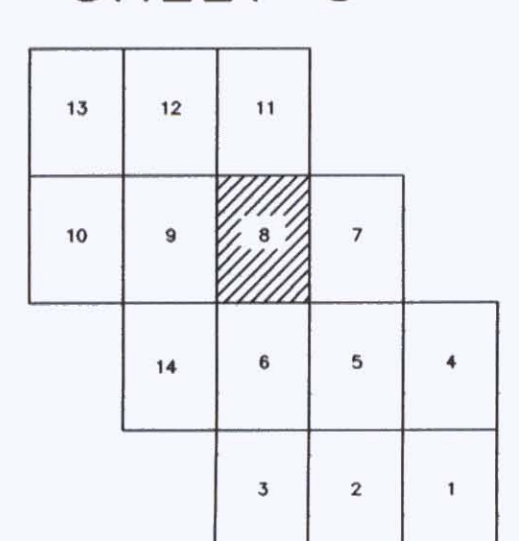
Compiled by: C. Bell, S. Casselman, K. Hottle Supervisor: K. Hottle Date drawn: Sept. 05, 1997

Drawn by: Victor Fisher Revised by: Revised: Nov 18, 1997

Scale: 1:5000 N.T.S. 1156/2 File: KLUsheet10geology.dwg Map 3



SHEET 8



Contour Interval = 100 feet

1997 mapping indicated in green.

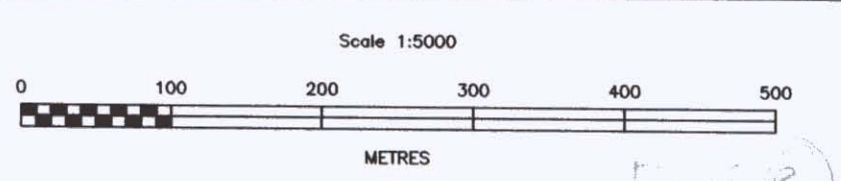
STRATIFIED ROCKS

Tertiary (Miocene - Pliocene)	Nw	Wongall Lava (undivided)	Basalt to Andesite flows, minor white to yellow tuffaceous pyroclastics and flows
Tertiary (Oligocene)	Os	Argillite Formation	Yellow-buff to gray-buff sandstone, pebbly sandstone, polymictic conglomerate
Upper Triassic - Cretaceous	UTrp		Dark Gray phyllite, minor graywacke and conglomerate
Upper Triassic	UTrs	McCarthy Formation	Argillaceous Limestone and dark Gray Argillite
	UTrs		White to creamy-white gypsum and anhydrite
	UTrs		Massive light Gray Limestone, Limestone breccia, and dark Gray well bedded Limestone
	UTrs		Dark green and massive conglomerated to massive basaltic and andesitic flows, locally interbedded with tuff, breccia, Shale, Limestone, pillow lava and Conglomerate occur at base

INTRUSIVE ROCKS

Lower Permian	Ps	Hosan Creek Formation	This bedded siliceous Argillite, siltstone, Shale, graywacke, Conglomerate, local thin basalt flows
	Pv	Hosan Creek Formation	Buff to Gray bioclastic Limestone
Pennsylvanian	RPv	Sheldon Creek Formation	Andesite to basaltic tuffs and flows
Tertiary (Miocene)	IMf	Wongall Plutonic Suite	Buff to creamy-white granodiorite, diorite, gabbro
	IMd	Boak's Brook Stock	Light buff-gray biotite diorite, medium grained
Triassic	Tb	Maple Creek Gabbro	Gabbro and anorthositic gabbro sill, medium grained
	Tb		Peridotite, feldspathic peridotite with minor pyroxene and dunite, medium grained
	Tmg	Kluane-type Ultramafite	Gray medium grained to fine grained locally Marginal Gabbro

Symbol	Description
●	silt sample locations
×	rock sample locations
—	fault
— / —	bedding (vertical, inclined)
— / — / —	cleavage (vertical, inclined)
— / — / — / —	foliation
— / — / — / — / —	lineation
— / — / — / — / — / —	shearing (vertical, inclined)
— / — / — / — / — / — / —	jointing
— / — / — / — / — / — / — / —	outcrop boundary
— / — / — / — / — / — / — / — / —	contact (defined, assumed)
— / — / — / — / — / — / — / — / — / —	traverse path showing direction of travel
— / — / — / — / — / — / — / — / — / — / —	property and park boundaries



INCO EXPLORATION

Project: KLU PROJECT Area: KLUANE LAKE, YUKON TERRITORY

GEOLOGY AND SAMPLE LOCATIONS

Compiled by: C. Bell, S. Casselman, K. Hostle Supervisor: K. Hostle Date drawn: Sept. 08, 1997

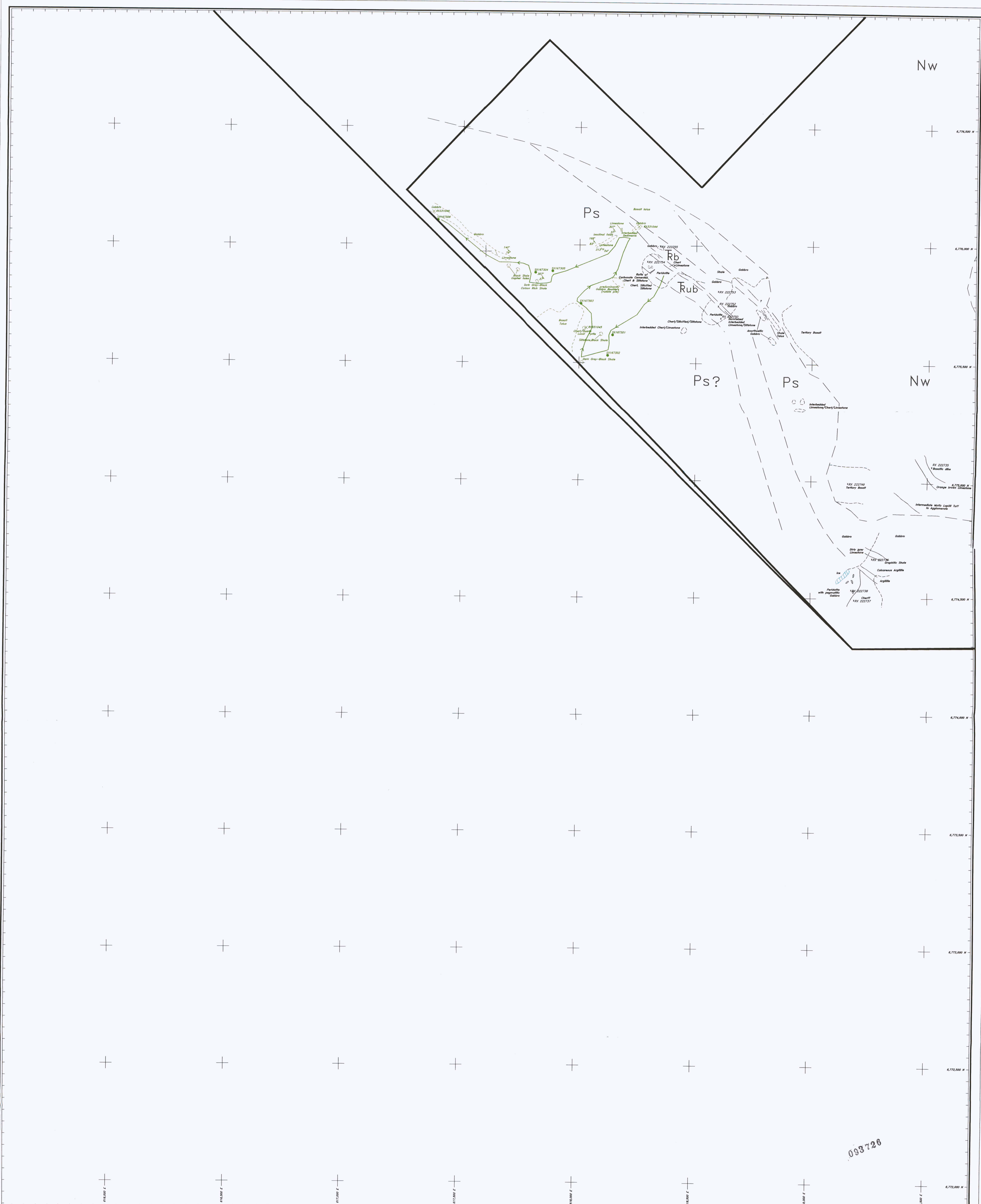
Drawn by: Victor Fisher Revised by: Reviewed: Nov. 19, 1997

Scale: 1:5000 N.T.S. 1156/2 File: KLUsheet08.dwg Map 3

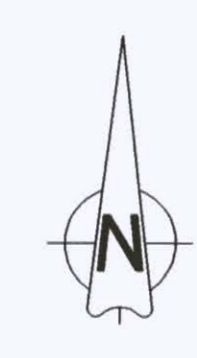
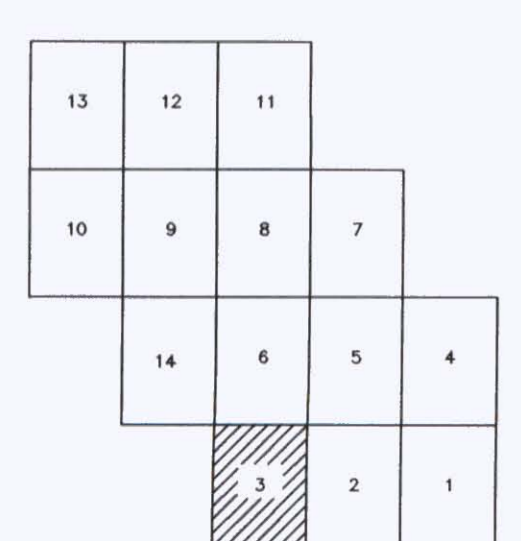
Nw

Nw

093726



SHEET 3



Contour interval = 100 feet

1987 mapping indicated in green.

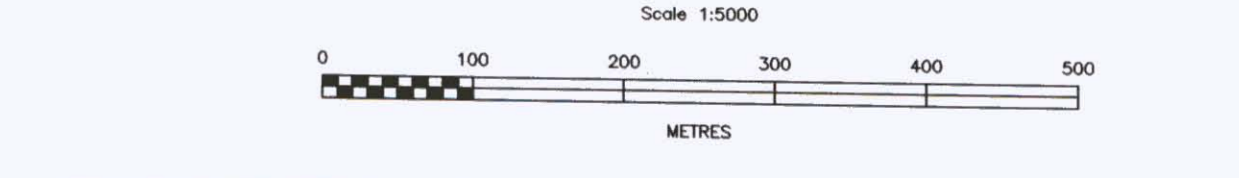
STRATIFIED ROCKS

Tertiary (Miocene - Pliocene)		
Nw	Wrangell Lava (undivided)	Basalt to andesite flows, minor white to yellow felsic pyroclastics and flows
Os	Angulimacine Formation	Yellow-buff to gray-buff sandstone, pebbly sandstone, polymictic conglomerate
Upper Triassic - Cretaceous		
U3c		Dark gray phyllite, minor greywacke and conglomerate
Upper Triassic		
U1b	McCarthy Formation	Argillaceous limestone and dark gray argillite
U1c		White to creamy-white gypsum and anhydrite
U1a	Chilona and Minto Formations	Massive light gray limestone, limestone breccia, and dark gray well bedded limestone
U1h	Minto Greenstone	Dark green and maroon amegdaloidal to massive basaltic and andesitic flows, locally interbedded with tuff, breccia, shale, limestone, pillow lava and conglomerate occur at base

INTRUSIVE ROCKS

Lower Permian		
P3	Hosen Creek Formation	This bedded siliceous argillite, siltstone, shale, greywacke, conglomerate, local thin basalt flows
Pc	Hosen Creek Formation	Buff to gray bioclastic limestone
Pennsylvanian		
Pv	Station Creek Formation	Andesite to basaltic tuffs and flows
Triassic		
IMf	Wrangell Plutonic Suite	Buff to creamy-white granodiorite, diorite, gabbro dykes and sills, fine grained
IMd	Back's Brook Stock	Light buff-gray biotite diorite, medium grained
Triassic		
Md	Maple Creek Gabbro	Gabbro and anorthositic gabbro sills, medium grained
Ku	Kluane-type Ultramafics	Peridotite, feldspathic peridotite sills with minor pyroxenite and dunite, medium grained
Tmg	Kluane-type chilled gabbro	Gray medium grained to fine grained locally marginal Gabbro

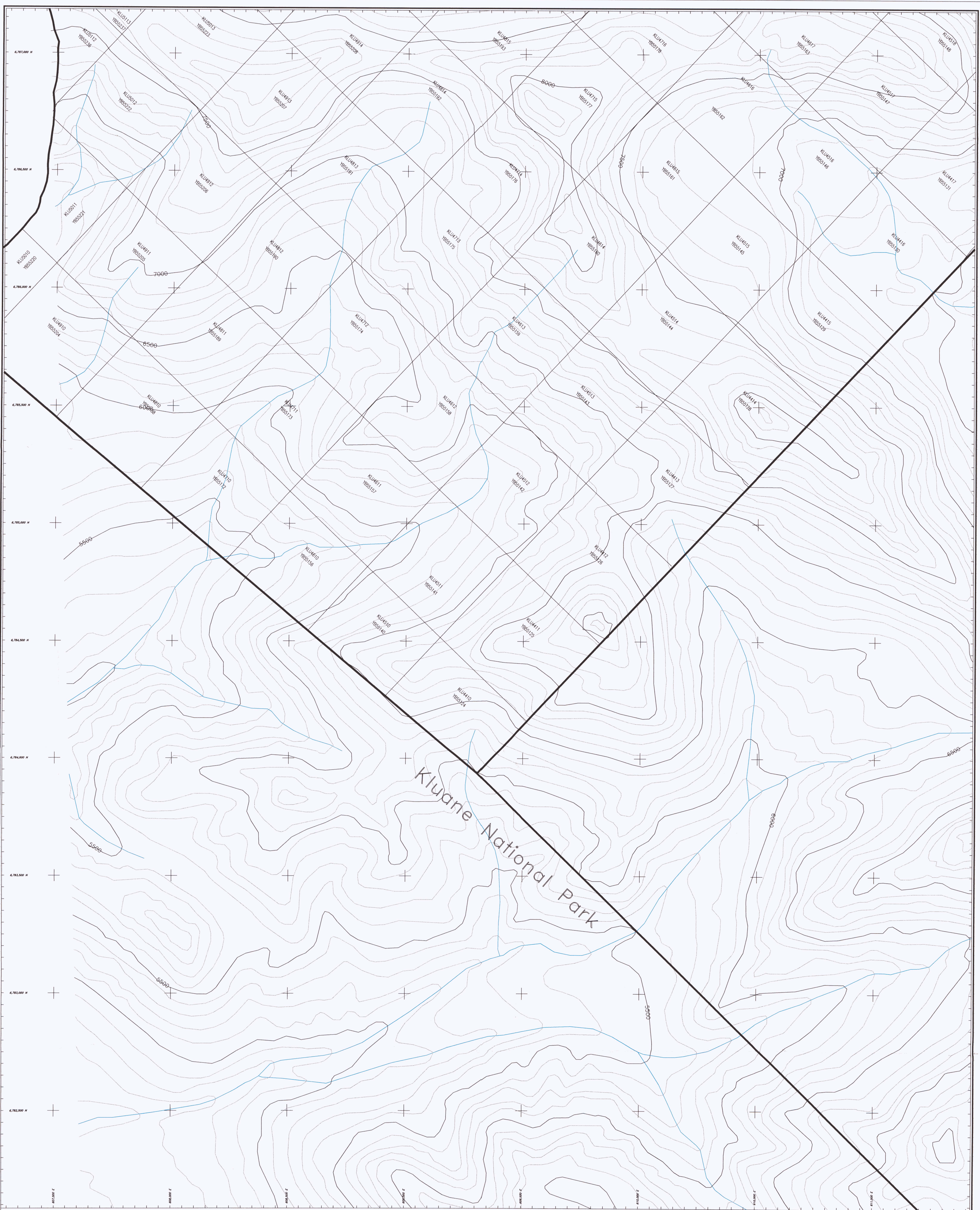
- SIH Sample Locations
- X Rock Sample Locations
- fault
- /// bedding (vertical, inclined)
- /// cleavage (vertical, inclined)
- fallation
- lineation
- /// shearing (vertical, inclined)
- jointing
- outcrop boundary
- contact (defined, assumed)
- traverse path showing direction of travel
- property and park boundaries



INCO EXPLORATION
 Project: KLU PROJECT Area: KLUANE LAKE, YUKON TERRITORY

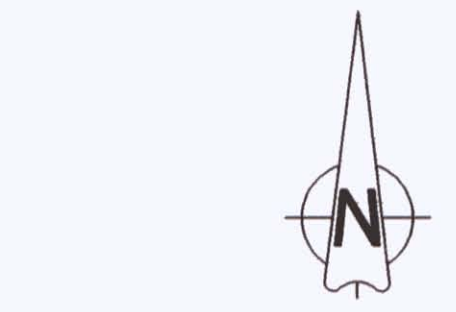
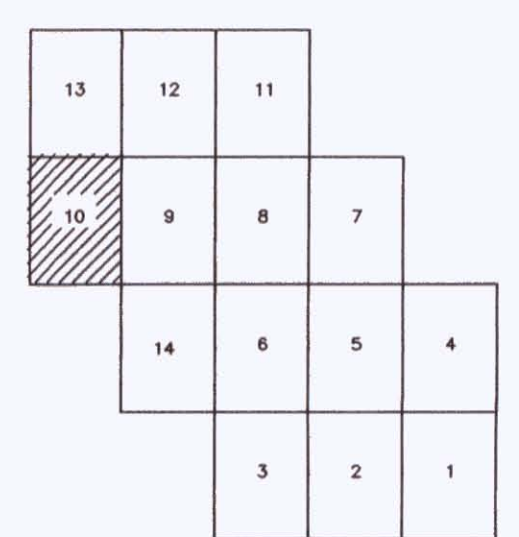
Geology and Sample Locations

Compiled by: C. Bell, S. Casselman, K. Hottle	Supervisor: K. Hottle	Date drawn: Sept. 28, 1997
Drawn by: Victor Fisher	Revised by: Victor Fisher	Revised: Nov. 20, 1997
Scale: 1:5000	N.T.S. 1156/2	File: KLUsheet3geology.dwg
		Map 3

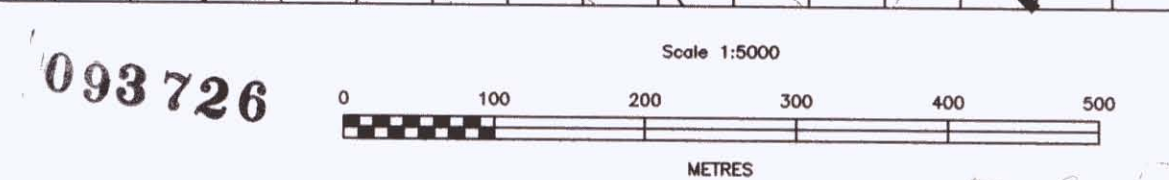


Kluane National Park

SHEET 10



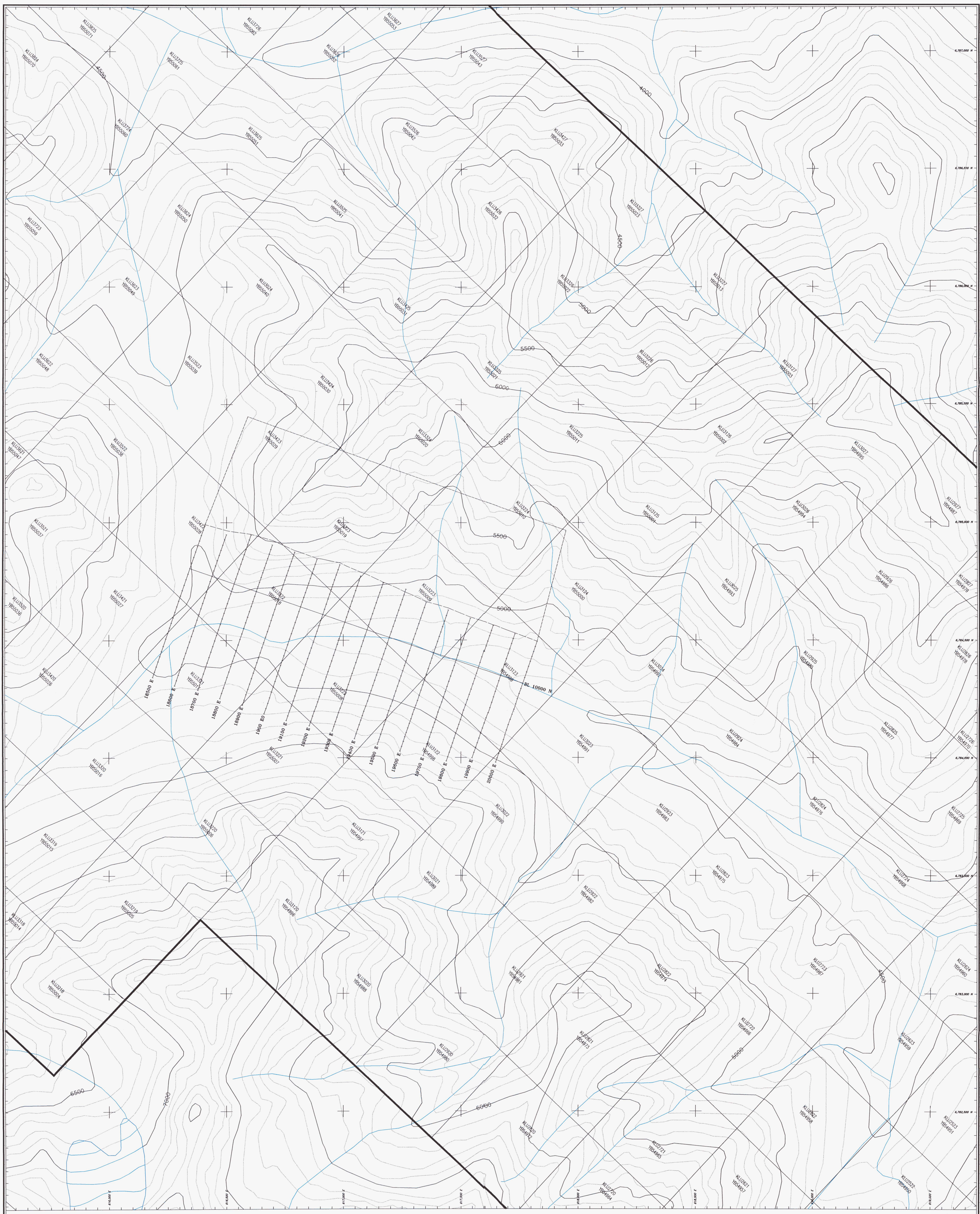
Contour Interval = 100 feet
 ——— Property and Park Boundaries



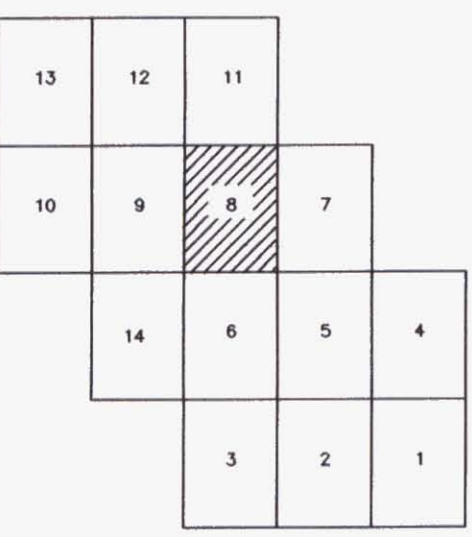
093 726
 Scale 1:5000
 METRES

INCO
 EXPLORATION
 Anchorage AK
 4400 Business Park Blvd.
 Suite 48
 99503

Project: KLU PROJECT		Area: KLIANE LAKE, YUKON TERRITORY	
CLAIM MAP: SHEET 10			
Compiled by: C. Bell, S. Casselman, K. Hattie	Supervisor: K. Hattie	Date drawn: Sept. 08, 1997	
Drawn by: Victor Fisher	Revised by:	Revised: Nov. 19, 1997	
Scale: 1:5000	N.T.S. 1:1562/2	File: KLUsheet10.dwg	Map: 2

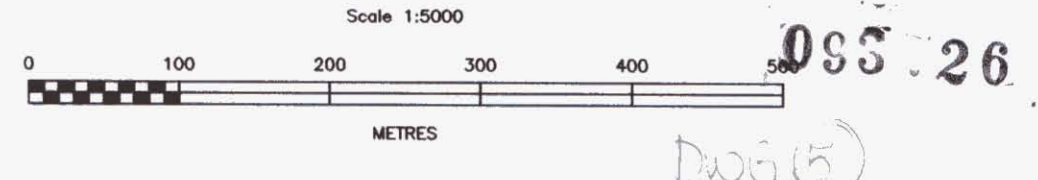


SHEET 8



Contour Interval = 100 feet

— Grid Line
 - - - UTEM Survey Loop

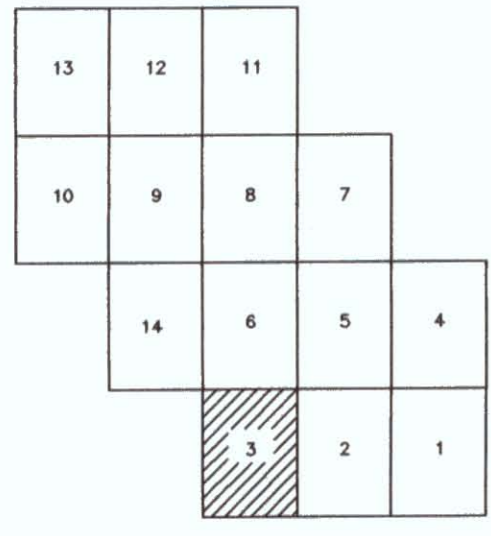


		Anchorage AK 4400 Business Park Blvd. Suite 48 99503	
Project: KLU PROJECT		Area: KLIANE LAKE, YUKON TERRITORY	
CLAIM MAP: SHEET 8			
Compiled by: C. Bell, S. Casselman, K. Hottle	Supervisor: K. Hottle	Date drawn: Sept 08, 1997	
Drawn by: Victor Fisher	Revised by:	Nov 19, 1997	
Scale: 1:5000	N.T.S. 1:150/2	File: KLUsheet08.dwg	Map 2



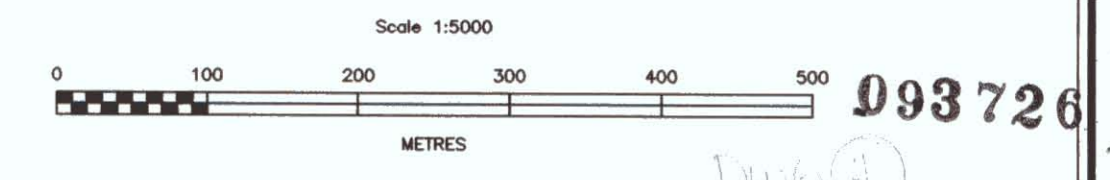
Right On Mtn

SHEET 3

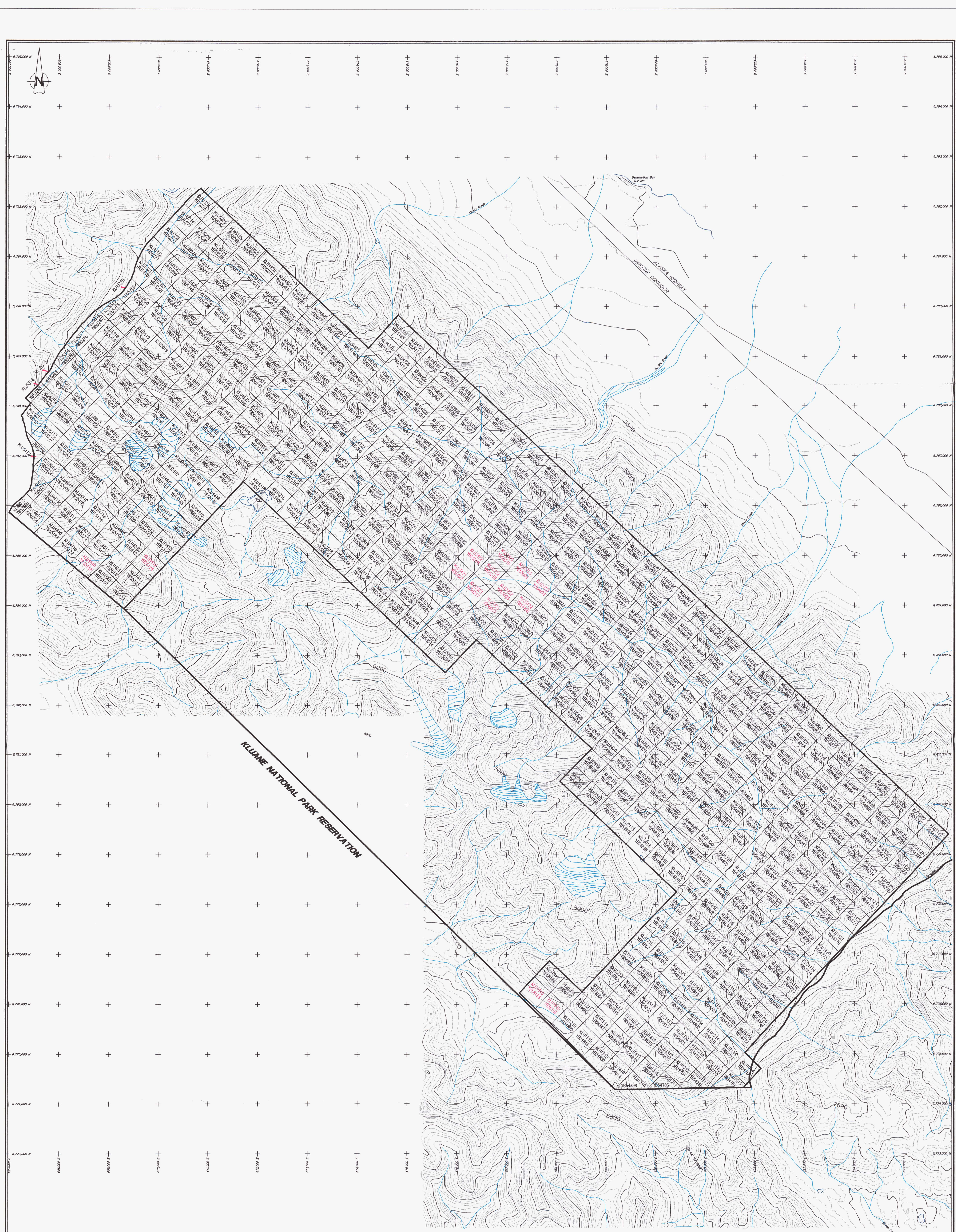


Contour interval = 100 feet

Property and Park Boundaries



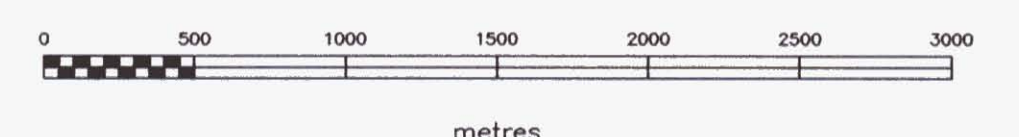
		Anchorage AK 4400 Business Park Blvd. Suite 45 99503
Project: KLU PROJECT	Area: KLIANE LAKE, YUKON TERRITORY	
CLAIM MAP: SHEET 3		
Compiled by: C. Bell, S. Casselman, K. Hottle	Supervisor: K. Hottle	Date drawn: Sept 08, 1997
Drawn by: Victor Fisher	Revised by: Victor Fisher	Nov 19, 1997
Scale: 1:5000	N.T.S. 1156/2	File: KLUsheet3claims.dwg
		Map 2



03726

Contour interval = 100 feet

Scale 1:25000



Claims Worked In 1997 Shown In Red

		Anchorage AK 4400 Business Park Blvd. Suite 48 99503	
Project: KLU PROJECT		Area: KLUANE LAKE, YUKON TERRITORY	
DETAILED CLAIM LOCATION MAP			
Compiled by: C. Bell, S. Casselman, K. Hottle	Supervisor: K. Hottle	Date drawn: Sept. 05, 1997	
Drawn by: Victor Fisher	Revised by:	Revised: Nov 14, 1997	
Scale: 1:25000	N.T.S. 1156/2	File: klu claims 1997.dwg	Map 1